





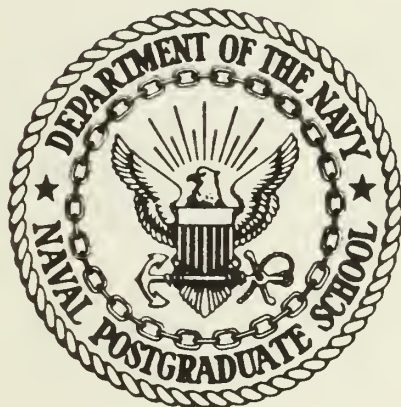


DUDLEY KNOX LIBRARY  
NAVAL POSTGRADUATE SCHOOL  
MONTEREY, CALIFORNIA 93943



# NAVAL POSTGRADUATE SCHOOL

## Monterey, California



# THESIS

AN INVESTIGATION OF THE WATERS OF  
THE EAST GREENLAND CURRENT

by

Mark D. Tunnicliffe

September 1985

Thesis Advisor:

Robert H. Bourke

Approved for Public Release; Distribution Unlimited

Prepared for:

Director, Arctic Submarine Laboratory,

Naval Ocean Systems Center,

San Diego, Ca., 92152

T227863

NAVAL POSTGRADUATE SCHOOL  
Monterey, California

Rear Admiral R. H. Schumaker  
Superintendent

D. A. Schradly  
Provost

This thesis prepared in conjunction with research sponsored by Arctic Submarine Laboratory, Naval Ocean Systems Center, San Diego, California under N66001-84-WR-00376. Reproduction of all or part of this report is authorized.

Released by:

REPORT DOCUMENTATION PAGE		READ INSTRUCTIONS BEFORE COMPLETING FORM
1. REPORT NUMBER NPS 68-85-025	2. GOVT ACCESSION NO.	3. RECIPIENT'S CATALOG NUMBER
4. TITLE (and Subtitle) AN INVESTIGATION OF THE WATERS OF THE EAST GREENLAND CURRENT		5. TYPE OF REPORT & PERIOD COVERED FINAL 1 Aug. 1984 - 30 Sept. 1985
		6. PERFORMING ORG. REPORT NUMBER
7. AUTHOR(s) Mark D. Tunnicliffe in conjunction with R.H. Bourke and R.G. Paquette		8. CONTRACT OR GRANT NUMBER(s) N66001-84-WR-00376
9. PERFORMING ORGANIZATION NAME AND ADDRESS Naval Postgraduate School, Monterey, California, 93943		10. PROGRAM ELEMENT, PROJECT, TASK AREA & WORK UNIT NUMBERS
11. CONTROLLING OFFICE NAME AND ADDRESS Arctic Submarine Laboratory, Code 54, Bldg. 371, Naval Ocean Systems Center, San Diego, California, 92152		12. REPORT DATE September 1985
		13. NUMBER OF PAGES 136
14. MONITORING AGENCY NAME & ADDRESS (if different from Controlling Office)		15. SECURITY CLASS. (of this report) Unclassified
		15a. DECLASSIFICATION/DOWNGRADING SCHEDULE
16. DISTRIBUTION STATEMENT (of this Report) Approved for public release; distribution unlimited.		
17. DISTRIBUTION STATEMENT (of the abstract entered in Block 20, if different from Report)		
18. SUPPLEMENTARY NOTES		
19. KEY WORDS (Continue on reverse side if necessary and identify by block number) East Greenland Current      MIZEX Icebreaker      East Greenland Polar Front NORTHWIND      Marginal Ice Zone Greenland Sea      Continental Shelf		
20. ABSTRACT (Continue on reverse side if necessary and identify by block number) A dense network of conductivity-temperature-depth (CTD) measurements made over the eastern Greenland continental shelf and slope between 81°N and 75°N provided new detail on the water properties and circulation on the shelf and at the adjacent East Greenland Polar Front (EGPF). The EGPF approaches the shelf break rapidly between 80°N and 78°N remaining 20 to 30 km east of it thereafter at least until 75°N. A filament of Atlantic Water (AW) was found close to the eastern side of the front which became generally cooler with		

decreasing latitude, suggesting that the majority of the contribution of the West Spitzbergen Current to the southward flowing Return Atlantic Current occurs north of 78°N. The portion of the shelf investigated is cut by several troughs generally oriented east-west; two of which are joined by a north-south depression west of Belgica Bank. Dynamic topography, water properties and ice movement suggest an anti-cyclonic surface circulation over this system of troughs and banks with AIW advecting up the troughs from the east.



Approved for public release; distribution is unlimited.

An Investigation of the Waters of the  
East Greenland Current

by

Mark D. Tunnickliffe  
LCDR, Canadian Forces  
B.Sc., McMaster University, 1972

Submitted in partial fulfillment of the  
requirements for the degree of

MASTER OF SCIENCE IN OCEANOGRAPHY

from the

NAVAL POSTGRADUATE SCHOOL  
September 1985

---

## ABSTRACT

A dense network of conductivity-temperature-depth (CTD) measurements made over the eastern Greenland continental shelf and slope between 81°N and 75°N provided new detail on the water properties and circulation on the shelf and at the adjacent East Greenland Polar Front (EGPF). The EGPF approaches the shelf break rapidly between 80°N and 78°N remaining 20 to 30 km east of it thereafter at least until 75°N. A filament of Atlantic Water (AW) was found close to the eastern side of the front which became generally cooler with decreasing latitude, suggesting that the majority of the contribution of the West Spitzbergen Current to the southward flowing Return Atlantic Current occurs north of 78°N. The portion of the shelf investigated is cut by several troughs generally oriented east-west; two of which are joined by a north-south depression west of Belgica Bank. Dynamic topography, water properties and ice movement suggest an anti-cyclonic surface circulation over this system of troughs and banks with AIW advecting up the troughs from the east.

## TABLE OF CONTENTS

I.	INTRODUCTION . . . . .	12
A.	PURPOSE . . . . .	12
B.	BACKGROUND . . . . .	13
	1. General . . . . .	13
	2. General Circulation . . . . .	14
	3. Water Masses . . . . .	15
	4. Current Velocities and Transports . . . . .	17
	5. The East Greenland Polar Front . . . . .	18
	6. Finestructure and Mesoscale Features at the EGPF . . . . .	18
C.	APPROACH . . . . .	19
II.	METHODS AND MEASUREMENTS . . . . .	21
A.	MISSION SUMMARY . . . . .	21
B.	INSTRUMENTATION . . . . .	21
	1. CTD . . . . .	21
	2. Data Recording and Display . . . . .	22
	3. Navigation . . . . .	24
C.	DATA PROCESSING AND COMPUTATIONS . . . . .	24
	1. Data Processing . . . . .	24
	2. Resolution . . . . .	25
	3. Computations . . . . .	25
D.	BATHYMETRY . . . . .	27
E.	ICE COVERAGE . . . . .	28
III.	OBSERVATIONS AND RESULTS . . . . .	33
A.	INTRODUCTION . . . . .	33
B.	THE EAST GREENLAND POLAR FRONT . . . . .	33
	1. Water Characteristics . . . . .	37

2.	Proximity to the Shelf Break . . . . .	41
3.	The Return Atlantic Current . . . . .	42
4.	Displacement of the Surficial Front . . . . .	46
5.	Finestructure . . . . .	47
6.	Mesoscale Features . . . . .	49
7.	Frontal Variability . . . . .	50
C.	THE CONTINENTAL SHELF . . . . .	64
1.	Introduction . . . . .	64
2.	Regional Hydrography . . . . .	64
3.	Shelf Water Masses . . . . .	81
D.	CIRCULATION AND TRANSPORT . . . . .	90
1.	Introduction . . . . .	90
2.	Dynamic Topography . . . . .	93
3.	Vertical Sections of Baroclinic Velocity . . . . .	99
4.	Circulation . . . . .	112
IV.	CONCLUSIONS . . . . .	118
	APPENDIX A: MOLLOY DEEP . . . . .	120
	LIST OF REFERENCES . . . . .	126
	INITIAL DISTRIBUTION LIST . . . . .	129



## LIST OF TABLES

I	Freezing Stress in the Northern Greenland Sea . .	29
II	A Summary of Frontal Characteristics for Transects Across the EGPF . . . . .	36
III	Frontal Geostrophic Current Sections . . . . .	102

## LIST OF FIGURES

1.1	General circulation and bathymetry of the Greenland Sea . . . . .	15
2.1	A map depicting the NORTHWIND 1984 cruise track and CTD locations . . . . .	23
2.2	Bathymetry of the northeast continental shelf of Greenland . . . . .	28
2.3	Observed ice conditions . . . . .	31
2.4	A NOAA 7 visual image of the ice margin on 27 Aug 1984 . . . . .	32
3.1	Location of transects across the EGPF . . . . .	34
3.2	A T/S plot of stations at the EGPF . . . . .	38
3.3	A T/S plot of stations within the RAC . . . . .	44
3.4	Transect 1 . . . . .	51
3.5	Transect 2 . . . . .	52
3.6	Transect 3 . . . . .	53
3.7	Transect 4 . . . . .	54
3.8	Transect 5 . . . . .	55
3.9	Transect 6 . . . . .	56
3.10	Transect 7 . . . . .	57
3.11	Transect 8 . . . . .	58
3.12	Transect 9a . . . . .	59
3.13	Transect 10 . . . . .	60
3.14	Transect 11 . . . . .	61
3.15	Transect 12 . . . . .	62
3.16	Transect 13 . . . . .	63
3.17	Location of transects made on the shelf . . . . .	65
3.18	Transect 9 . . . . .	70
3.19	Transect 14 . . . . .	71

3.20	Transect 15 . . . . .	72
3.21	Transect 16 . . . . .	73
3.22	Transect 17 . . . . .	74
3.23	Transect 18 . . . . .	75
3.24	Transect 19 . . . . .	76
3.25	Transect 20 . . . . .	77
3.26	Transect 21 . . . . .	78
3.27	Transect 22 . . . . .	79
3.28	Transect 23 . . . . .	80
3.29	A TS plot of typical shelf stations . . . . .	82
3.30	Thickness of the -1.7°C layer . . . . .	84
3.31	Surface temperature distribution . . . . .	87
3.32	Surface temperature distribution - Deviation from freezing . . . . .	88
3.33	Surface salinity distribution . . . . .	89
3.34	Bottom temperatures - deviation from the freezing point . . . . .	91
3.35	Distribution of bottom salinities . . . . .	92
3.36	Dynamic height: surface referenced to 150 dbars . .	94
3.37	Dynamic height: surface referenced to 200 dbars . .	95
3.38	Dynamic height: surface referenced to 500 dbars . .	96
3.39	Dynamic height: 150 dbars referenced to 500 dbars . . . . .	97
3.40	Location of vertical baroclinic current sections . . . . .	100
3.41	Sections 1 - 3 . . . . .	105
3.42	Sections 4 - 6 . . . . .	106
3.43	Sections 7 - 9 . . . . .	107
3.44	Sections 10 - 12 . . . . .	108
3.45	Sections 13a and 13b . . . . .	109
3.46	Sections 14 - 16 . . . . .	110
3.47	Sections 17 - 19 . . . . .	112
3.48	Sections 20 and 21 . . . . .	113

3.49	General circulation over the shelf and at the adjacent EGPF . . . . .	116
3.50	Sea ice drift 1976 After Vinje (1977) . . . . .	117
A.1	Bathymetric and ice structure at Molloy Deep . .	123
A.2	Transect across Molloy Deep . . . . .	124
A.3	Baroclinic velocity field near Molloy Deep . . .	125



## ACKNOWLEDGEMENTS

Funding for the work described in this thesis was provided by the Arctic Submarine Laboratory, Naval Ocean Systems Center, San Diego, California under Work Order N-66001-84-WR00376.

I wish to thank Dr. R.H. Bourke and Dr. R.G. Paquette for their advice and guidance during the analysis of the results and the preparation of this thesis. The assistance from Dr. J.L. Newton is also gratefully acknowledged. The success of the cruise and the large quantity of data acquired is to a great extent a reflection of the enthusiasm of the crew of the USCGC NORTHWIND, and in particular to the personal interest of her Commanding Officer, Captain W. Caster.

Finally, I wish to acknowledge the support of my wife, Nancy, whom I deserted with two small children to cruise amid the ice and who defended me from interruption while this thesis was being written.

## I. INTRODUCTION

### A. PURPOSE

The cruise of the USCGC NORTHWIND to the north-east coast of Greenland during the summer of 1984 provided, by means of a relatively dense network of conductivity-temperature-depth recorder (CTD) stations, a wealth of information on the circulation, water masses, and hydrographic structure of the major oceanographic feature in this region, the East Greenland Current. This cruise, the third in a series of hydrographic surveys designed to investigate the East Greenland Current (EGC) north of  $75^{\circ}\text{N}$ , provided information on the characteristics of the water overlying the continental shelf and the area immediately east of the shelf break between  $75^{\circ}45'\text{N}$  and  $81^{\circ}20'\text{N}$ . This thesis presents an analysis of the information collected during that cruise.

The major purpose of the cruise was to investigate the water masses and circulation over the troughs and banks of the shelf. An additional objective was to make a series of crossings of the boundary between the EGC and the warmer Greenland Sea water to the east, and to determine what, if any, interactions occurred between this deeper region and the shelf waters. This boundary zone is characterized by a sharp temperature and salinity gradient and will be referred to as the East Greenland Polar Front (EGPF) after Wadhams et al. (1979, p. 1325).

Because of the normally heavy ice concentrations encountered on the shelf, even in summer, relatively little information has been obtained concerning the oceanographic features of this region. However, during the NORTHWIND 1984

cruise, ice conditions over the shelf and in the marginal ice zone (MIZ) were unusually light, allowing the cruise objectives to be largely met. Only a small portion of the area of interest proved to be inaccessible.

The objective of the analysis of the CTD data presented in this thesis will be to:

- characterize the north-south development of the EGPF using temperature-salinity transects and contours of the vertical baroclinic geostrophic current velocity field,
- describe the water masses found over the shelf region and observe how bathymetry and other factors affect the distribution of water characteristics, and
- make some inferences about the circulation over the shelf and at the front by examining the distribution of water characteristics and the dynamic topography.

## B. BACKGROUND

### 1. General

The EGC is the major outlet for Arctic Ocean surface water into the Atlantic Ocean. The presence of this current, which carries significant quantities of ice through Fram Strait between Greenland and Svalbard and through the Denmark Strait to Cap Farvel, has been known for some time. Aagaard and Coachman (1968a) provide a comprehensive review of studies of the EGC up to and including the 1964 and 1965 EDISTO expeditions. Some direct current measurements along much of the north-south extent of the EGC were made during the drift of the ice island ARLIS II during the winter of 1964/65, and another three were made over Belgica Bank by EDISTO in the summer of 1965. An under-ice investigation of the EGC was conducted by HMS/M SOVEREIGN in the fall of

1976 using a recording velocimeter (Wadhams et al.,1979). Beginning with the summer 1979 WESTWIND expedition, a series of Arctic Submarine Laboratory sponsored cruises commenced high resolution CTD surveys of the northern portion of the EGC. The WESTWIND 1979 cruise (Newton and Piper, 1981; Newton, in preparation) penetrated the shelf at 77°N and 80°N, while the autumn 1981 NORTHWIND cruise (Perdue,1981; Paquette et al.,1985) executed a series of transects across the EGPF east of the continental slope between 76°N and 78°N.

## 2. General Circulation

The general bathymetry and circulation in the Greenland Sea is presented in Fig. 1.1. This figure (taken from Paquette et al.,1985) indicates the estimated circulation pattern based on various sources up to and including the results of the NORTHWIND 1981 cruise. The surface circulation in the Greenland Sea is dominated by a large cyclonic gyre bounded to the south by the Jan Mayen Current and to the east by the Norwegian and West Spitzbergen Currents. In the northern portion of the Greenland Sea, the West Spitzbergen Current (WSC) splits, with a portion turning westward and subsequently submerging and turning southward. This branch of relatively warm water, called the Return Atlantic Current (RAC), together with the EGC, accounts for the flow of water in the western portion of the Greenland Sea. The RAC consists of relatively warm and saline water compared to the cold fresher surface waters of the EGC, and the conjunction of the two provides the sharp east-west gradient of water properties which comprise the EGPF. Paquette et al. (1985) characterize the RAC as being less than 100 km in breadth and submerged under the EGPF at depths of 50 to 300 m.



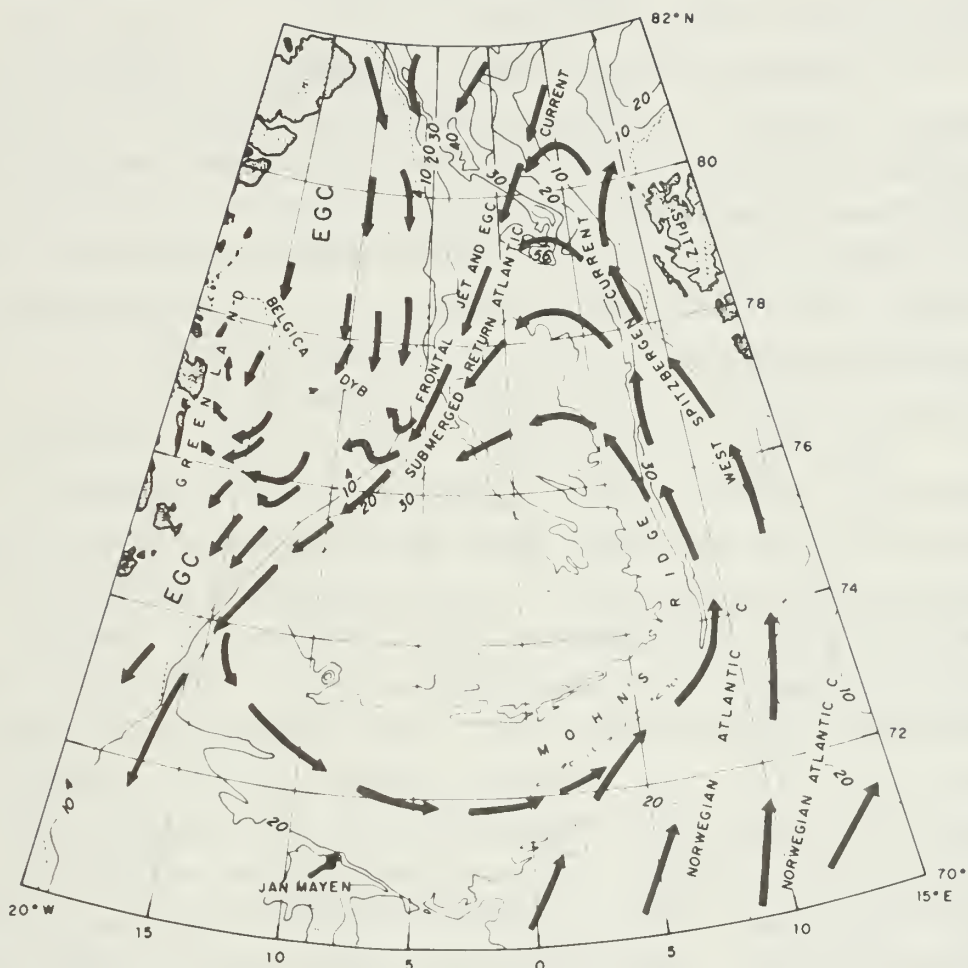


Figure 1.1 A map showing the general bathymetry and circulation in the Greenland Sea (from Paquette et al., 1985, p. 4867). Note that Belgica "Dyb" in this figure is referred to as Belgica Trough in this work.

### 3. Water Masses

Aagaard and Coachman (1968a) have identified three major water types found in the EGC. Their definitions, which have been accepted by much of the succeeding literature, are adopted here.

The Polar Water (PW) fraction extends from the surface to 150 to 200 m and is colder than  $0^{\circ}\text{C}$ . This layer increases rapidly in salinity with increasing depth. Surface salinities often are less than 30.0 and increase to about 34.5 at the bottom of the layer. The PW fraction of the EGC is generated in the Arctic Ocean but its characteristics are modified somewhat by local processes such as ice melt and freezing as well as insolation and mixing.

Atlantic Intermediate Water (AIW) is found both under the PW and, at the EGPF, to the east of it. AIW consists of water warmer than  $0^{\circ}\text{C}$  with salinities increasing from the PW maximum to a value between 34.88 and 35.00 at about 400 m, remaining relatively constant thereafter. The Swift and Aagaard (1981, p.1111) lower limits for Atlantic Water (AW), temperature  $3^{\circ}\text{C}$ , salinity 34.9, set the upper limits for AIW. Aagaard and Coachman (1968b, p. 282) state that the AIW fraction of the EGC has its origin in the WSC, deriving from a westward movement of warm Atlantic Water (AW) beginning north of  $75^{\circ}\text{N}$  and continuing over a range of latitudes to at least  $80^{\circ}\text{N}$ . Not all of the upper layer of the AIW can be formed by simple mixing of PW with the AW found in the WSC. Paquette et al. (1985, p. 4878) demonstrate that the AIW overlain by PW contains a fraction which is too cold to have been formed by mixing and suggest that double diffusion, local freezing, or advection from the north may be responsible.

Underlying the AIW at depths generally greater than 800 m is the Greenland Sea Deep Water (GSDW). It is

comprised of water colder than  $0^{\circ}\text{C}$  and limited by a narrow salinity range of 34.87 to 34.95.

#### 4. Current Velocities and Transports

The current velocity of the EGC shows considerable spatial variation and probably large scale temporal variation as well. Aagaard and Coachman (1968a) summarized the current meter measurements made during the diagonal passage of the EGC by the ice island ARLIS II in the winter of 1965 as well as those by EDISTO over Belgica Bank in the same year. They concluded that the surface current velocity increases to the south from 0.04 m/s southeast of Belgica Bank to 0.14 m/s at  $70^{\circ}\text{N}$  and decreases in speed over the continental shelf. They also noted that there appeared to be no large decrease in velocity with depth, at least to depths of 340 m in winter, although they conceded that the baroclinic contribution to the current flow may be more significant in summer. On the basis of these results they computed a volume transport of 35 Sv, an order of magnitude higher than previous estimates (e.g. Vowinckel and Orvig (1962), Mosby (1962)).

Baroclinic estimates of current velocities north of  $75^{\circ}\text{N}$  vary somewhat from year to year, as may be expected, but in general show highest values over the shelf break in the region of the EGPF and decrease westward. Maximum values of 0.23 m/s were reported by Aagaard and Coachman (1968b, p. 280) from the 1965 EDISTO Nansen bottle/reversing thermometer data, and 0.15 to 0.20 m/s by Newton (in preparation) from the 1979 WESTWIND results. Both of these calculations were made with respect to a 200 dbar level of assumed no net motion. Paquette et al. (1985) suggest that the frontal jet may exhibit much higher velocities. The closer station spacing across the front made during the NORTHWIND 1981 cruise and the use of a 500 dbar reference indicated speeds up to 0.96 m/s at  $77^{\circ}25'\text{N}$  just inside the ice edge.

## 5. The East Greenland Polar Front

The eastern edge of the EGC is characterized by a strong east-west gradient in temperature and salinity which marks the East Greenland Polar Front and which forms a boundary between the PW of the EGC and the AIW and AW of the central Greenland Sea to the east. At the EGPF, the isotherms and isohalines characterizing the PW of the EGC and the underlying AIW turn sharply upward toward the east. The slope of the front appears to show considerable spatial and temporal variability. For example, Aagaard and Coachman (1968b) reported a mean slope of 1 m/km over a range of 120 km derived from a transect taken across the EGPF at 75°N in 1965. Newton and Piper (1981) report a mean slope of 3.3 m/km over 60 km at 78°N in 1979. Perdue (1982) noted mean slopes of 1.5 m/km to 20 m/km between 78°N and 76°N. In a subsequent transect conducted eight days later, this latter value, which was derived from a transect conducted at the mouth of Belgica Trough, was reduced to 8.5 m/km.

The EGPF is the location of the fastest currents in the EGC. Paquette et al. (1985, p. 4877) present a section showing baroclinic north-south components of current velocity derived from the NORTHWIND 1981 data at 78°N which shows a narrow, shallow jet (35 km wide, 100 m deep, as defined by the 0.05 m/s isotach) at the EGPF.

## 6. Finestructure and Mesoscale Features at the EGPF

The relatively high vertical-resolution sampling provided by the CTD measurements made during the WESTWIND 1979, NORTHWIND 1981, and the present cruise has permitted resolution of finestructure in the EGPF. During NORTHWIND 1981, lenses of alternating cool and warm water with peak-to-peak temperature excursions of up to 1.0°C were noted in the AIW between 75 and 300 m by Paquette et al. (1985). They



propose that this interleaving of water of different temperatures is the result of parcels of AIW or AW east of the front, at or near the surface, which have undergone cooling and slight dilution and have descended westward along the sloping isopycnals of the front.

Another feature of the front is the presence of meanders and eddies, usually in the AIW just east of the EGPF. Paquette et al. (1985, p.4874), compared the EDISTO 1965 and NORTHWIND 1981 cruises and noted a cyclonic eddy in much the same location in both cases. This eddy, generally located at about  $79^{\circ}30'N$ ,  $001^{\circ}E$  is quasi-permanent and appears to be associated with the 5570 m Molloy Deep. Further discussion on this phenomenon is provided in Appendix A.

Newton (in preparation) noted a front configuration at  $79^{\circ}N$  during the WESTWIND 1979 cruise which was consistent with the cyclonic circulation associated with the Molloy Deep feature together with appeared to be a parcel of PW detached from the EGC east of the front. He observed that the density structure of this 30 km feature was consistent with an anticyclonic eddy with a Rossby radius of deformation of about 10km.

## C. APPROACH

The succeeding chapters present an analysis of the results of the NORTHWIND 1984 data making comparisons with previous work. One of the most significant features of this cruise, compared with previous ones, was the large amount of high resolution data collected on the continental shelf between  $76^{\circ}N$  and  $81^{\circ}N$ . Since previous bathymetries of part of this region have been somewhat sparse or inaccurate, a new plot of the bottom topography with adequate resolution for the purposes of this work was developed based on depth

observations made at each CTD station. Supplemental depth data obtained from the CTD stations of the WESTWIND 1979 and NORTHWIND 1981 cruises was incorporated as well. This bathymetry, along with a review of the method and instruments employed, and a synopsis of the ice conditions encountered is presented in Chapter 2.

Results of the data analyses are included in Chapter 3. The water masses, structure and development of the EGPF are presented using temperature-salinity cross-sections across the front as well as temperature-salinity (T/S) plots of the water structure at individual stations in the frontal region. A similar approach is used to examine the hydrography of the shelf. Additionally, an analysis of the circulation pattern at the front and on the shelf is presented using dynamic topography, distribution of water properties and, in one instance, ice drift.

## II. METHODS AND MEASUREMENTS

### A. MISSION SUMMARY

Between 22 August and 16 September 1985, the USCGC NORTHWIND conducted an extensive hydrographic survey of the waters of the East Greenland Current including the shelf waters of the northeast Greenland coast. In the course of this cruise, NORTHWIND made a series of crossings of the continental shelf break between 80°N and 75°30'N, many of which extended inward close to the Greenland coast. Detailed transects were conducted over prominent shelf features such as Ob' and Belgica Banks, Belgica Trough and Westwind Trough (see Fig. 2.2 for the location of the place names listed). The ship approached the coast closely enough to conduct surveys in Ingolf's Fjord and Dijmphna Sund in the north, and along the east and south coasts of Ile de France further south. NORTHWIND covered almost 6500 km in the course of conducting 333 CTD stations. Operations were augmented and assisted with the use of the ship's Arctic Survey Boat in shallow water and by the NORTHWIND's two helicopters which conducted some 45 sorties in ice reconnaissance. The cruise track and location of CTD stations are shown in Fig. 2.1.

### B. INSTRUMENTATION

#### 1. CTD

The Neil Brown Instrument Systems (NBIS) Mark III CTD was the primary instrument used to make the oceanographic observations. A wire cage, supported by a metal frame, was appended to the base of the instrument to protect

the sensors against impact with ice and with the ocean floor. No significant deterioration of sensor response due to this adaptation has been observed (see also Paquette et al. 1985, p. 4876). The CTD was fitted with a calibrated 3200 decibar pressure sensor which provided adequate depth resolution for the purposes of the cruise and facilitated making deeper casts off the shelf.

The temperature and conductivity sensors were calibrated before and after the cruise. Because of a possible error in one or the other measurement, a comparison of pre- and post-cruise conductivity calibrations was inconclusive for accuracy levels better than 0.5 S ( $0.005 \text{ ohm}^{-1}\text{cm}^{-1}$ ). Evidence of long-term stability in both temperature and conductivity was provided by a comparison of salinity measurements taken at two adjacent stations - one made at the beginning of the cruise and one towards the end - which suggested that a difference no greater than 0.001 ppt was likely to have occurred. This comparison was made at depths below 600 m where the salinity profile is quite stable.

None of the difficulties noted by Perdue (1982, p. 62) with water freezing in the sensors between casts was experienced during this cruise since the ambient air temperature was greater than  $-2^{\circ}\text{C}$  for much of the time. The CTD sensors were conditioned prior to each recording by repeated flushing to 50 m. The lack of any notable or consistent differences in the near-surface measurements made during the up and down traverses of the CTD showed that this technique was adequate.

## 2. Data Recording and Display

The data were passed from the CTD via the NBIS deck unit to a Hewlett-Packard 9835B computer where it was stored on magnetic tape cassettes. For flexibility in storing data, and to economize on tape usage, the computer and tapes were

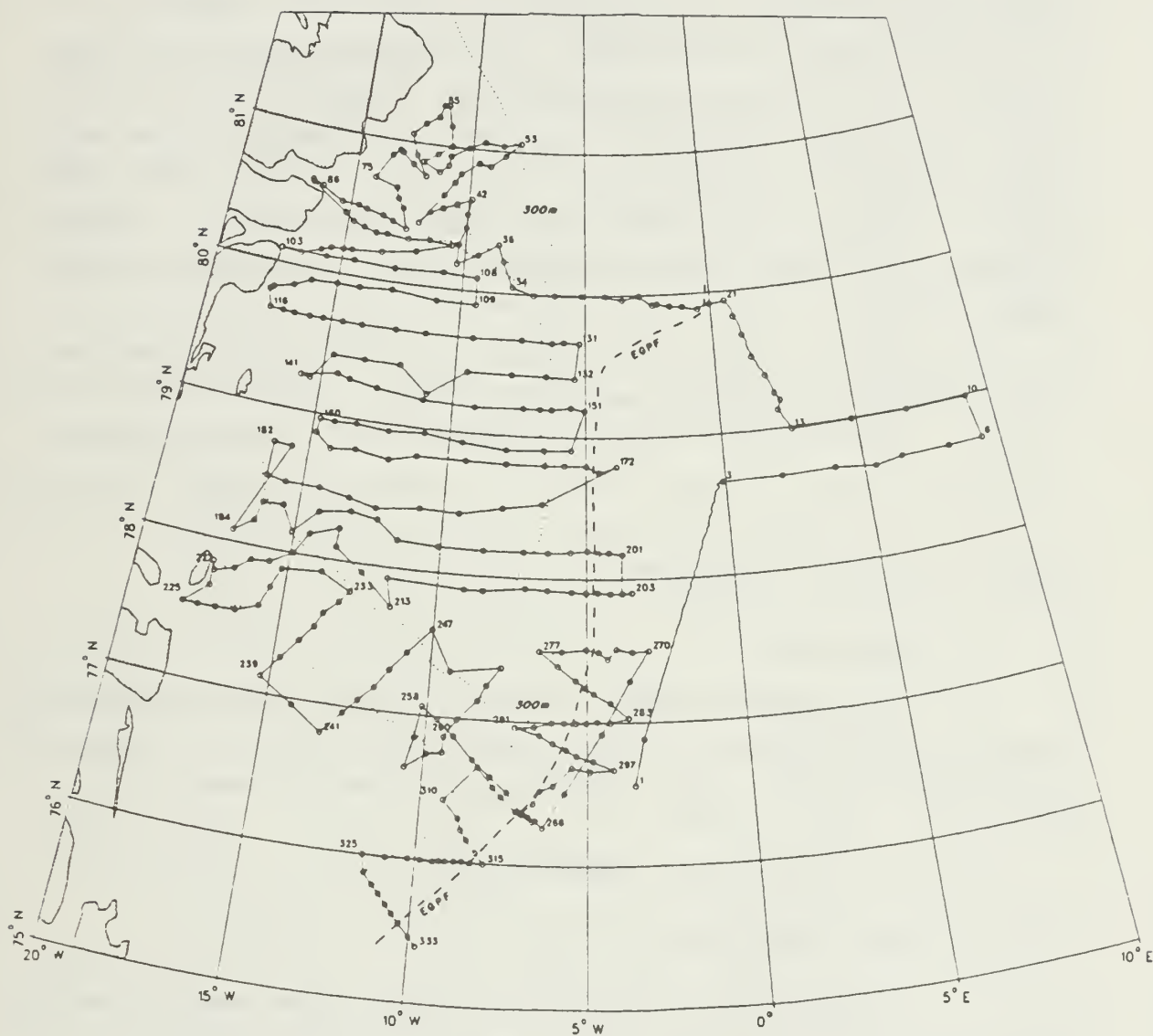


Figure 2.1 A map showing the NORTHWIND 1984 cruise track and CTD station locations. The location of the EGPF and the 300 m isobath are also shown.



formatted to accept either 3500, 2625, 1750, or 875 binary data records. This allowed tapes to store data to approximately 1200, 900, 600, or 300 m, respectively. When it became clear that the supply of tapes was going to be limiting, only the data from the down casts were recorded. However, the 10 kHz modulated audio signal from the CTD for both up and down casts was recorded on a back-up Sony audio tape recorder. Additionally, in water of less than 150 m depth, both up and down casts were recorded in digital format since both sets of data would then fit on the minimum length file.

Data for both up and down casts at all stations were immediately plotted on a Hewlett-Packard 9872A X-Y flat bed plotter and later, on the back-up H-P 9225B plotter. Temperature and salinity plots of the up casts were plotted on the same graph as the down casts (offset by half a scale unit) to permit comparison.

### 3. Navigation

The primary navigation aid was the Magnavox MX 1107 Satellite Navigation System, which provided an average of two fixes per hour with a mean accuracy of 0.5 km.

## C. DATA PROCESSING AND COMPUTATIONS

### 1. Data Processing

A number of spikes in the CTD data were noted as temperature and salinity profiles were generated on the X-Y plotter. The causes of such spikes are not certain but are possibly due to a combination of plankton or ice particles passing through the conductivity cell, power surges, slip-ring noise, or instrument peculiarities. The spikes were occasionally serious enough to cause the plotting routine to fail completely. This problem was solved by modifying the



H-P computer program to ignore out-of-range single data points.

Upon conclusion of the cruise, the data were transferred to a tape format more suitable for processing by the NPS IBM 3033 computer. At this point the data were edited to remove single spurious data points and data mis-sequenced in terms of depth (caused by the roll of the ship during a cast). The temperature and conductivity were corrected for dynamic response errors, thus compensating for the salinity spikes produced by the mismatch of response time in conductivity and temperature, empirically found to be 23 and 110 ms, respectively. The resulting despiked salinities were smoothed with a five point centered running mean.

## 2. Resolution

The data sampling rate was set to provide for one conductivity/temperature/pressure recording every 36 cm based on a CTD lowering rate of 1 m/s, providing a vertical resolution in the data of about three points per meter. To monitor the lowering/raising rate of the CTD, the H-P computer was programmed to display the actual depth and the ideal depth, based on the 1 m/s lowering rate, of the CTD continuously throughout the cast.

A subset of this data was constructed consisting of one point every 5 m. This subset was used for various ancillary purposes not requiring the full resolution of the original data set such as in the construction of vertical baroclinic velocity profiles and the calculation of volume transports.

## 3. Computations

Dynamic heights, based on the geostrophic approximation were calculated with reference primarily to the 500 dbar level. Additional computations were made with reference

to the 200 and 150 dbar levels which provided an opportunity to compare the differences resulting from the selection of different reference levels as well as providing an appropriate basis for comparison with earlier work (for example, Paquette et al., 1985; Newton, in preparation) in which different reference levels are used.

Over portions of the shelf where the bottom was often shallower than the reference level selected for dynamic height computations, the reference level and the isosteres from the nearest adjacent deep-water station were projected horizontally into the sea bottom, following the technique of Helland-Hansen (1934). As pointed out by Fomin (1964, p. 153), this method assumes that the velocity of the gradient current at the bottom is zero and therefore that the horizontal pressure gradient is zero. Since this latter assumption is probably not true, the use of this technique introduces some error into the calculations. As pointed out by Paquette et al. (1985), the regions of greatest velocity are over deeper water and are therefore not subject to this inconsistency. The use of a 150 dbar reference level (Fig. 3.36) avoids much of this difficulty since relatively few such extrapolations were needed. However, use of this reference level neglects the information inherent in deeper waters.

The vertical baroclinic velocity cross-sections developed are also normally referenced to 500 dbar with a 300 dbar reference level used when necessary. Reference levels are noted with the appropriate figures. The Helland-Hansen (1934) technique was also applied to these sections when required.

Volume transports were calculated for baroclinic current velocities referenced to 500 dbar or 300 dbar as indicated above. They were obtained from vertical trapezoidal integration of the baroclinic velocity curve between each pair of stations in a section with a 5 m vertical grid.

#### D. BATHYMETRY

In order to relate some of the observed oceanographic phenomena to the shelf topography (where appropriate), and since older charts were not sufficiently accurate, a bathymetric map of the shelf between  $75^{\circ}\text{N}$  and  $82^{\circ}\text{N}$  was constructed (Fig. 2.2). Bottom contours were constructed based upon the water depth at CTD stations occupied during the WESTWIND 1979 and NORTHWIND 1981 and 1984 cruises to this region. Required details not available from these data were obtained from using older charts (Perry et al., 1980).

The eastern continental shelf of Greenland between  $77^{\circ}\text{N}$  and  $81^{\circ}\text{N}$  is transversely cut by a number of troughs and depressions. The most notable of these, Belgica Trough (which may also be referred to elsewhere as Belgica Dyb or Belgica Strath), cuts the shelf from the shelf break at  $77^{\circ}\text{N}$  westward to just north of Ile de France at  $78^{\circ}\text{N}$ . The mean depth of this trough is somewhat greater than 300 m but deeper depressions, in excess of 500 m at the shoreward end, were noted during the cruise.

Contiguous to Belgica Trough, and running northward parallel to the coast, is another deep depression tentatively named Norske Trough after the island nearby. Depths in excess of 600 m were noted near its southern end but much of it, particularly the portion closest to the shore, could not be investigated due to the presence of fast ice covering much of the area.

Norske Trough is connected at its northern end to Westwind Trough which extends southeasterly from Ingolf's Fjord. Westwind Trough is somewhat shallower than Belgica Trough, the axial depth being about 300 m.

Less well defined and running almost north/south is a depression east of the shallowest portion of Belgica Bank. This depression lies between Belgica and Westwind Troughs and parallels the coastline.

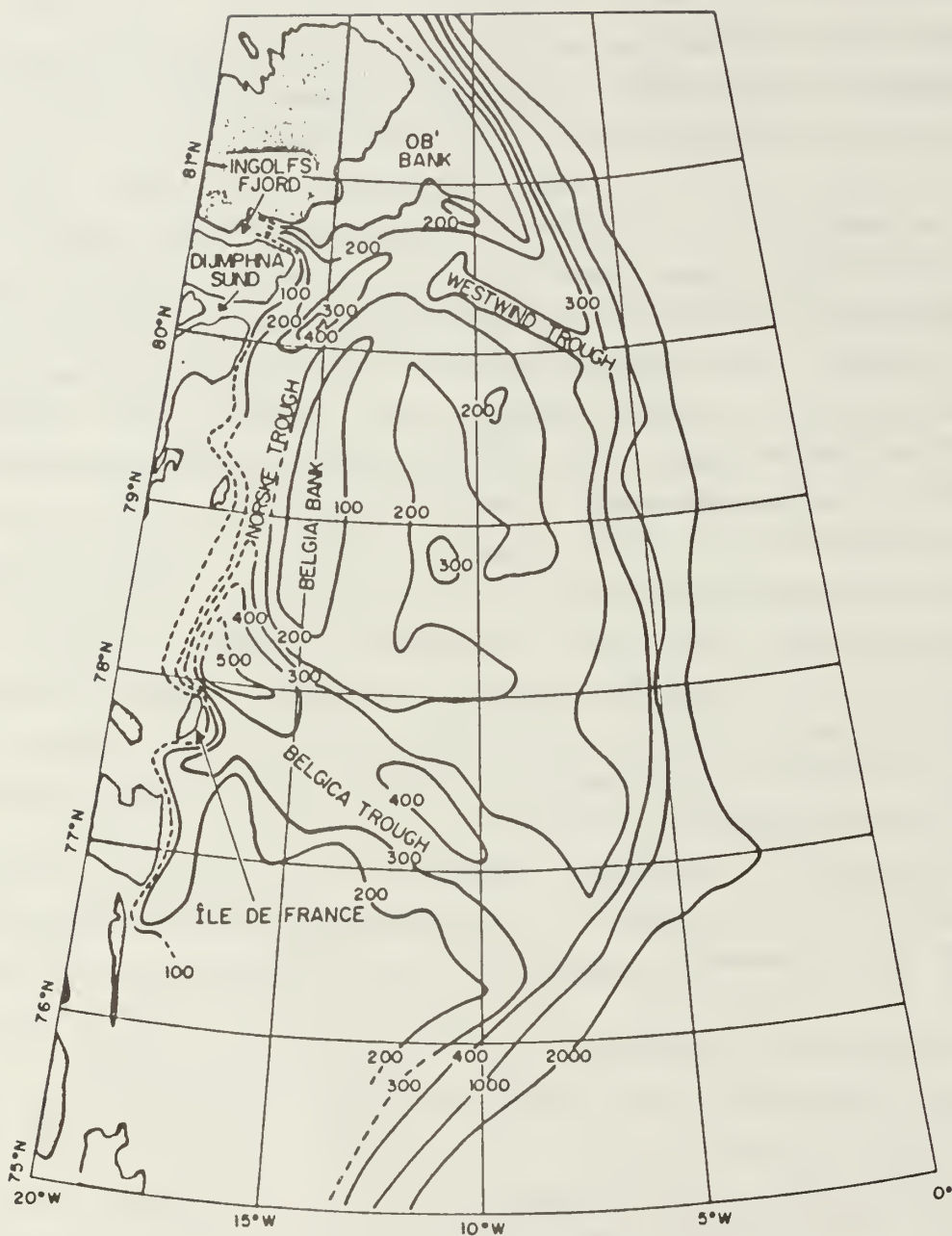


Figure 2.2 A map showing the bathymetry of the north-east continental shelf of Greenland. This map was produced by contouring depths measured at CTD stations during the 1979 WESTWIND and 1981 and 1984 NORTHWIND cruises.

## E. ICE COVERAGE

During this cruise NORTHWIND was able to penetrate many areas on the shelf not accessible on previous cruises because of the relatively low ice concentrations encountered. This variation in ice coverage is due ultimately to variations in seasonal weather. Some indication of the relative mildness of the 1983/84 winter season can be gained from the freezing degree days in the general area during the freezing season. Table I indicates the Celsius freezing degree days experienced at three meteorological stations: Damatshaven at 76°48'N on the east Greenland coast, Barentsberg on Svalbard and Malye Karmakuly on the southern end of Novaya Zemlya. The data suggest that over a wide range in the area north of the Greenland and Norwegian Seas that the winter of 1983/84 was relatively mild.

TABLE I  
Freezing Stress in the Northern Greenland Sea

Station/Year	Freezing Degree Days (°C)		
	1979	1981	1984
Damatshaven	4583	4871	4558
Barentsberg	N/A	3268	2234
Malye Karmakuly	3342	2793	1788

Ice coverage is a function of local climatic conditions (as indicated by the number of freezing and warming degree days) as well as wind and circulation. It is also, to some extent a function of the climatic conditions in the regions from which ice might advect. According to Wadhams (1983, p. 110), ice in Fram Strait is derived from two sources.



The ice within 100 km of the MIZ has advected from north of the Barents and Kara Seas westward across the north of Svalbard into the Strait. The ice in the western part of Fram Strait from 79°N - 84°N has advected across the North Pole region and is comprised of a greater fraction of multi-year ice. Therefore presumably, climatic conditions in the Soviet arctic will also have a significant impact on the ice coverage in the Greenland Sea MIZ.

The ice conditions encountered by NORTHWIND throughout the 1984 cruise are indicated in Fig. 2.3. Concentrations are taken from ice density observations made in the local area during each CTD cast. It is not a fully accurate indicator of the actual ice conditions in the region not only because of its non-synoptic nature but also because the ship occasionally had to skirt some of the densest concentrations which are therefore not recorded. However, it does best indicate the local ice conditions at the time of each CTD cast. A photographic view of the ice conditions as recorded by the NOAA 7 meteorological satellite (visual band) on 27 August is shown in Fig. 2.4. It is representative of NOAA 7 photographs taken throughout the period of the cruise.

Despite differences in their derivations, both Figs. 2.3 and 2.4 show many similar features, including:

- low ice concentration to the north (80°N) especially near the coast,
- a somewhat less well developed marginal ice zone (MIZ) north of 78°N, and
- the presence of a solid mass of fast ice covering much of the inshore portion of Norske Trough.





Figure 2.3 Distribution of ice coverage. This non-synoptic representation of the ice coverage, indicated in tenths, is based on the ice concentration noted at each CTD station. The ice margin on 27 August as determined from a NOAA 7 photograph on that date is also indicated for comparison.



Figure 2.4 A NOAA 7 visual image of the ice margin on 27 August 1984. This photograph, typical of the situation in August/September 1984, shows little ice coverage at  $80^{\circ}$  N with ice increasing somewhat by  $75^{\circ}$  N.

### III. OBSERVATIONS AND RESULTS

#### A. INTRODUCTION

The distribution of water properties over the north-east Greenland shelf and in the East Greenland Current is primarily depicted in this chapter using temperature and salinity transects. The area has been divided into two regions for consideration: the front, located east of the shelf break, and the shelf proper and its associated banks and troughs. Sequences of transects in each region were produced showing the development of the EGC and its water properties with respect to bathymetry, latitude, or proximity to the coast, as appropriate.

The circulation of water on the shelf is inferred from dynamic topographies, the horizontal advection of water properties as well as by examining the geostrophic baroclinic current velocity in vertical cross-section over a series of sections made at various latitudes. Results from this analysis could be confirmed in one instance using satellite photographs indicating ice motion.

#### B. THE EAST GREENLAND POLAR FRONT

NORTHWIND crossed the shelf break seventeen times between  $80^{\circ}\text{N}$  and  $75^{\circ}45'\text{N}$  during this cruise, but not all of these crossings included the East Greenland Polar Front (EGPF). The locations of thirteen temperature-salinity transects made in the vicinity of the front is indicated in Fig. 3.1. They are numbered sequentially from north to south, not necessarily in the order in which they were conducted. Each of the transects was reasonably synoptic being completed over time spans of 5 to 25 hours during the 25

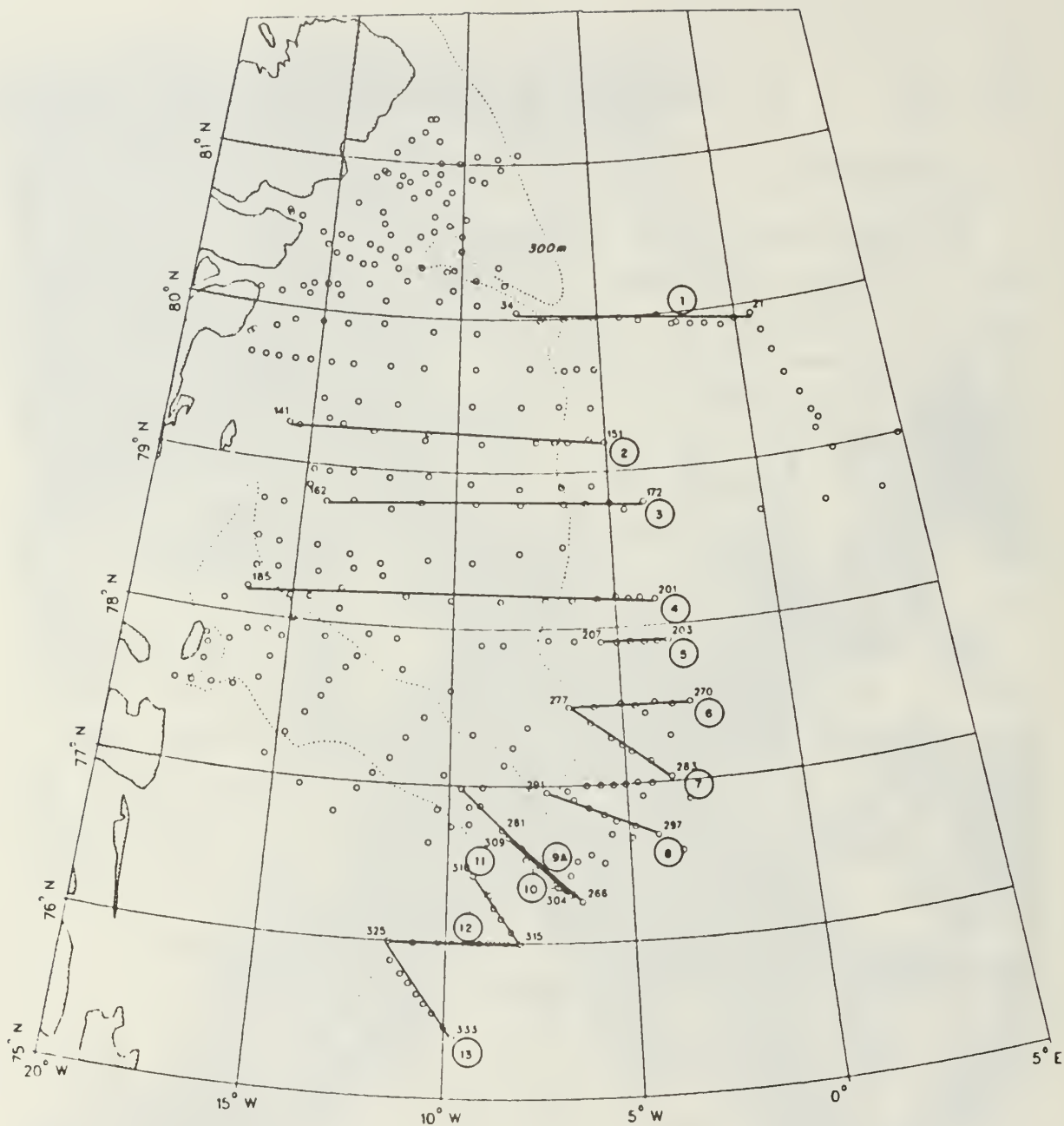


Figure 3.1 A map showing the location of transects made across the continental shelf break.



August - 16 September period. One (Transect 9a) was repeated three days later (as Transect 10); otherwise transects are separated by 15 to 30 minutes of latitude and run perpendicular to the direction of the front with the exception of Transect 12 which crosses the front at about  $45^\circ$ .

Transects 1 to 13 are shown in Figs. 3.4 to 3.16 at the end of this section. To facilitate the observation of the north-south evolution of the front as shown in these transects, a number of characteristics were quantified using consistent though somewhat arbitrary criteria. The mean slope of the front is derived by noting the depth of the  $0^\circ\text{C}$  isotherm at the point where it clearly turns upward and the location of its intersection with the surface (or the upper boundary of the lower front in the case of a split front) and then determining the horizontal distance over which this vertical displacement takes place. While this determination is clearly somewhat arbitrary, particularly in the case of the more northerly transects, where the front was split into upper and lower parts horizontally displaced from each other, it could be made with reasonable consistency in most cases. Additionally, since the shape of the front (again as defined by the behaviour of the  $0^\circ\text{C}$  isotherm) is concave with respect to the PW, instantaneous slopes of the front at its eastern extremity were considerably greater than the mean values calculated. The west-east horizontal thermal gradient was calculated by noting the distance between the  $-1.5^\circ\text{C}$  and  $2.0^\circ\text{C}$  isotherms at 50 m. Distances from the shelf were measured from the 400 m isobath to the point at which the  $0^\circ\text{C}$  isotherm intersects 50 m depth. A summary of the frontal transects and the results of these calculations is provided in Table II.

A detailed description of the water masses and processes occurring along the EGPF at the onset of the freezing season and over a lesser range of latitudes has already been made

TABLE II  
A Summary of Frontal Characteristics  
for Transects Across the EGPf

TRANSECT	START DATE	MEAN LATITUDE	MEAN SLOPE OF FRONT (m/km)	THERMAL GRADIENT (°C/km)	DISTANCE OF FRONT FROM SHELF BREAK (km)	MAXIMUM TEMPERATURE AT FRONT (°C)	DEPTH OF POLAR WATER AT SHELF BREAK (m)	MAX. GEOSTROPHIC BAROCLINIC VELOCITY (m/s)	STATIONS (W - E)	REMARKS
1	25 Aug	79°55'N	2.8	0.92	123	4.9	190	0.37	34-21	Split front. "Warm surface water" west of front. GSDW at 800 m.
2	2 Sep	79°12'N	4.8	N/A	36*	N/A	180	0.12	141-151	Shows only the lower part of front.
3	3 Sep	78°48'N	5.8	1.9	18	5.5	200	0.39	162-172	Split front. Filamented AIW west of front.
4	5 Sep	78°10'N	5.5	1.75	19	5.3	160	0.38	194-201	
5	7 Sep	77°54'	N/A	N/A	N/A	N/A	155	0.32	207-203	Thermal extrusion at front.
6	12 Sep	77°30'N	5.3	0.83	23	5.0*	180	0.46	277-270	Split front.
7	12 Sep	77°15'N	4.8	1.75	25	4.7	175	0.38	277-283	
8	13 Sep	76°50'N	3.3	0.34	16	3.7	120	0.30	291-297	Weak surface front.
9	11 Sep	76°30'N	2.6	0.34	19	3.2	115	0.38	258-266	First transect at the mouth of Belgica Trough.
10	14 Sep	76°30'N	4.3	0.56	30	3.1	170	0.38	309-304	Second transect at the mouth of Belgica Trough.
11	14 Sep	76°15'N	3.8	0.58	34	3.8	145	0.47	310-315	
12	15 Sep	76°00'N	N/A	0.39	35	3.8	130	0.36	325-315	Front ill-defined due to extensive finestructure.
13	15 Sep	75°45'N	3.9	0.25	40	3.9	140	0.36	325-333	

N/A - A reasonable estimate could not be provided.

\* - Estimate

# - A very small filament.



(Paquette et al., 1985; Perdue, 1982). However, the present sequence of transects show more clearly the development of a number of characteristics of the EGPF as the EGC moves southward. In the following sections, the location of the front with respect to the shelf, frontal water masses, the nature of the RAC associated with the EGPF, finestructure, and mesoscale features are discussed.

## 1. Water Characteristics

A characteristic of the PW close to the EGPF appears to be a cold ( $<-1.5^{\circ}\text{C}$ ), relatively saline (about 34.0) fraction which lies close to the bottom of the PW layer at about 100 m. Another temperature minimum occurs at a salinity of about 32.3 to 32.8 in many, but not, all frontal stations. This "double minimum" feature, shown in Fig. 3.2, persists down the length of the EGPF although the temperature of the high salinity minimum rises somewhat from less than  $-1.7^{\circ}\text{C}$  (Station 24) at  $79^{\circ}55'\text{N}$  to  $-1.58^{\circ}\text{C}$  at  $75^{\circ}35'\text{N}$  (Station 330). There is also a reduction in salinity from 34.0 to 33.6 of the high salinity temperature minimum over this latitude range. Cold waters of such high salinities were generally not noted at stations on the shelf (Station 137 in Fig. 3.2 is a typical example) nor in waters east of the front (for example, Station 18 in Fig. 3.2). Another way of observing this feature is to note the behaviour of the lower  $-1.5^{\circ}\text{C}$  isotherm in the longer frontal transects (for example Fig. 3.4, 3.6 or 3.7). Over the shelf, the lower  $-1.5^{\circ}\text{C}$  isotherm is almost contiguous with the 33.0 isohaline but close to the EGPF, this isotherm changes to the depth at which the 34.0 isohaline is found. Typically, this happens 20 - 30 km west of the front. In Transect 1 (Fig. 3.4), where the EGPF lies 120 km east of the shelf break, this cold saline fraction is spread over an east-west distance of 75 km. Transect 1 also provides a

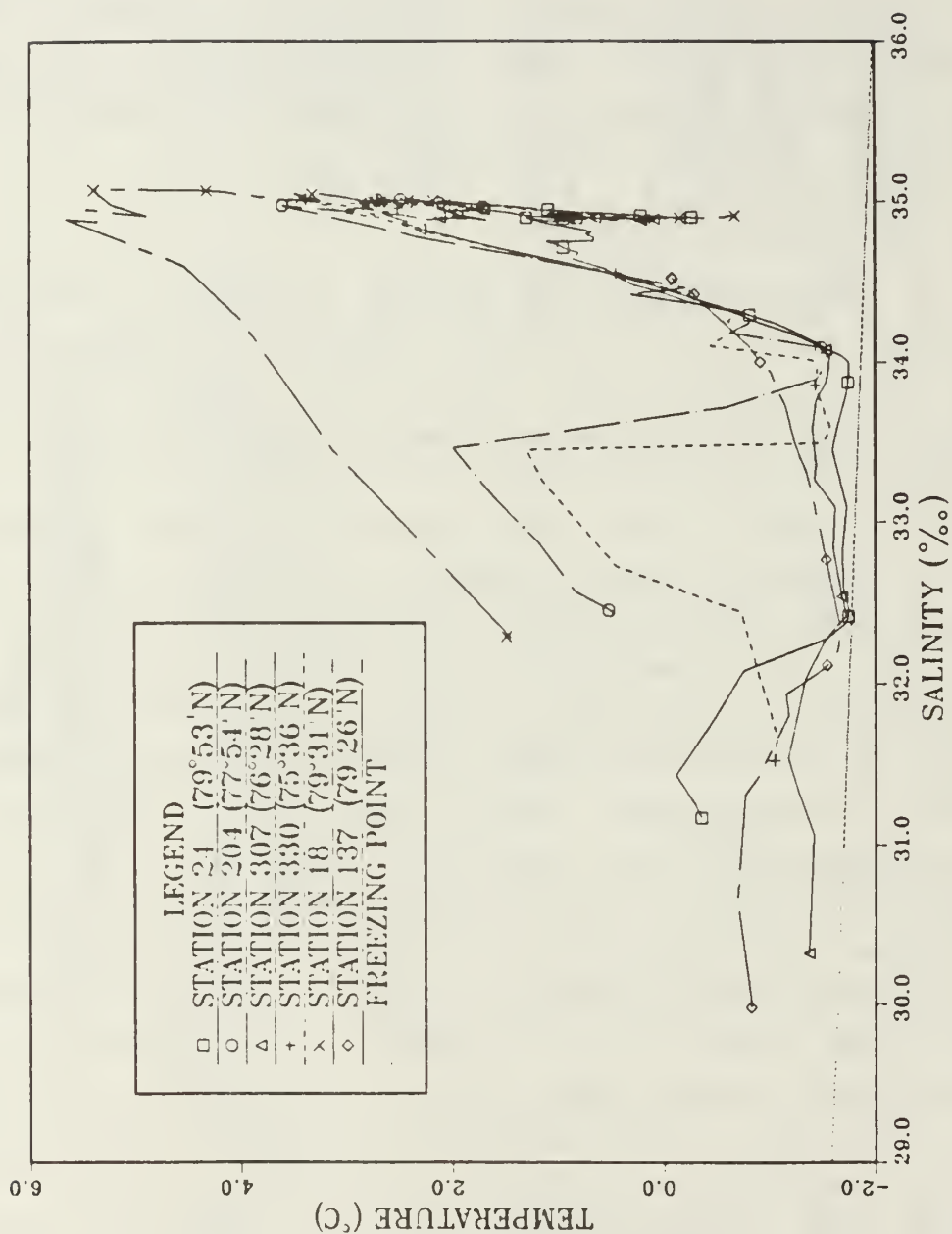


Figure 3.2 A temperature/salinity plot for stations close to the EGPF. Station 24 is the most northerly, Station 307 is the most southerly. Station 137 is a typical shelf station, is provided for comparison. Station 18 lies east of the front. Symbols are at 50 m intervals.

typical example of the superposition of two cold water masses of different salinities in the proximity of the front.

The formation of the cold, saline fraction has led to some speculation. Kiillerich (1945, p. 28) discussed the temperature-salinity characteristics of the water in Fram Strait as observed by the BELGICA 1905 expedition. He postulated that the characteristics of the water were defined by the mixing of "AW" ( $2.1^{\circ}\text{C}$ , 34.97), and "PW" ( $-1.85^{\circ}\text{C}$ , 34.00) which he stated was formed beneath the ice of the polar sea. Paquette et al. (1985, p. 4878) defined a cold temperature source for mixing as locally available PW of lowest salinity ( $-1.5^{\circ}\text{C}$ , 30.5). They observed that simple mixing between this PW and AW ( $3.5^{\circ}\text{C}$ , 35.1) would not account for the "knee" structure they observed in temperature-salinity diagrams constructed from NORTHWIND 1981 observations made at  $78^{\circ}\text{N}$ . Their knee at  $-1.2^{\circ}\text{C}$  and 34.1 appears similar to the apex observed at about  $-1.5^{\circ}\text{C}$  and 34.0 in Fig. 3.2. They suggest that the knee is primarily formed by the advection of AIW from the east under the upper layers of Arctic Ocean water at which interface some modification, possibly by double diffusion, occurs.

If one assumes that the cold saline fraction has advected into the area of the EGC covered by this study, the question of its origin is raised. Certainly Kiillerich's assumption of origin appears somewhat general in light of more recent data on Arctic Ocean water properties. For example, in none of the winter 1964/65 stations occupied by the ice island ARLIS II in the western Arctic Ocean was water which was more saline than 34.00, colder than  $-1.5^{\circ}\text{C}$  (Tripp and Kusunoki, 1967). Water approximating Kiillerich's "PW" was only noted by Tripp and Kusunoki further south ( $72^{\circ}\text{N}$  -  $78^{\circ}\text{N}$ ) off the east Greenland coast where water with temperatures less than  $-1.8^{\circ}\text{C}$  with

salinities in the range 33.4 - 34.4 were found in the upper 100 m. This suggests that a source in the western and central Arctic Ocean is not responsible for the cold saline fraction.

Aagaard et al. (1981) discussed the formation of such cold saline water in the Arctic Ocean and suggest two mechanisms: salinization of cold surface waters by brine rejection during freezing, and the cooling of AW. The latter mechanism, they proposed, might occur when AW upwells from a deep position and is cooled and freshened. The second mechanism, which they explored in some detail, involves the salinization of shallow shelf water by brine rejection during winter freezing. In particular, they noted that the region between Spitzbergen and Franz Joseph Land requires relatively little ice growth to raise the upper 50 m to a salinity of 34.5. Cold saline water produced in this location or similar regions in the Kara and Barents seas farther east advecting into the eastern portion of Fram Strait could account for the cold saline fraction noted in the frontal station in Fig. 3.2.

The question of the path of such advection is then raised since the near-surface circulation appears to be predominantly eastward in these locations. Water formed on these shelf areas might be postulated to move off the shelf region and subsequently follow the same path as the first year ice within the eastern 100 km of the MIZ in Fram Strait which Wadhams (1983, p. 110) suggests originates north of the Barents and Kara Seas. Such a speculated flow might be resolved by the conduct of several zonal transects in the northern portion of Fram Strait and a comparison of the water properties in the northeastern portion of the Strait with those north of the Barents and Kara Seas.

In summer, as the cold saline fraction moves south in the EGC, some local modifications would occur. Warming by

diffusion of heat from underlying AIW could account for the slight erosion, with decreasing latitude, of the apex in the T-S properties in Fig. 3.2. The lack of such a sharp knee in the T-S diagram at 34.0 for stations west of the frontal region may result from a longer period of erosion in the slower moving portions of the current over the shelf or perhaps because the PW over the shelf originates from a different portion of the Arctic Ocean than that in the frontal region. This latter suggestion appears to be consistent with the hypothesis of Wadhams (1983, p. 110) that the ice in this portion of the current was derived from deep within the Arctic Ocean. It is also supported by the observations of Tripp and Kusunoki (1967) of temperatures greater than  $-1.5^{\circ}\text{C}$  for water more saline than 34.00 in the central Arctic.

## 2. Proximity to the Shelf Break

Transect 1 (Fig. 3.4) at  $79^{\circ}55'\text{N}$  is the only transect in which the front is displaced any significant distance (123 km) from the shelf break (here defined as the 400 m isobath). The front appears to have moved significantly closer to the shelf by  $79^{\circ}12'\text{N}$  (Transect 2; Fig. 3.5) and at Transect 3 (Fig. 3.6), the front is about 20 km from the shelf. From here southward (at least until  $75^{\circ}55'\text{N}$ ), the front remains within 15 to 40 km of the shelf break.

The front south of  $79^{\circ}\text{N}$  appears to be steered by bathymetry. Aagaard and Coachman (1968b, p. 269) note that the front and the shelf break coincide as far south as  $73^{\circ}\text{N}$ , at which point PW extends eastward again, associated with the flow of the Jan Mayen Polar Current.

The location of the front north of  $78^{\circ}\text{N}$  varies somewhat from year to year as can be seen by interannual comparisons along  $79^{\circ}\text{N}$ . As indicated above, in 1984 the front at  $79^{\circ}\text{N}$  was about 20 km from the shelf break, while Newton and



Piper (1981, p. 35) observed it at a distance of 120 km in 1979. Paquette et al. (1985, p. 4874) show the front in 1981 split into an upper and lower portion 45 to 90 km from the shelf break. The EDISTO 1965 data does not provide sufficient spatial resolution for satisfactory comparison but Aagaard and Coachman (1968b, p. 268) show the front at that time generally departing from the shelf north of 77°30'N and approximately 150 km west of it by 80°N.

Since the position of the EGPF appears to be controlled by bathymetry for much of its extent north of 73°N, its behaviour above 78°N leads to some speculation. By about 80°N the position of the front, as indicated by the location of the ice edge, has changed orientation from essentially meridional as it is further south, to to a zonal configuration near 81°N (see, for example, Fig. 2.4). The location of the ice edge in summer is largely controlled by the position of the EGPF although closer to Svalbard the WSC may be more influential in determining the ice cover in that area. As will be discussed in the next section, the majority of the warm water which marks the EGPF turns into the southward flowing EGC from the east between 79°N to 81°N causing the front to veer west in this region. Since this warm water is derived from the WSC it is reasonable to assume that the position of the front north of 78°N will vary somewhat with the strength of the WSC. Aagaard and Coachman (1968a, p. 197), citing the work of Soviet oceanographers, note that there are strong seasonal fluctuations in the strength of the WSC and such fluctuations are probably reflected in the behaviour of the EGC (although the nature of the coupling between the two is open to debate).

### 3. The Return Atlantic Current

In most of the frontal transects, a warm filament of dilute AW (i.e.  $>3.0^{\circ}\text{C}$ ,  $<34.9$ ) is found close to the main

thermal expression of the front between 100 m and 25 m. Transects 1 (Fig. 3.4) and 3 (Fig. 3.6) show good examples of this. In Fig. 3.6 a filament of AW is separated by AIW from AW of similar characteristics lying some 30 km farther east. The filaments are often substantial in size - up to 200 m in thickness and 20 km in horizontal extent - as defined by the 3°C isotherm. The north-south dimensions of the filaments are undefined. These filaments appear to be embedded in the core of RAC water described by Paquette et al (1985, p. 4869) from the NORTHWIND early winter 1981 data although in none of the transects from that cruise were temperatures found as high as those noted in the present cruise. A temperature-salinity (T/S) plot (Fig. 3.3) of some of the stations at which this feature was noted, from 79°55'N (Station 23) southward along the front to 77°15'N (Station 280), shows that the water characteristics of this core vary somewhat with latitude. The salinity of the core generally decreases with latitude and, after an initial increase in temperature at Station 23, the temperature maximum also decreases with latitude. However, there is no indication whether the core is continuous or fragmented over this range.

The variation in maximum temperature of this core is also indicated in Table II. The maximum temperature of the core initially rises from 4.9°C at 80°N to 5.8°C at 78°10'N after which it decreases to 3.9°C at 75°44'N. Not surprisingly, the east-west thermal gradient at the front, measured at 50 m, also follows this trend with maximum values noted between 78°48'N and 77°15'N and thereafter decreasing southward. The initially lower temperature at 80°N might be expected if one assumes that the westward flowing arm of the WSC has a north-south temperature gradient with maximum temperatures close to the zonal ice edge in Fram Strait. At 80°N, the westward flowing water comes from under the ice

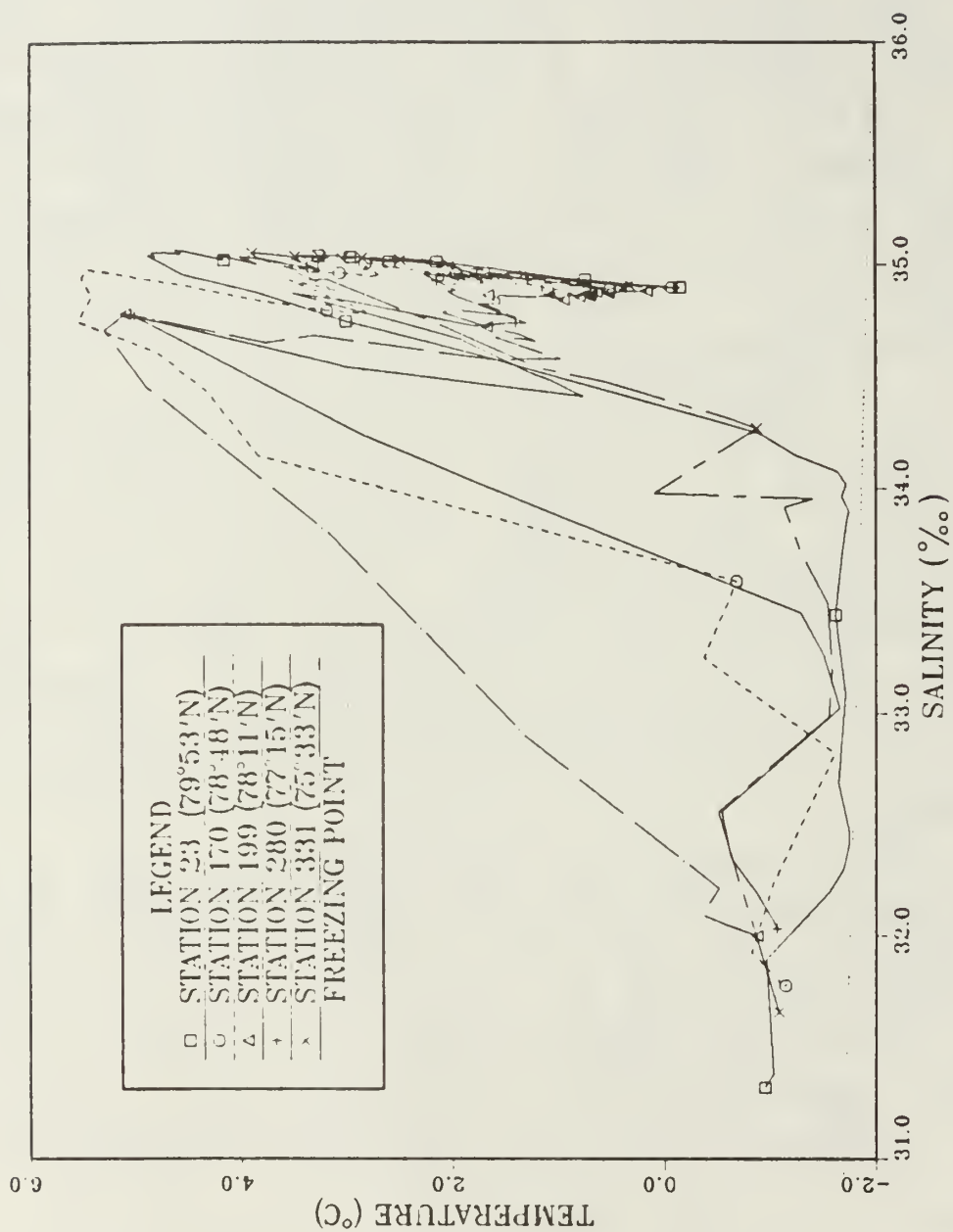


Figure 3.3 A temperature/salinity plot of stations near the EGPF showing elements of the warm core of RAC often found close to the eastern side of the front.

while at  $79^{\circ}\text{N}$  -  $78^{\circ}\text{N}$  it comes from the warmest portion of this westward flow.

The warm core of RAC water, found close to the front in most of the frontal transects presented here, was also observed during other cruises. Data from NORTHWIND 1981 showed the core cooling from  $>3^{\circ}\text{C}$  at  $78^{\circ}\text{N}$  to  $>2.5^{\circ}\text{N}$  at  $76^{\circ}\text{N}$  and fragmented farther southward. A  $79^{\circ}\text{N}$  frontal transect from the 1979 WESTWIND cruise (Newton and Piper, 1981) shows a large ( $>2^{\circ}\text{C}$ ) core extending from 150 m to the surface lying close to the eastern side of the EGPF. The core temperature was reduced considerably in the  $78^{\circ}\text{N}$  frontal transect conducted later in the cruise.

The variation in temperature with latitude of this warm core is consistent with the hypothesis that the majority of the input of AW into the RAC comes from the westward turning arm of the WSC above  $78^{\circ}\text{N}$ . If this is so, then presumably this input water is subjected to atmospheric cooling and mixing along the frontal region, thus reducing the size of the high temperature core and its maximum temperature, as observed. If, on the other hand, the westward turning of the WSC occurred to a significant degree over a broader range of latitudes, say from  $75^{\circ}\text{N}$  (at which latitude, one would expect surface temperatures in the WSC to be about  $10^{\circ}\text{C}$ ), as suggested by Aagaard and Coachman (1968b, p283), the temperature of the water immediately to the east of the EGPF should increase with decreasing latitude, a feature generally not observed.

To summarize, it is hypothesized that the WSC splits into two sections near Svalbard, one of which turns westward between about  $78^{\circ}\text{N}$  and  $80^{\circ}\text{N}$ , north of the dome of cooler water which characterizes the central Greenland Sea. This westward turning arm interacts with the southward moving polar waters of the EGC influencing the position of the EGPF and the ice margin in the region. Such an interaction may be

reflected in the slightly cooler maximum temperature of the RAC noted in Transect 1 at 79°55'N than in transects immediately southward. This picture might be resolved by conducting a transect north along the 5°E meridian through Fram Strait on a future cruise.

#### 4. Displacement of the Surficial Front

The front north of 77°30'N is divided between a lower portion from 200 to 25 m and a shallower surface front. In Transects 1 (Fig. 3.4) and 3 (Fig. 3.6), the surface front was not encountered and was displaced at least 30 km east of the subsurface position. Transect 6 (Fig. 3.9) clearly shows the separate upper and lower fronts. South of this transect, the surface expression of the front is either weak or continuous with the subsurface portion.

This division of the front is probably due to the large area of dilute surface water formed by the melting of sea ice. At 77°30'N and southward, the ice edge becomes considerably better defined and it closely follows the shelf break contours. To the north, the melting of sea ice has been more extensive, possibly as a result of the advection of warm AW from the WSC onto the northern shelf, resulting in an expanse of cool dilute surface water.

The location of the surface expression of the EGPF is probably primarily influenced by the growth or retreat of the ice margin. An example of such a process might be the action of offshore winds which blow substantial quantities of ice seaward into warmer water, causing the ice to melt, cooling and diluting a large expanse of surface water. Since the ice edge can move faster than the front due to the inertia of the water, the effect is seen as a shallow surface front displaced seaward of the subsurface front. This same type of displacement can occur in a region of rapid ice growth. Perdue (1981, p.38) shows several



transects in the region of 76°30'N to 78°N from the NORTHWIND autumn 1981 cruise in which the surface expression of the front was extended 20 - 40 km seaward of the lower part. He ascribed this extension of the front to the rapid expansion of the ice margin followed by a retreat, leaving a layer of PW to the east. Presumably this PW was initially AIW which had been conditioned by the melting process.

## 5. Finestructure

Some notable examples of finestructure can be seen in a few of the transects from the NORTHWIND 1984 cruise. Transect 12 (Fig. 3.15) at 76°N is an example of a frontal crossing in which the finestructure is so highly developed that the precise location of the front is obscured. Generally the finestructure observed was limited to the frontal region and usually became more developed in the southern transects (little or none was noted in Transects 1 through 4, for example). Finestructure primarily consisted of an interleaving of AIW and PW, generally in the upper 100 m immediately east of the EGPF. Considerable temperature fluctuations over a short vertical distance were noted in some instances. For example, near the 60 m depth at Station 320 in Transect 12 (Fig. 3.15), the temperature varied from -1.5°C to 2.0°C and back again over 24 m. Presumably finestructure of this nature could be formed by AIW at or near the surface being cooled east of the EGPF and descending westward along an isopycnal into the region of the front. The finestructure was more developed to the south where the ice in the MIZ was more dense. The patchwork of open water and floes of melting ice in this region could generate parcels of water near the front with different salinity and temperature characteristics but similar densities.

Paquette et al. (1985, p. 4879) present a description of finestructure along the EGPF as noted during the

autumn 1981 NORTHWIND cruise. Based on an analysis of the fluxes and dynamics involved, they estimated the lifetimes and mean sizes of the finestructure elements. Finestructure observed during that cruise consisted of elements with peak to peak temperatures in excess of  $1.0^{\circ}\text{C}$  associated with the AIW along the front at depths just below the temperature maximum. Temperature-salinity cross-sections from the 1981 data show finestructure generally located between 70 and 300 m in the AIW sandwiched between lines of constant salinity. They proposed that finestructure consists of filaments of anomalously warm or cool water with a mean length of 27 km in the along front direction. Given this, it is understandable that the  $45^{\circ}$  orientation of Transect 12 in 1984 with respect to the front would exaggerate the appearance of the finestructure elements compared to the other transects in the region which are positioned normal to the front.

Finestructure noted during the 1984 cruise generally followed this pattern. Transects 7 (Fig. 3.10) and 6 (Fig. 3.9) provide examples of interleaving layers of AIW between 50 and 300 m, generally confined between the 34.7 and 34.9 isohalines. However, the horizontal extent of the development of this finestructure is not as great as that noted in the transects presented for the 1981 cruise in which lenses of AIW warmer than  $1.5^{\circ}\text{C}$  were noted under the PW up to 90 km west of the front.

In none of the transects published from the 1981 NORTHWIND cruise (Paquette et al., 1985; Perdue 1982) is there any notable finestructure development consisting of AIW in the PW fraction immediately to the west of the front. This, however is noted fairly frequently in several of the frontal transects developed from the 1984 data. For example, a lens of AIW at 60 m depth located 20 km west of the front is imbedded in the PW layer in Transect 11 (Fig. 3.14),

while in Transect 12 (Fig. 3.15), the PW fraction near the front contains AIW finestructure lenses up to 50 km west of the front. Finestructure in the PW layer was observed in several stations taken near the EGPF at the mouth of Belgica Trough in the early fall of 1979 (Newton and Piper, 1981). These show significant AIW interleaving with the PW layer between 75 and 20 m.

## 6. Mesoscale Features

A striking example of a larger scale interleaving of PW and AIW was noted in Transect 5 (Fig. 3.8) along  $77^{\circ}54'N$ . The front, as defined at Transects 4 and 6, lies close to the  $5^{\circ}W$  meridian which runs between Stations 206 and 205 in Transect 5. The extrusion of cold water seen in this transect extends some 20 km beyond the presumed location of the front and is sandwiched between the 33.5 and 34.5 isohalines. The form of this extrusion is reminiscent of an eddy about to be detached. But because the isopycnals in the upper 150 m rise monotonically from west to east (and are almost horizontal across the extrusion itself), the mass distribution is not indicative of an eddy-like rotation (see also Section 8 in Fig. 3.43).

A significant displacement of isotherms and isohalines appears to have occurred in the AIW layer at Station 28 in Transect 1 (Fig. 3.4). As indicated in the vertical contours of baroclinic velocity shown in Section 1 of Fig. 3.41, the distortion in the mass field at this location may be suggestive of a weak eddy-like rotation. If this feature does represent an eddy, it would be an anticyclonic one with a radius of about 15 km, comparable to a typical Rossby radius of deformation at this latitude. Similar features were also noted during the WESTWIND 1979 (Newton, in preparation) and NORTHWIND 1981 (Paquette et al., 1985, p. 4870) cruises.

## 7. Frontal Variability

Two transects, 9a (Fig. 3.12) and 10 (Fig. 3.13), were made three days apart across the same section of the front adjacent to the entrance to Belgica Trough. These transects were separated by no more than 3 km and provided an opportunity to observe the temporal variability of the EGPF in this area. A comparison of these two transects indicates that the surface expression of the front and the region of its initial upward development at 150 m are coincident in each crossing. However, between 11 and 14 September, the front itself changed shape from concave to convex, the portion at 50 m bowing eastward some 25 km. Also at 200 m, the 2°C isotherm has been displaced westward somewhat and its vertical development shortened. Additionally, cold ( $<0^{\circ}\text{C}$ ), saline (34.88) water, characteristic of GSDW is observed as shallow as 300 m at Station 266 in 11 September but is absent in the 14 September transect.

The EGPF has been frequently noted to vary in position over relatively short periods of time. Aagaard and Coachman (1968b, p. 272), reviewing a sequence of stations occupied by EDISTO in 1965 at 73°N, noted a lateral fluctuation in excess of 90 km in the position of the front. They speculated that large scale eddies or a variation in intensity of the circulation in the Greenland Sea may be responsible.

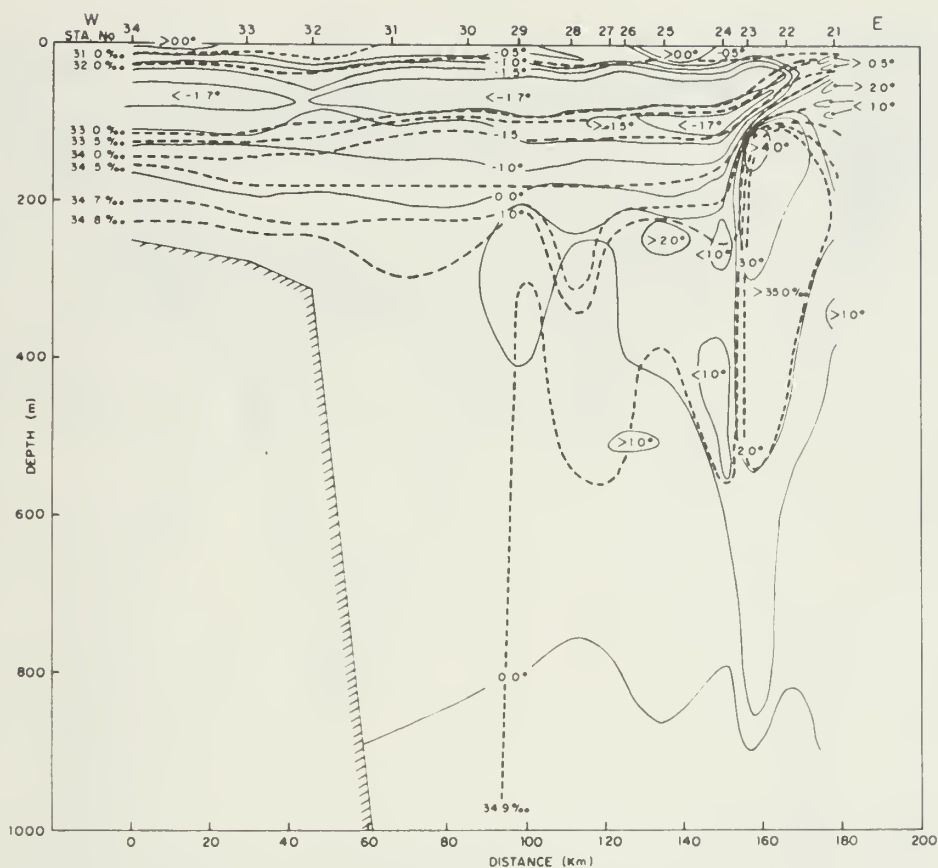


Figure 3.4 Transect 1 along  $79^\circ 55'N$ . In this transect, the front is shown displaced about 120 km east of the shelf break. In this figure and in all succeeding transects, isotherms are shown as solid lines and isohalines as dashed lines. The vertical scale of this figure is compressed to show the water properties below 500 m.



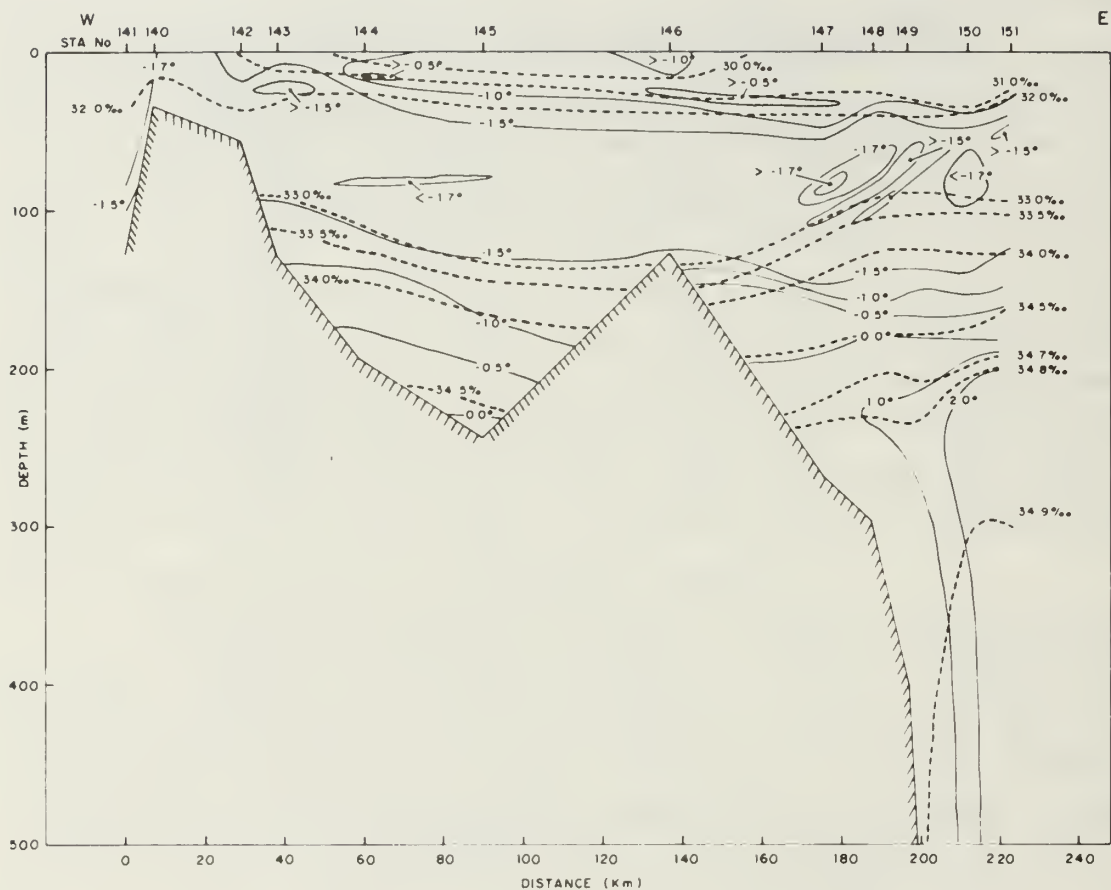


Figure 3.5 Transect 2 along  $79^{\circ}12'N$ . The EGPF was not included in this transect but the upward turning of the isopleths at Station 151 suggest that the front is probably located within 50 km of the shelf break at this latitude.

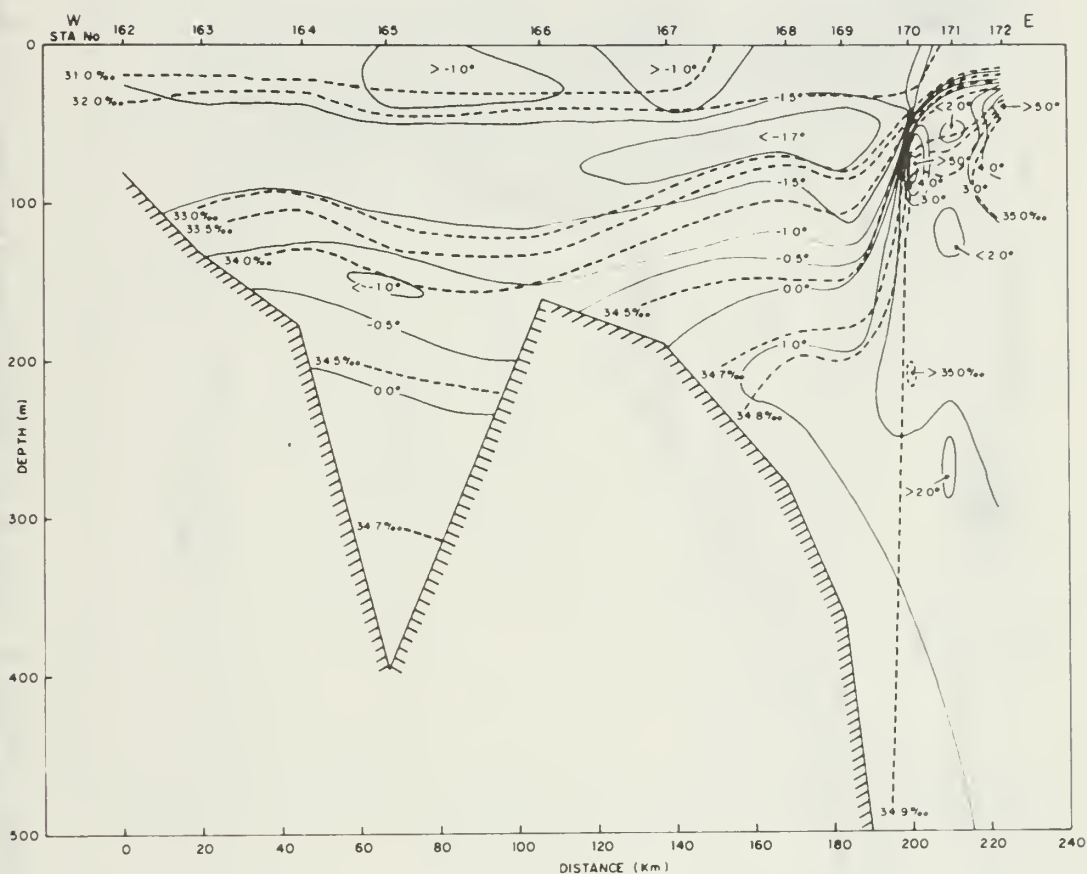


Figure 3.6 Transect 3 along  $78^{\circ}46'N$ . The subsurface expression of the EGPF is located 18 km east of the shelf break. A warm filament of AW, separated by more than 20 km from water of similar properties, lies close to the east side of the EGPF.

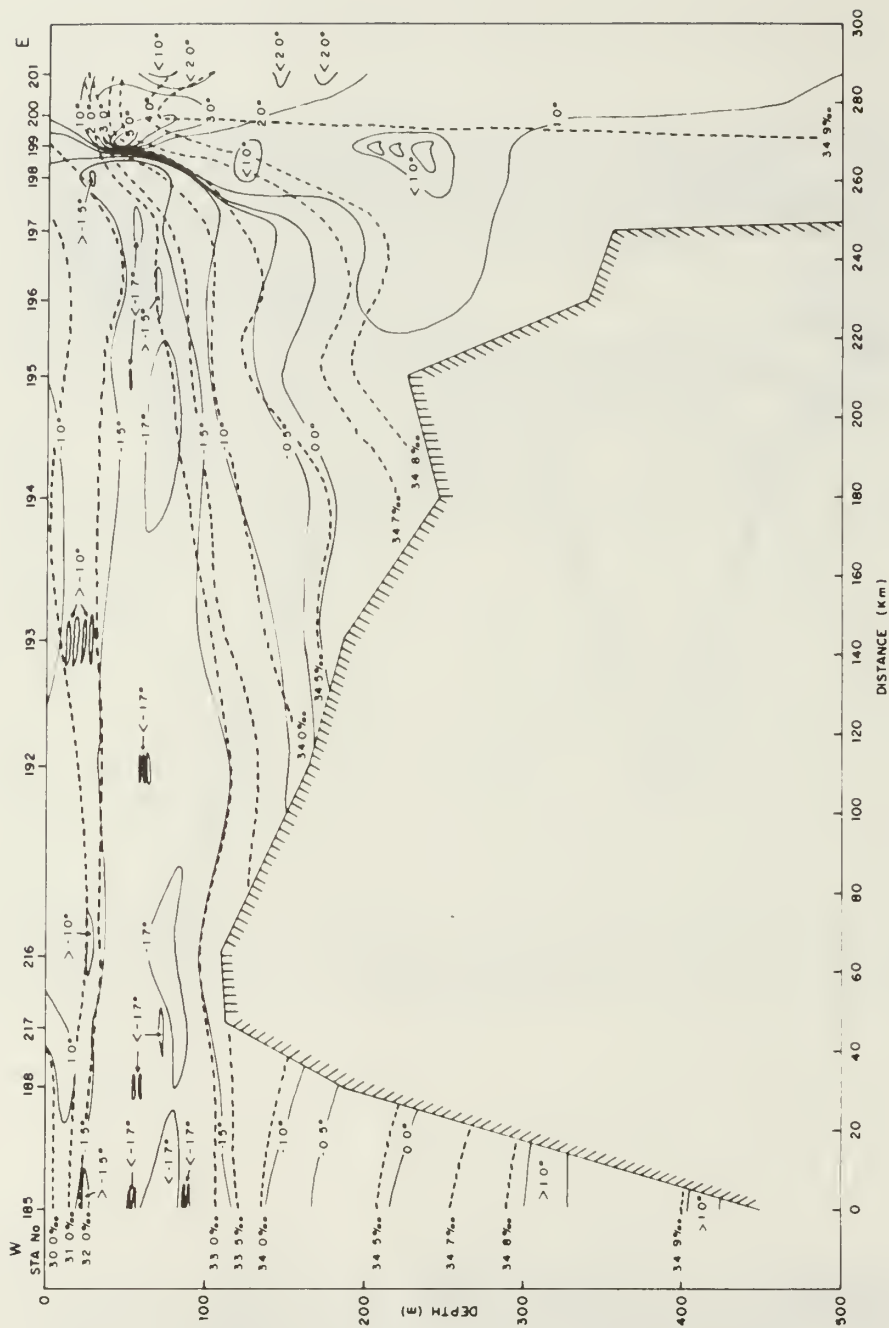


Figure 3.7 Transect 4 along 78°10'N. This transect covers most of Belgica Bank and a portion of Norske Trough in the west, as well as the EGPF.

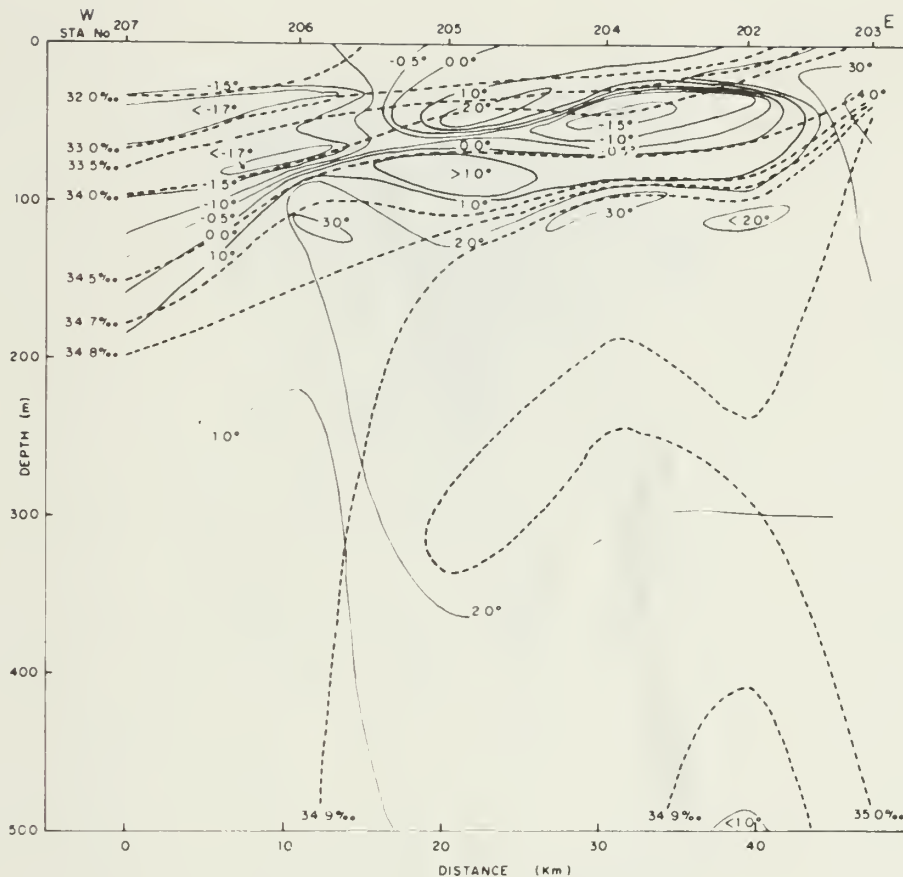


Figure 3.8 Transect 5 along 77°50'N. This transect shows the horizontal extrusion of PW some 20 km east of the EGPF possibly developing into an eddy. The horizontal scale of this figure has been expanded for clarity.

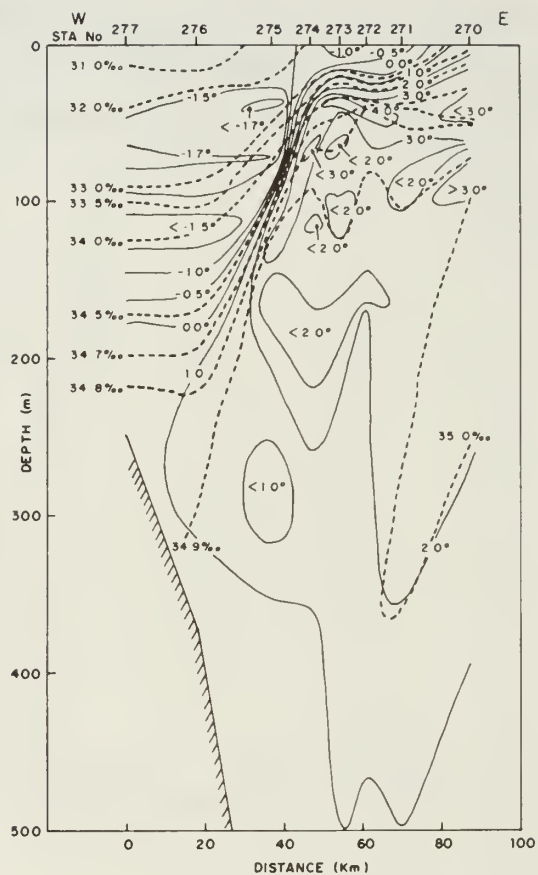


Figure 3.9 Transect 6 along 77°30'N. In this transect the EGPF is split into an upper and lower front.



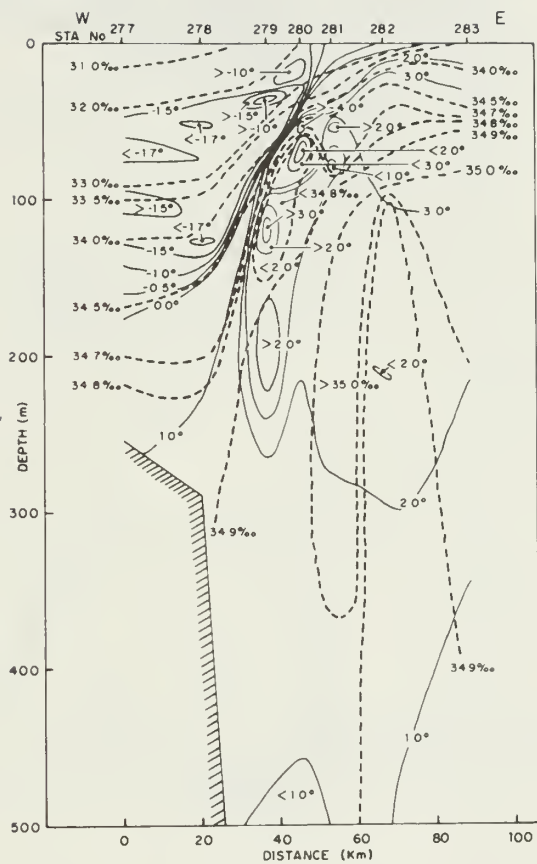


Figure 3.10 Transect 7 along 77°15'N.



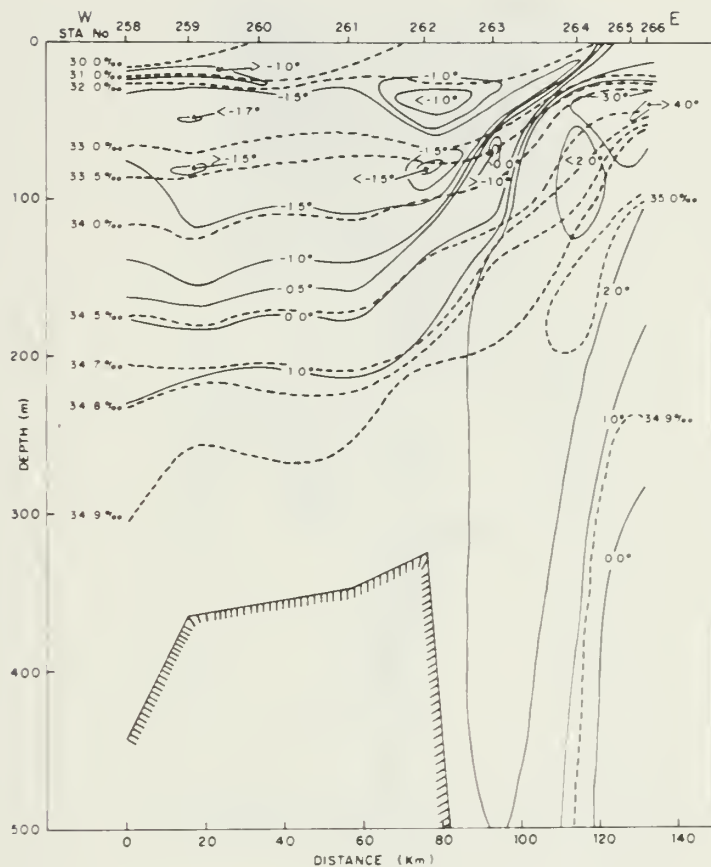


Figure 3.12 Transect 9a at  $76^{\circ}30'N$  at the mouth of Belgica Trough. Compare this transect with Transect 10 (Figure 3.13) made 3 days later. Cold saline water is evident at depths below 300 m at Station 266.

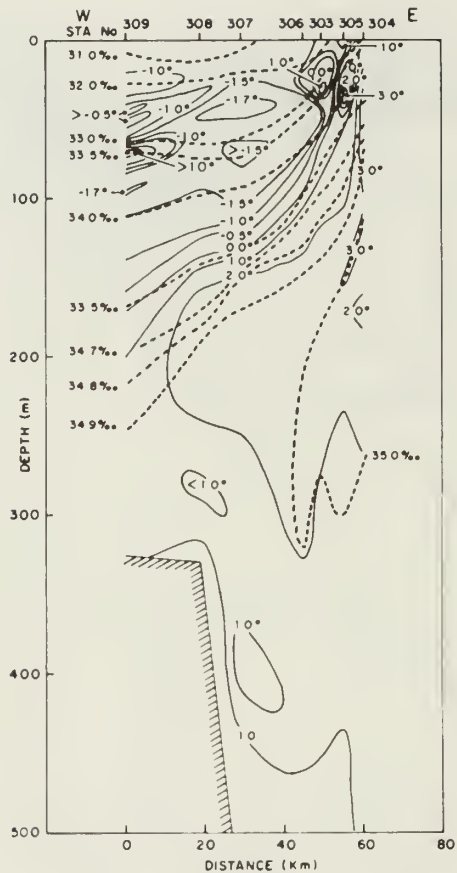


Figure 3.13 Transect 10 at the mouth of Belgica Trough. The shape of the EGPF has changed and the cold deep water noted in Figure 3.12 is not evident here.

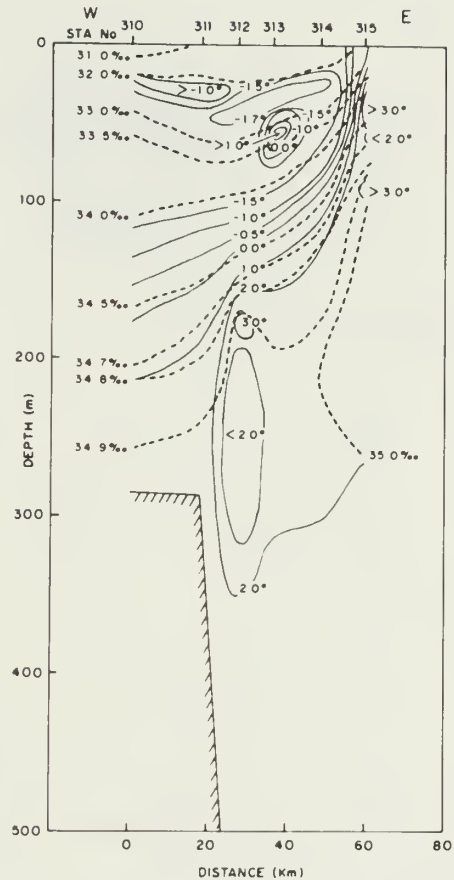


Figure 3.14 Transect 11 at 76°15'N. Some finestructure consisting of AIW in the PW layer is evident.







## C. THE CONTINENTAL SHELF

### 1. Introduction

NORTHWIND completed ten transects of the shelf in the vicinity of Belgica Bank as well as several transverse crossings of Belgica Trough, Norske Trough, and Westwind Trough. Transects were also constructed from stations taken along the axes of these troughs. The location of transects made on the shelf is shown in Fig. 3.1; those made in the troughs are shown in Fig. 3.17.

The waters of the continental shelf consist primarily of PW more or less conditioned by local processes. These include sea ice melting and freezing, surface radiation cooling and insolation, and dilution by continental run-off and the melting of glacial ice, particularly near the northern fjords. The lower boundary of the PW on the shelf remains, for the most part at about 200 m, thinning to about 150 m near the shelf break at 76°N.

This next sub-section will first present a brief description of the oceanographic features of the major areas on the northern shelf, i.e., the above named troughs and bank. Following sub-sections provide an expanded description of shelf water properties using a T/S diagram and horizontal plots of water characteristic distributions.

### 2. Regional Hydrography

#### a. Belgica Bank

Crossings which covered Belgica Bank are included in Transects 2 to 5 in Section B of this chapter (Figs. 3.5 - 3.8). The bank extends eastward from a crest (which at Northwind Shoal becomes as shallow as 15 m) to the shelf break some 180 km further east. PW is the dominant water over the bank occupying the upper 200 to 225 m in the west (where the bottom is deep enough) shoaling to about 150 m at the shelf break.

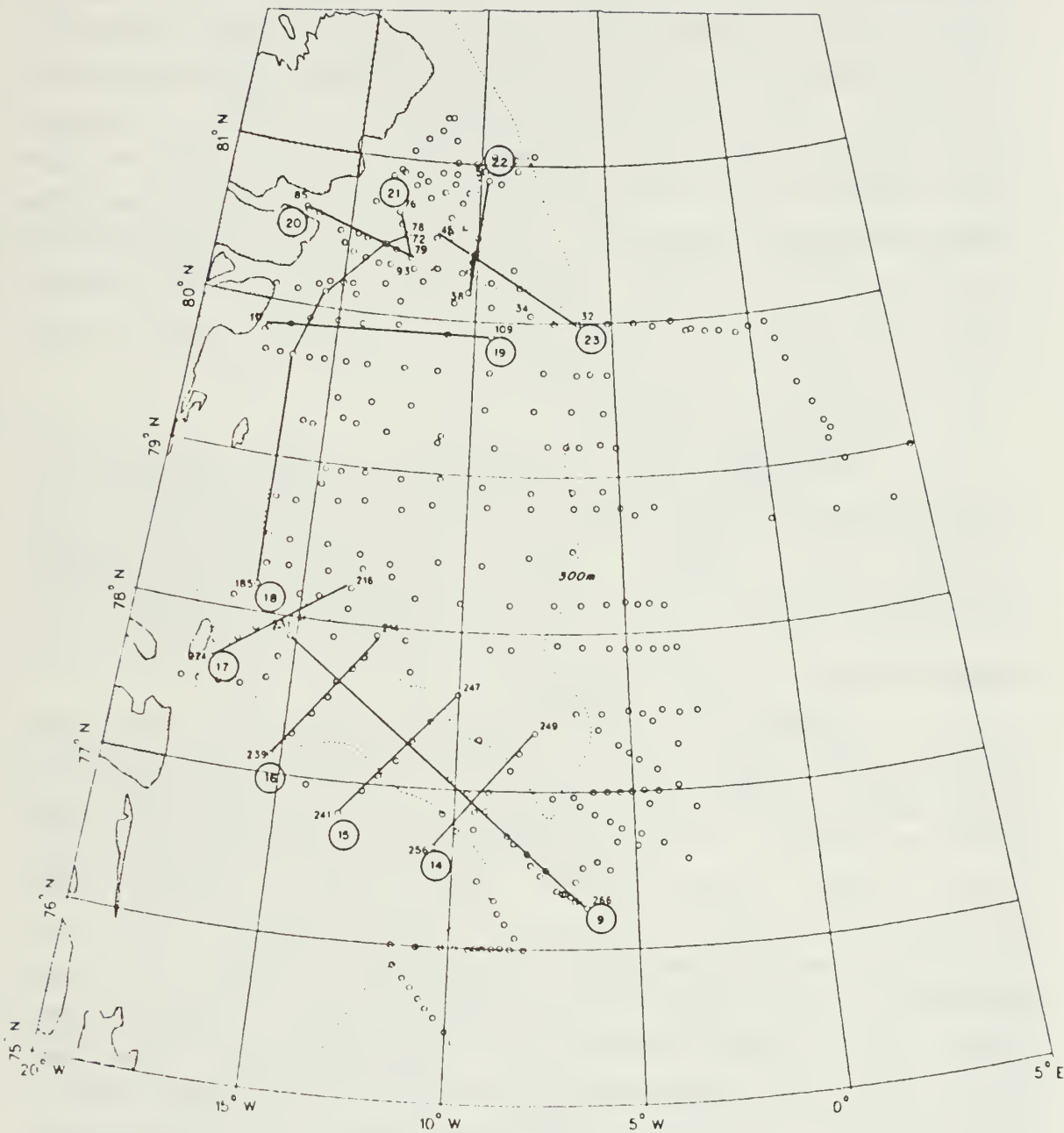


Figure 3.17 A map showing the location of transects conducted over the troughs which cut across the northeast Greenland shelf.

Underlying the PW, in areas where the shelf is deep enough to accommodate it, is the AIW layer. The latter extends as far inland as 50 km west of the shelf break in the north and 100 km farther south. AIW is also found in pockets at the bottom of the trough east of the crest of Belgica Bank. The maximum temperature and salinity of this layer occurs close to the bottom on the bank so that AIW with the highest salinities and temperatures (generally not more than 34.8 and 1°C, respectively) are found over the deepest portions of the bank (see, for example, Figs. 3.34 and 3.35 compared to Fig. 2.2).

#### b. Belgica Trough

NORTHWIND made a series of four transverse crossings of Belgica Trough about 50 km apart (Transects 14 - 17 in Figs. 3.19 - 3.22). However, the development of water properties in this trough can best be seen in an axial transect (Transect 9, Fig. 3.18) constructed from stations occupied over a 3.5 day period.

Generally, temperature and salinity isopleths deepen to the west. This is, to some extent, more noticeable in the water below 100 m and is not inconsistent with what might be expected from a westward movement of AIW from the frontal region up the trough. The PW layer thickens from less than 150 m at the entrance of the trough to 220 m at its western end. Between Station 258 and 259 (Fig. 3.18) the salinity of the lower -1.5°C isotherm changes sharply from almost 34.0 to less than 33.5, suggesting that the cold saline fraction of PW discussed in Section B of this chapter has penetrated 60 km down the trough compared to its relatively minimal invasion onto Belgica Bank (see Transect 3, Fig. 3.6 for a comparative example). Pockets of this cold fraction can also be seen farther into the trough at Stations 245 and 231. Another feature of the PW layer is a



lens of water warmer than  $-1.0^{\circ}\text{C}$  centered at 25 m imbedded in cooler water and which extends throughout much of the length and breadth of the trough (see Figs. 3.18 and 3.21). This lens might be a remnant of summer warming and freshening by ice melt with the waters above being cooled somewhat due to the onset of fall or cooling by the passage of a melting ice floe. However, with the exception of Westwind Trough, this feature was observed nowhere else to such a degree on the shelf.

About half way along the trough, the PW at 65 m cools to  $-1.7^{\circ}\text{C}$  in a 15 m thick band generally centered over the deepest areas. Within this band, the temperature decreased to  $-1.81^{\circ}\text{C}$  at Station 257 (located 24 km south of Station 258 in Fig. 3.18), the coldest water encountered anywhere during this cruise. Further comments on the distribution and nature of this band of water are made in Section C of this chapter in conjunction with Fig. 3.30.

About half of the water mass in the trough consists of AIW which becomes cooler and less saline towards the northwest. Water with temperatures greater than  $1^{\circ}\text{C}$  and salinities exceeding 34.9 lie close to the bottom along almost the entire length of the trough.

#### c. Norske Trough

At its western end, Belgica Trough merges with Norske Trough which parallels the coast northward. Complete transverse sections of much of Norske Trough could not be completed due to the presence of fast ice which covered its western boundary. A partial crossing of the southern portion of the trough can be seen in the western part of Transect 4 (Fig. 3.7) and a complete crossing of the northern part in Transect 19 (Fig. 3.24). A non-synoptic axial transect (Transect 18, Fig. 3.23) presents some idea of the character of the water in this deep coastal depression.

The PW layer extends to 200 m at the southern extremity of Norske Trough becoming somewhat thinner (175 m) at its northern end. A temperature minimum is also present in this trough with values less than  $-1.7^{\circ}\text{C}$  centered at about 75 m in the south. This water has similar salinity characteristics to the temperature minimum described earlier in Belgica Trough - about 32.3 to 32.5 (see, for example Fig. 3.29). In the northern end of Norske Trough the  $-1.7^{\circ}\text{C}$  layer band is found at about 60 m. It is comprised of somewhat less saline water, lying almost exclusively between the 32.1 and 32.3 isohalines, and is thicker than the  $-1.7^{\circ}\text{C}$  band at the southern end. At Station 120 in Fig. 3.23 the two layers of cold water can be seen to overlap.

The AIW layer decreases in salinity and temperature towards the north. The maximum temperature and salinity in the water column is found near the bottom. With the exception of the extreme southern end, it is cooler than  $1^{\circ}\text{C}$  and fresher than 34.9.

#### d. Westwind Trough

At  $80^{\circ}30'\text{N}$  Norske Trough connects with Westwind Trough, an apparent extension of Ingolf's Fjord. As seen in the axial transect of Westwind Trough (Transect 23, Fig. 3.28), the 180 m thick PW layer has the same characteristics as in the northern portion of Norske Trough with the exception that the near-surface "warm" layer, described in connection with the Belgica Trough PW, is also present here. The  $-1.7^{\circ}\text{C}$  layer is defined by the 32.1 and 32.3 isohalines similar to that in the northern portion of Norske Trough.

The AIW layer is relatively cool and fresh compared to its properties in Belgica Trough. Compare, for example, Transect 23, Fig. 3.28 with Transect 9, Fig. 3.18 or the reflection of the properties of the AIW at the bottom as presented in Figs. 3.34 and 3.35. Maximum temperatures

are about  $0.5^{\circ}\text{C}$  and salinities are about 34.8. Given that the 34.8 isohalines in Westwind Trough and Belgica Trough are generally at the same depth (about 240 m), the difference in bottom characteristics is probably, in part, a reflection of the greater depth of Belgica Trough. However, as Fig. 3.4 shows, stations immediately seaward of Westwind Trough (e.g., 31, 32) did not show any salinities in excess of 34.9, even at depths in excess of 800 m. The somewhat cooler and more dilute AIW in Westwind Trough compared to that found at the bottom of Belgica Trough may also, therefore, be a reflection of the fact that the RAC, which is probably the source of warm ( $>1^{\circ}\text{C}$ ), saline water in both troughs, is located some 100 km farther seaward of the entrance to Westwind Trough than it is at the entrance to Belgica Trough.



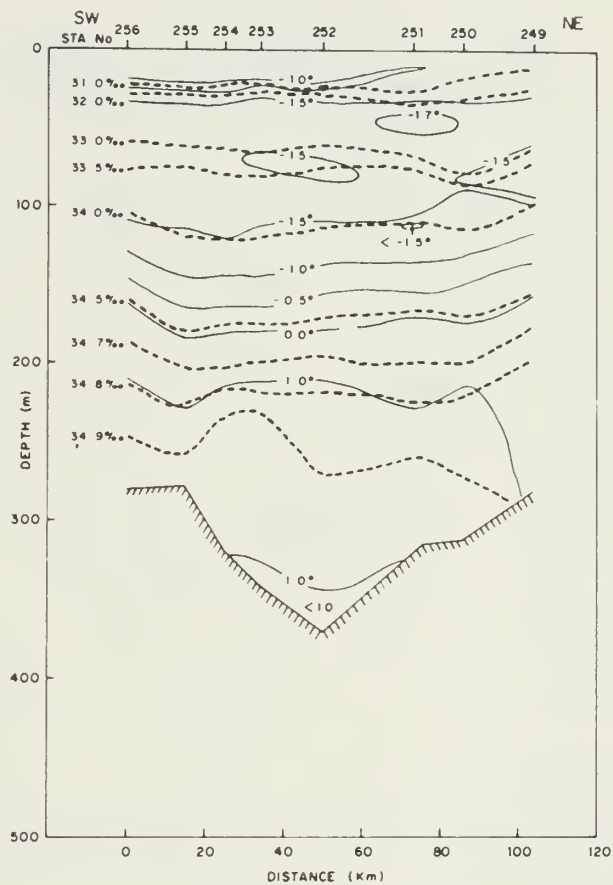


Figure 3.19 Transect 14 across Belgica Trough. This transect is located about 65 km west of the entrance to Belgica Trough.



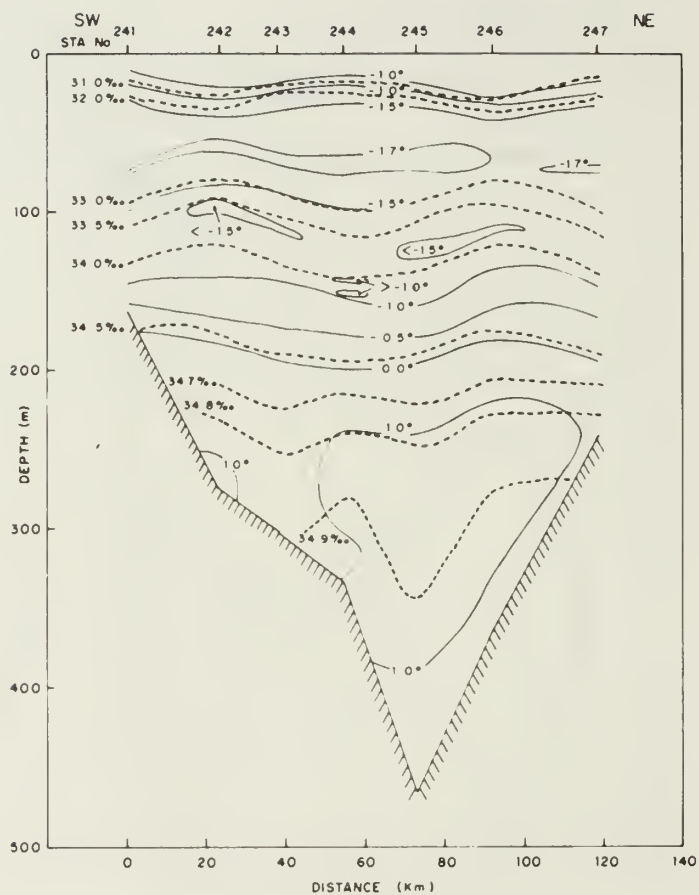


Figure 3.20 Transect 15 across Belgica Trough. This transect is located about 125 km west of the entrance to Belgica Trough.

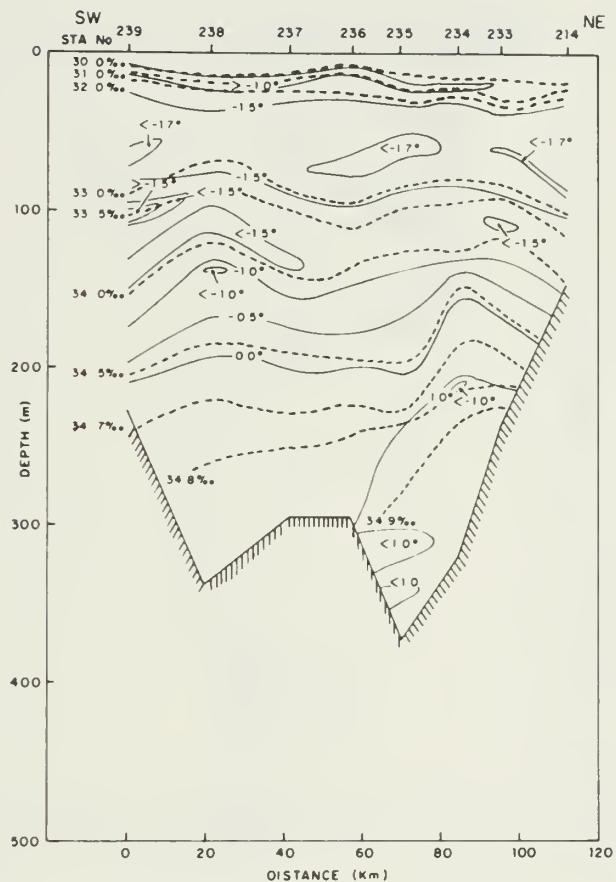


Figure 3.21 Transect 16 across Belgica Trough. This transect is located about 190 km west of the entrance to Belgica Trough.

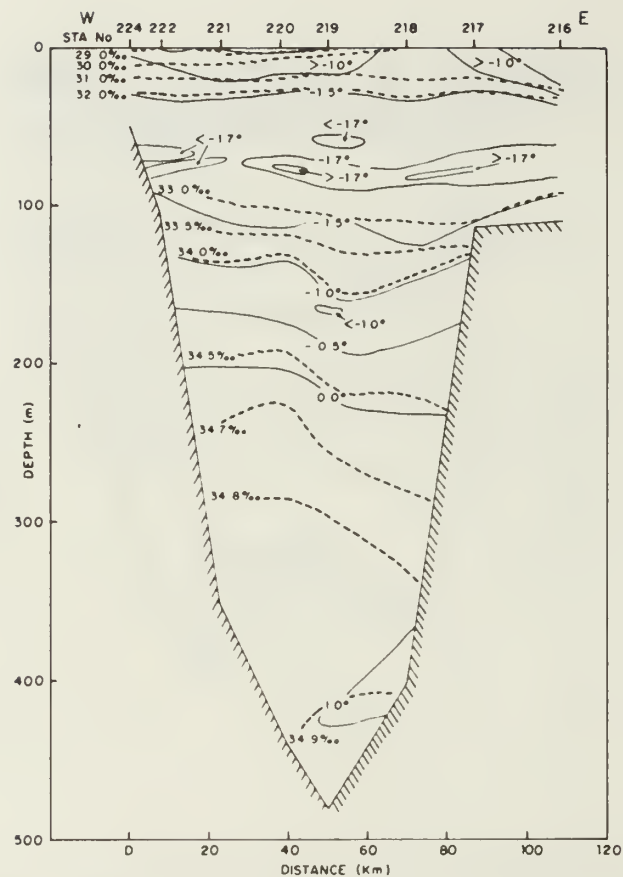


Figure 3.22 Transect 17 across Belgica Trough. This transect is located about 250 km west of the entrance to Belgica Trough.

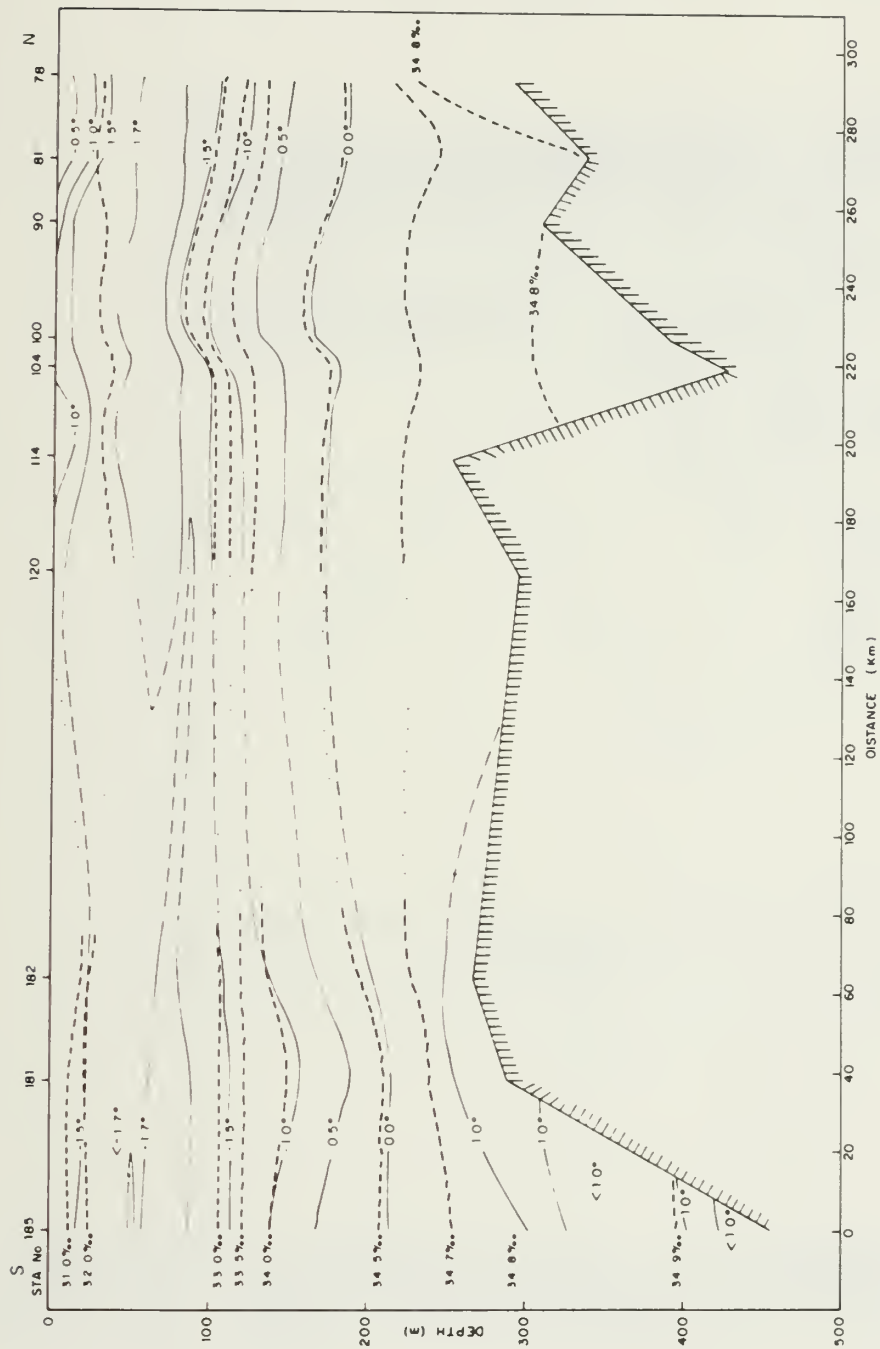


Figure 3.23 Transect 18 along the axis of Norske Trough. Two layers of  $< -1.7^\circ\text{C}$  water of different salinities are superposed at station 120.

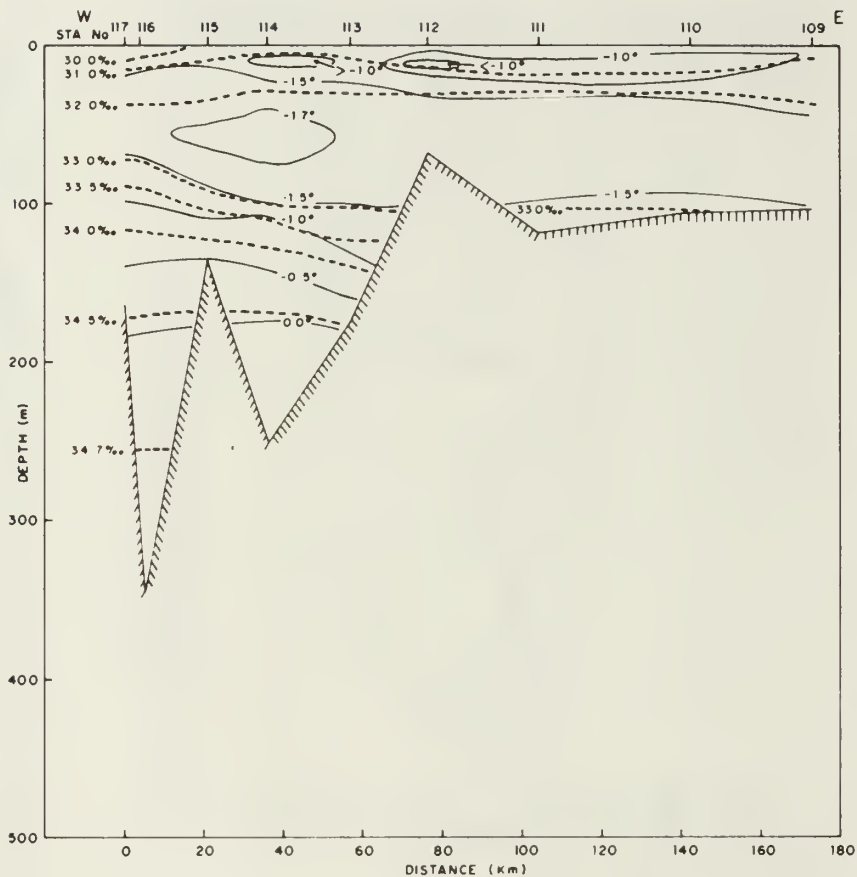


Figure 3.24 Transect 19 across the northern end of Norske Trough.

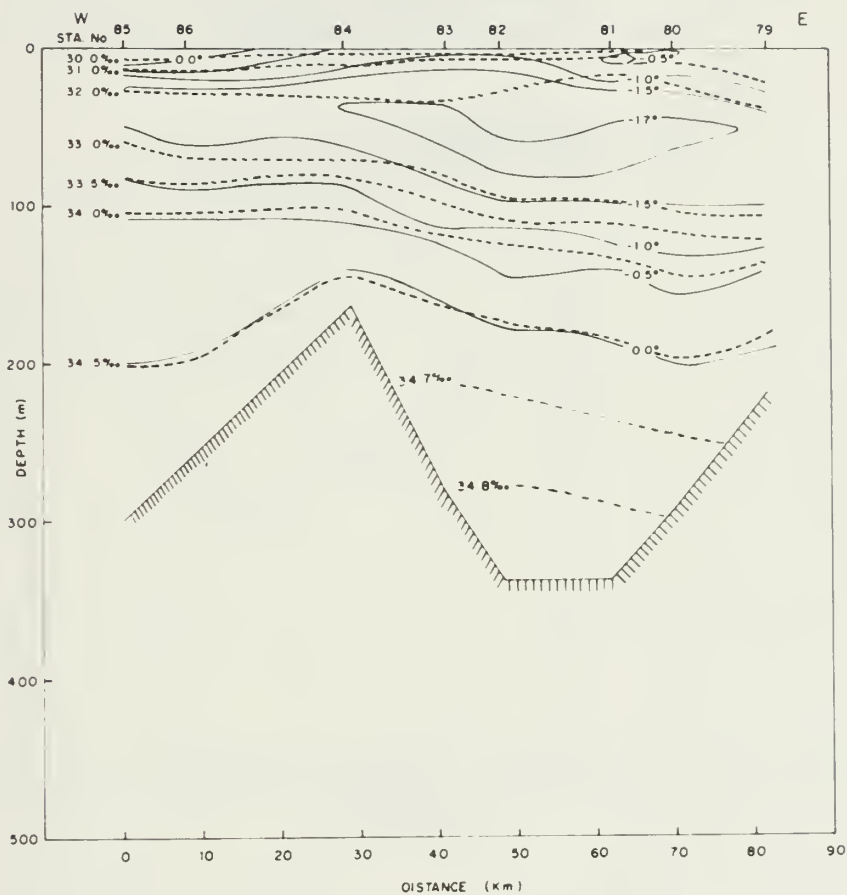


Figure 3.25 Transect 20 extending eastward from Ingolf's Fjord to Westwind Trough.



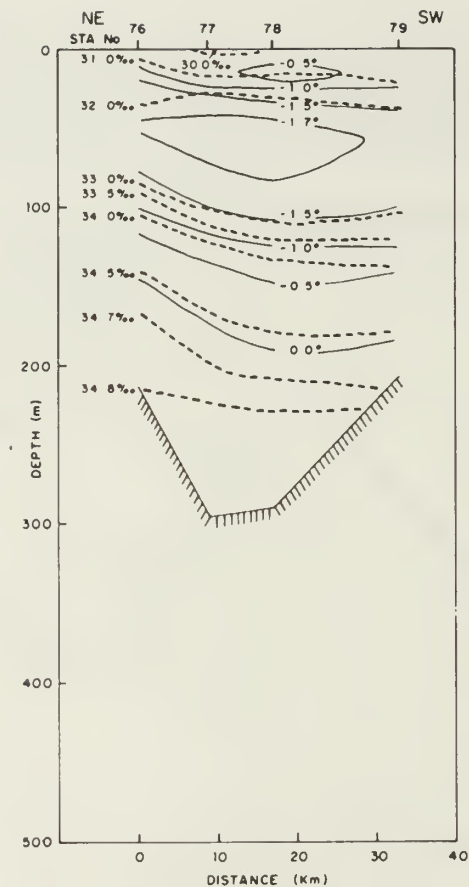


Figure 3.26 Transect 21 across Westwind Trough. This transect is located 150 km west of the entrance to Westwind Trough. In the northern portion of the shelf, the  $-1.7^{\circ}\text{C}$  water was confined to the troughs.

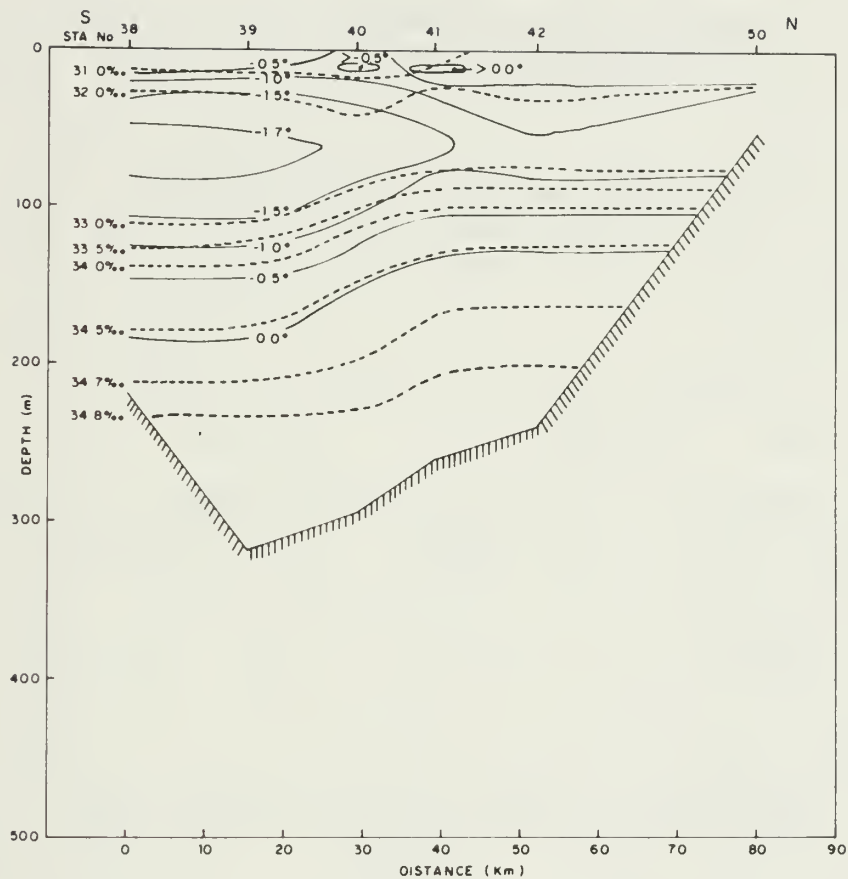


Figure 3.27 Transect 22 across Westwind Trough. This transect, located 95 km west of the entrance to Westwind Trough, does not completely cross the trough.

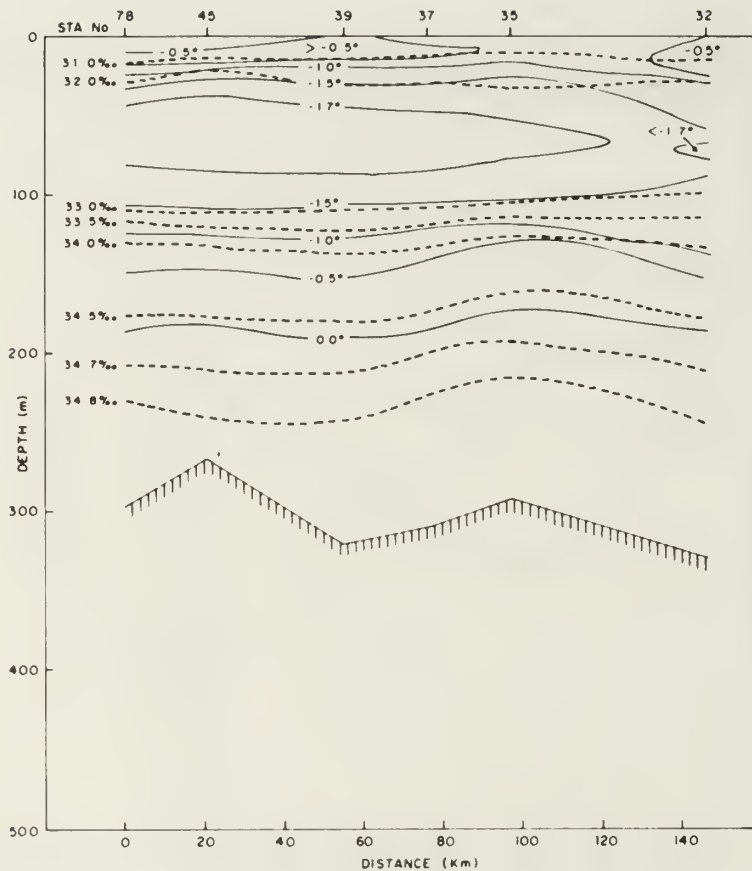


Figure 3.28 Transect 23 along the axis of Westwind Trough. The  $-1.7^{\circ}\text{C}$  water at Station 32 is slightly more saline than that farther east. Surface waters here are warmer than at more southerly locations on the shelf.

### 3. Shelf Water Masses

A comparative look at the relationship of water properties on the shelf is presented in the T/S plot shown in Fig. 3.29. Two stations (24 and 307) located east of the shelf and just west of the EGPF are also included for comparison. The figure includes Station 245 from the middle of Belgica Trough, Station 184 at the southern end of Norske Trough, Station 182 in the middle of Norske Trough, Station 120 at the northern end of Norske Trough and Station 37 in Westwind Trough. (Transects containing these stations may be found in Figs. 3.18, 3.23, and 3.28). Station 137, a typical shelf station taken over the middle of Belgica Bank is also included.

This temperature-salinity plot presents a consistent picture of the evolution of water properties in meridional and zonal directions. In general, cold low-salinity water is present everywhere with a temperature minimum located at about 75 m. A cold high-salinity (34.0) fraction is present only at the EGPF with the exception of Station 245. As noted previously, and in Fig.3.18, water of this character extends westward into much of Belgica Trough. All stations at which the depth is sufficient show some admixture of AIW/AW as indicated by a rise toward the T-S peak. This peak is best developed in the front itself and decreases in maximum temperature toward the south. Such a maximum is not reached in shallower stations. The near-surface temperature maximum is scattered but is generally associated with relatively warm water, both above and below.

#### a. Polar Water

An interesting feature of the shelf PW is that despite the greater source of heat inherent in the relatively large volume of AIW in the trough areas as compared to the shallow bank waters, the coldest temperature water

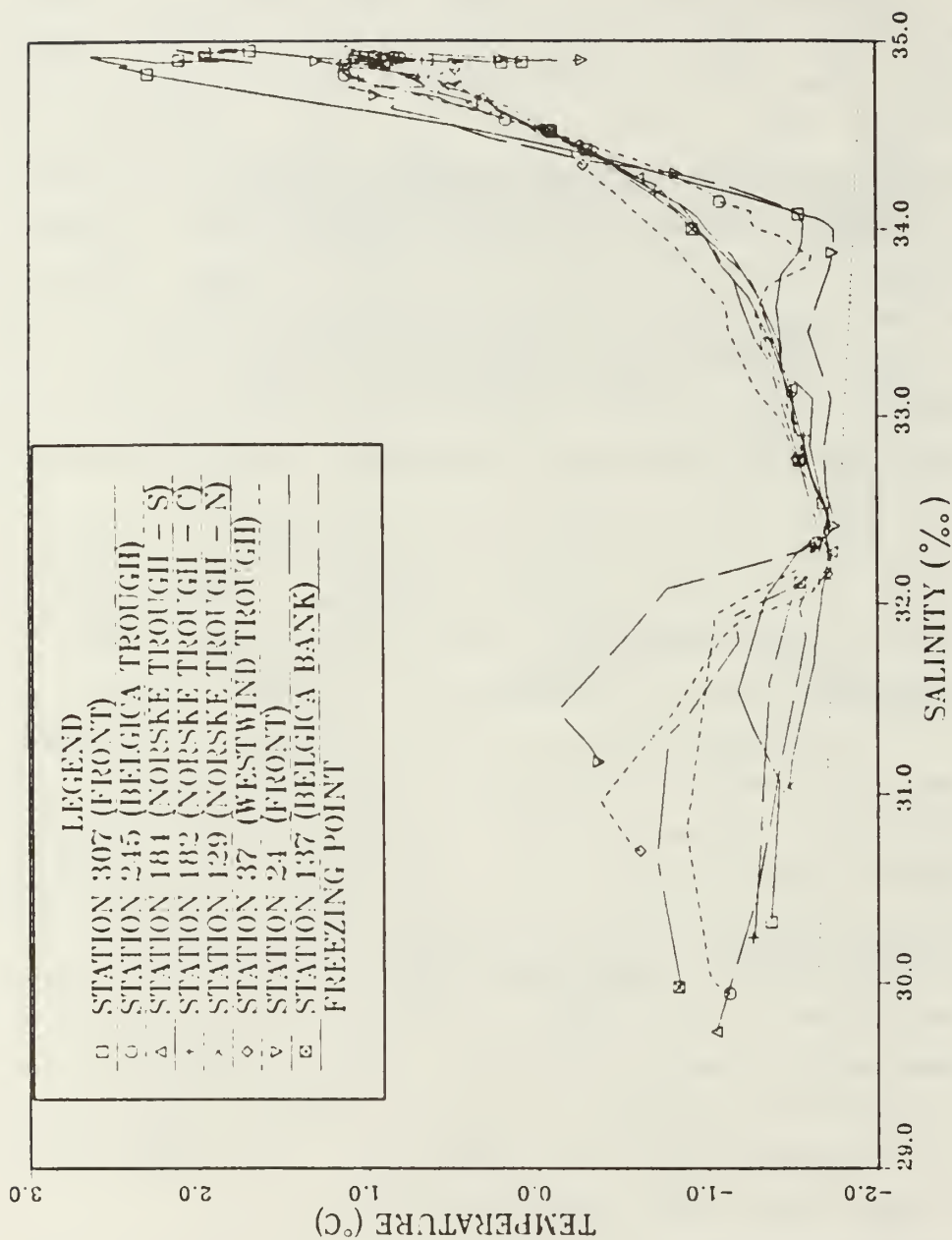


Figure 3.29 A temperature-salinity plot of typical shelf stations. Stations in the legend are listed in counterclockwise order from the mouth of Belgica Trough, through Norske Trough, and westward out Westwind Trough. Stations 307 and 24 are in the EGPF. Station 137 is on Belgica Bank. Symbols are 50 m apart.

west of the shelf break is almost exclusively found in the troughs. This is evident in a number of the transects presented previously for the shelf (see for example, Figs. 3.20, 3.24 and 3.26) where water colder than  $-1.7^{\circ}\text{C}$  is found only over the trough areas. Generally, this cold water layer does not seem to have advected onto the adjacent banks in the north, despite the fact that this layer is located shallower than the bottom of the bank. This feature is most evident in Fig. 3.30 where the thickness of the  $<-1.7^{\circ}\text{C}$  layer has been contoured in 15 m intervals. The  $-1.7^{\circ}\text{C}$  water is particularly clearly associated with deeper water in the northern portion of Norske Trough and in Westwind Trough where, as previously noted, it is bounded almost precisely by the 32.1 and 32.3 isohalines. Farther south, over Belgica Trough and the surrounding bank waters, the cold layer is somewhat more saline (32.3 - 32.5) while to the east, in the frontal region, the  $-1.7^{\circ}\text{C}$  water had variable salinities from 32.3 to 32.9. At the front near  $80^{\circ}\text{N}$ , the more saline water discussed earlier achieved temperatures lower than  $-1.7^{\circ}\text{C}$  and is contoured in Fig. 3.30 as an underlying layer.

The basic structure of the PW has been described and accounted for by other authors. For example, Aagaard and Coachman (1968b, p. 277) describe the temperature minimum found in the summer PW layer at 50 m as a result of the warming and freshening of the surface layer above by insolation and ice melt and present an example of it from the 1965 EDISTO results. Newton and Piper (1981, p. 22), in discussing the WESTWIND 1979 results, noted that except for warming at the top by insolation and the bottom by the AIW layer, respectively, the PW consisted of a cold water mass of fairly uniform salinity. They noted a relatively large amount of water concentrated in a salinity range of 33.2 to 33.4 at the temperature minimum, a considerably greater





Figure 3.30 A plot contouring the thickness of the  $-1.7^{\circ}\text{C}$  layer in 15 m intervals. Over the shelf, water of this temperature is generally confined to the deeper areas, particularly in the north. Salinity ranges are shown by the contour line pattern as indicated.

value than the 32.1 - 32.5 noted for the  $<-1.7^{\circ}\text{C}$  water on the shelf observed in 1984. This appears to be a result of the greater freezing stress experienced in 1979 or perhaps to the presence of warmer, more dilute waters during the 1983/84 freezing cycle and reflected in the lower degree of ice coverage during the summer of 1984.

The surface properties of the shelf and frontal waters may also serve as useful indicators of local processes and advection. In general, the distribution of various water properties on and adjacent to the shelf appears to be primarily affected by proximity to the coast and the EGPF, bathymetry, circulation and, in the case of surface properties, reflects the ice concentration. For example, a plot of surface temperatures (Fig. 3.31) and a plot of the surface temperature as a function of the freezing point (Fig. 3.32) both clearly show the location of the EGPF. Isotherms are particularly densely packed near the mouth of Belgica Trough, a region where the gradient of ice concentration (Fig. 2.3) is also particularly steep. Surface temperatures in the northern portion of the shelf are slightly warmer than they are in the region near Belgica Trough, consistent with the lower ice concentrations in the north.

The surface salinity distribution (Fig. 3.33) shows the effect of coastal fresh water input and reflects some bathymetric features. For example, the surface water overlying Belgica Trough, Westwind Trough and possibly most of Norske Trough is, at  $<30.0$ , fresher than the surface water overlying the adjacent banks to the east. The shape of the 30.0 isohaline over Westwind Trough is suggestive of an eastward advection of low salinity water there. A local surface salinity high overlies the shallowest portion of Belgica Bank while a region of low salinity overlies the central portion of the bank. Isohalines are packed

relatively closely at the shelf break, reflecting the position of the EGPF.

A comparison of the above plots of surface properties with those developed from the WESTWIND 1979 cruise, shows some interesting similarities and differences. The plot of surface temperatures referenced to the freezing point (Newton, in preparation) from the 1979 data, also shows warmer surface temperatures over the northern shelf compared to the southern portion. Overall surface temperature values were lower than those in Fig. 3.32, while surface salinity values were about 1 ppt higher - reflecting the lighter ice concentrations in 1984. However, the isopleths of surface temperatures and salinities for the 1979 data which parallel the EGPF show a significant westward turning at about 77°N, just north of the entrance to Belgica Trough. This feature is not evident in Figs. 3.32 or 3.33 and may reflect a fluctuation in circulation in this region.

#### b. AIW

As pointed out with reference to the shelf temperature-salinity transects presented earlier, AIW is found in all trough areas and over the deeper parts of the shelf. The distribution of bottom temperatures (as deviations from freezing) and salinities are shown in Figs. 3.34 and 3.35. Values were available only for the shelf areas (since no CTD casts were made to the bottom east of the shelf break) and generally reflect near maximum temperatures and salinities for the AIW on the shelf. The warmest and most saline waters on the shelf are found along the axis of Belgica Trough, the southern part of Norske Trough and, to a lesser extent, along the axis of Westwind Trough. Where bottom topographic features extend up into the PW layer, both salinities and temperatures decrease, particularly over

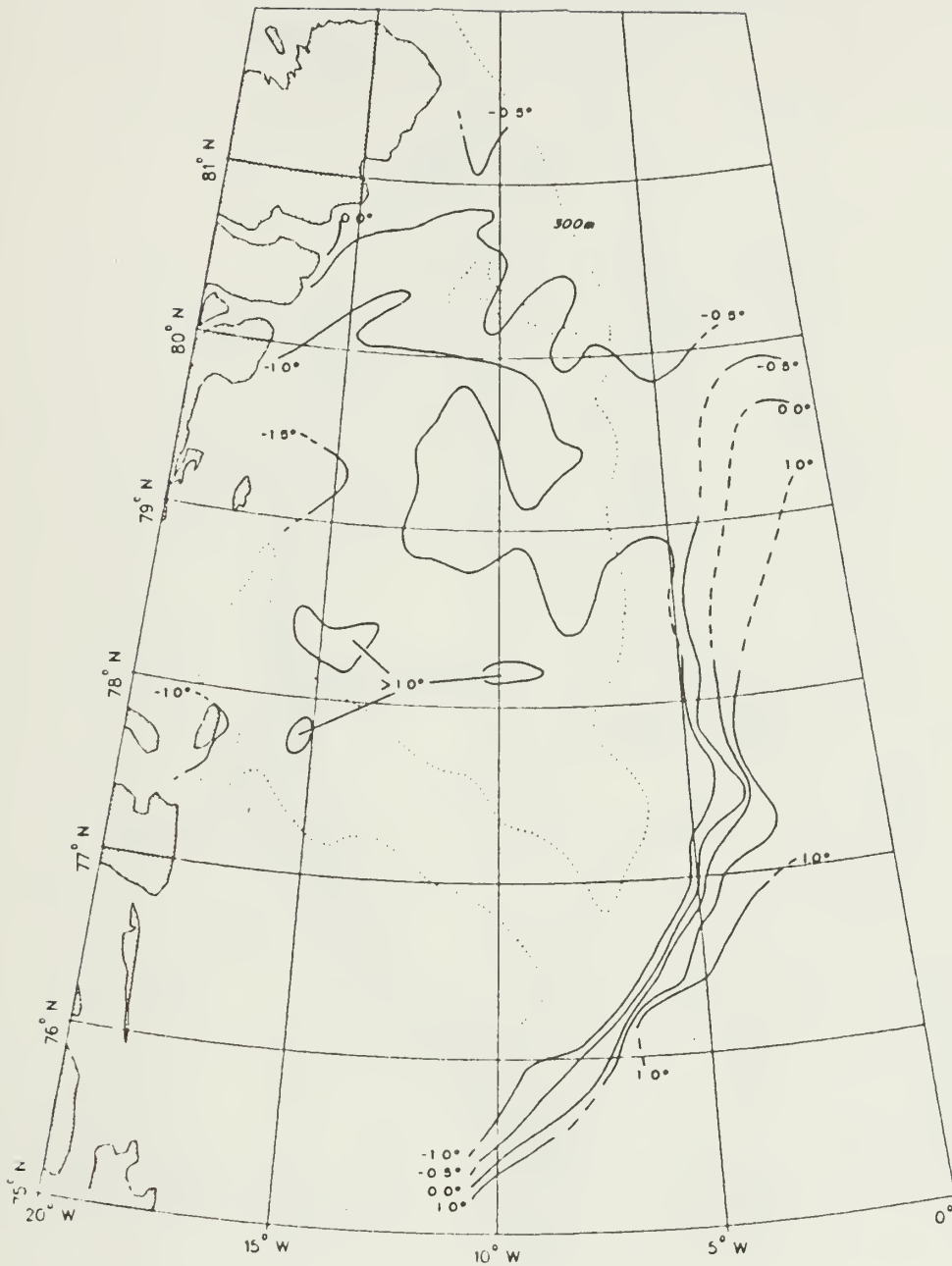


Figure 3.31 Temperature of the surface layer. Isotherms clearly show the position of the EGPF. Warmest temperatures over the shelf are near Ob' Bank.

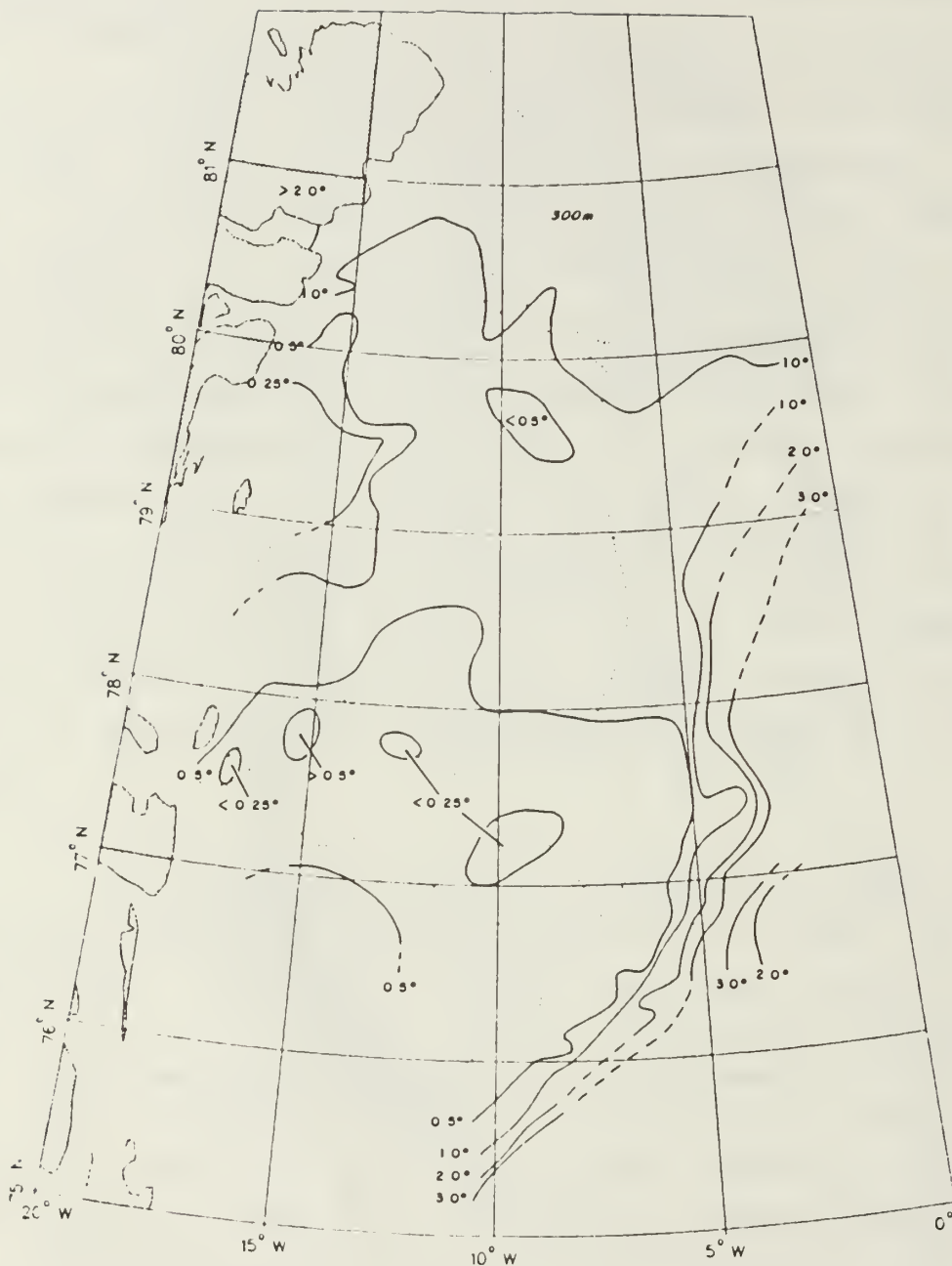


Figure 3.34 Temperature deviation from freezing at the bottom. Values reflect bathymetry and suggest that the warm water in Belgica Trough, Norske Trough, and Westwind Trough probably advected from the east.

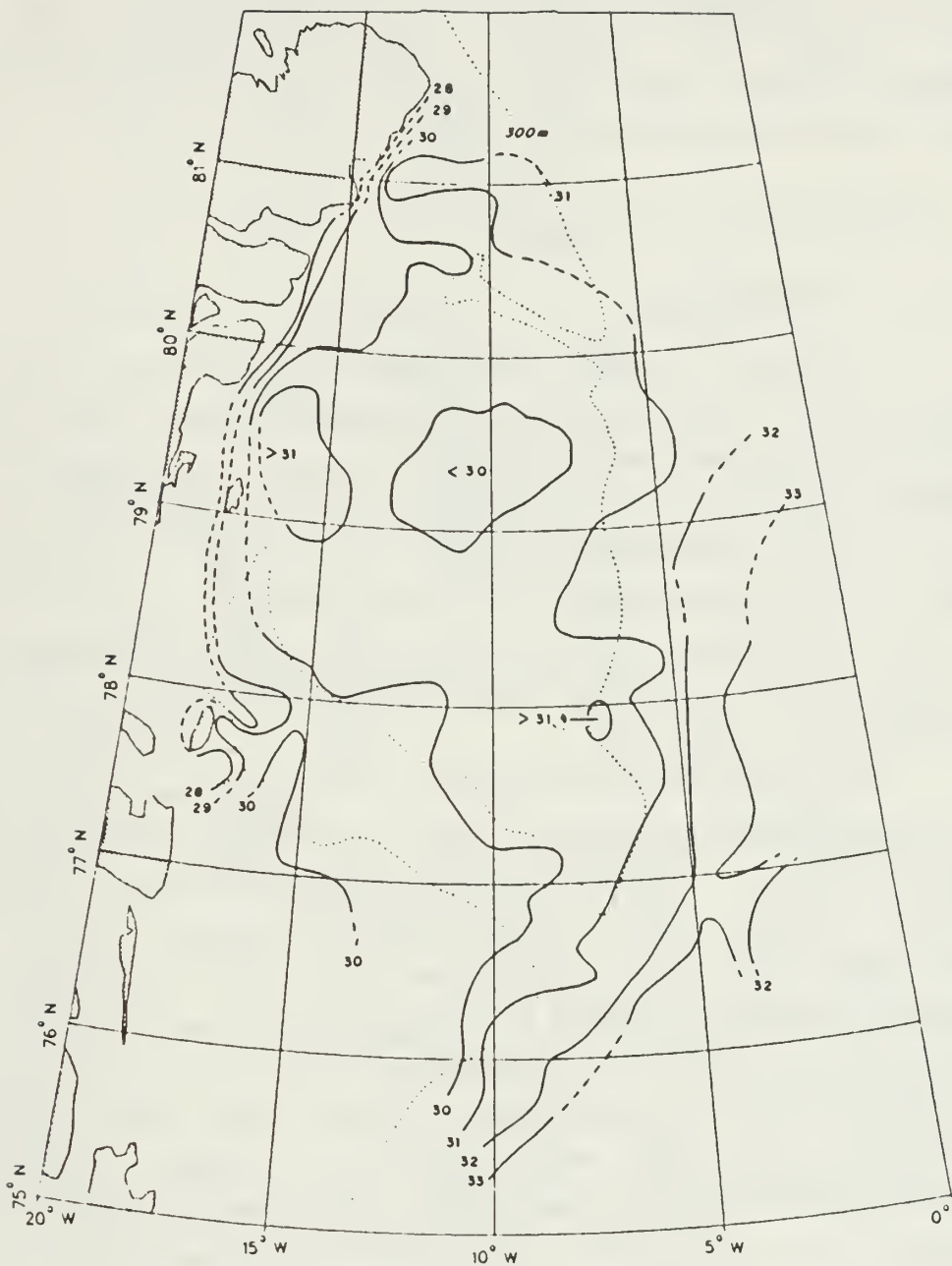


Figure 3.33 Salinity of the surface layer. Salinities over the central shelf are low. The configuration of the 30.0 isohaline over Westwind Trough suggests a westward flow.



the crest of Belgica Bank. The distribution of bottom water properties suggests that AIW is intruding under the PW up the troughs from the east, both at Westwind Trough and Belgica Trough since there is no apparent source of such warm saline water on the shelf.

## D. CIRCULATION AND TRANSPORT

### 1. Introduction

Without reliable long-term current meter data, it is difficult to make definitive statements about the absolute movement of water, particularly over such a relatively wide, shallow-water regime with rapidly varying bathymetry such as exists on the northeast Greenland shelf. It is difficult to make a good approximation of the barotropic component of the current and indeed, frictional and boundary influences may be significant, raising the question as to how geostrophic the current in fact is.

The question of validity of dynamic heights obtained by extrapolation in shallow water was considered by Reid and Mantyla (1976). These authors extrapolated the slopes of dynamic heights into shallow water regions rather than projecting them horizontally as has been done here. In comparing dynamic heights for coastal stations in relatively shallow water with tide gauges and current measurements in the North Pacific periphery, they found good agreement between the tide gage measurements and dynamic heights and between geostrophic currents and current measurements. This appeared to be valid for time scales long enough for quasi-geostrophic equilibrium to be achieved. In the area of their study, this period was on the order of several days to several weeks. For this reason, considerable reality is expected from the baroclinic geostrophic currents computed in the present work. Therefore, in the following sections,

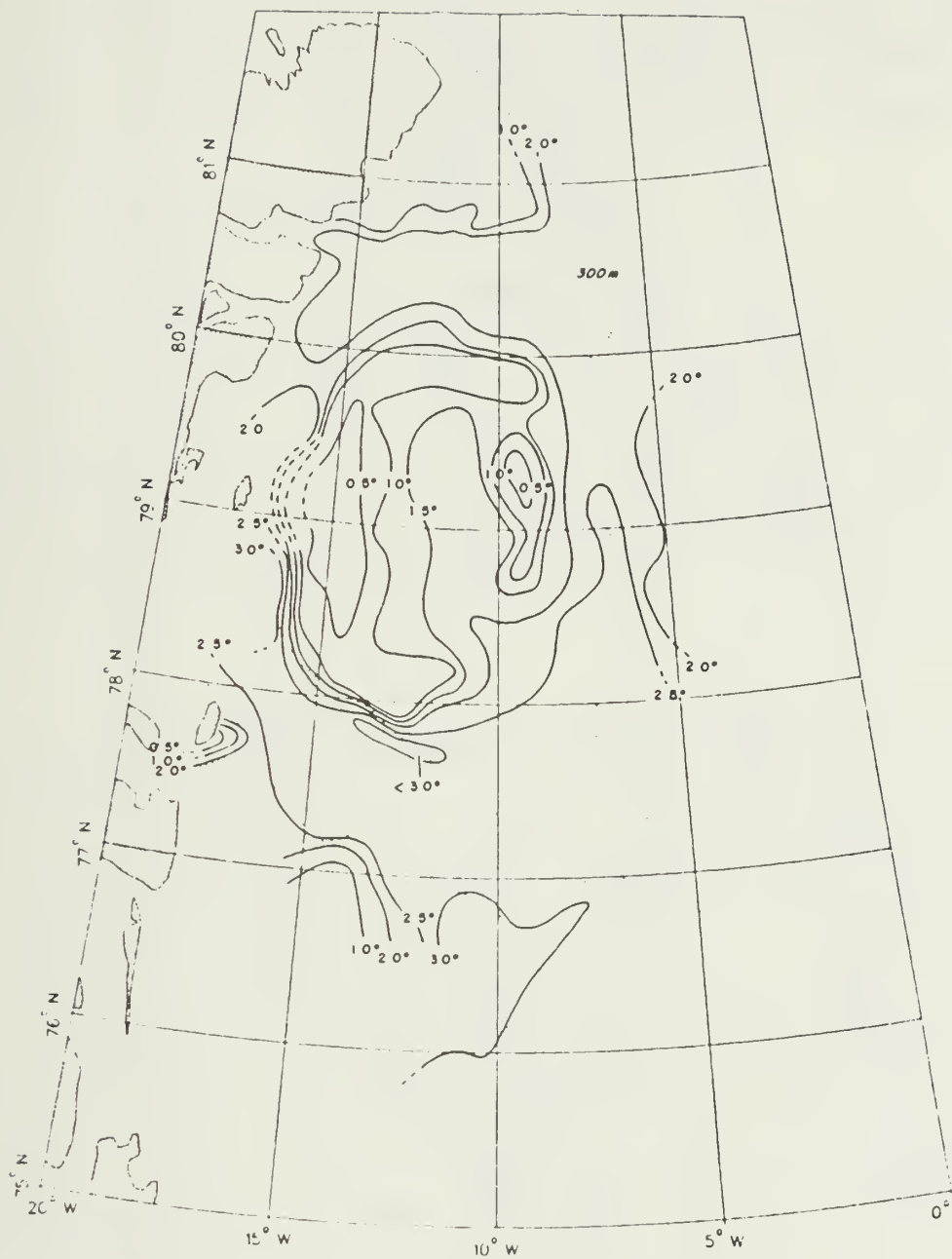


Figure 3.32 Temperature departures from the freezing point in the surface layer. Minimum values are found over the southern shelf where the ice concentration is high.

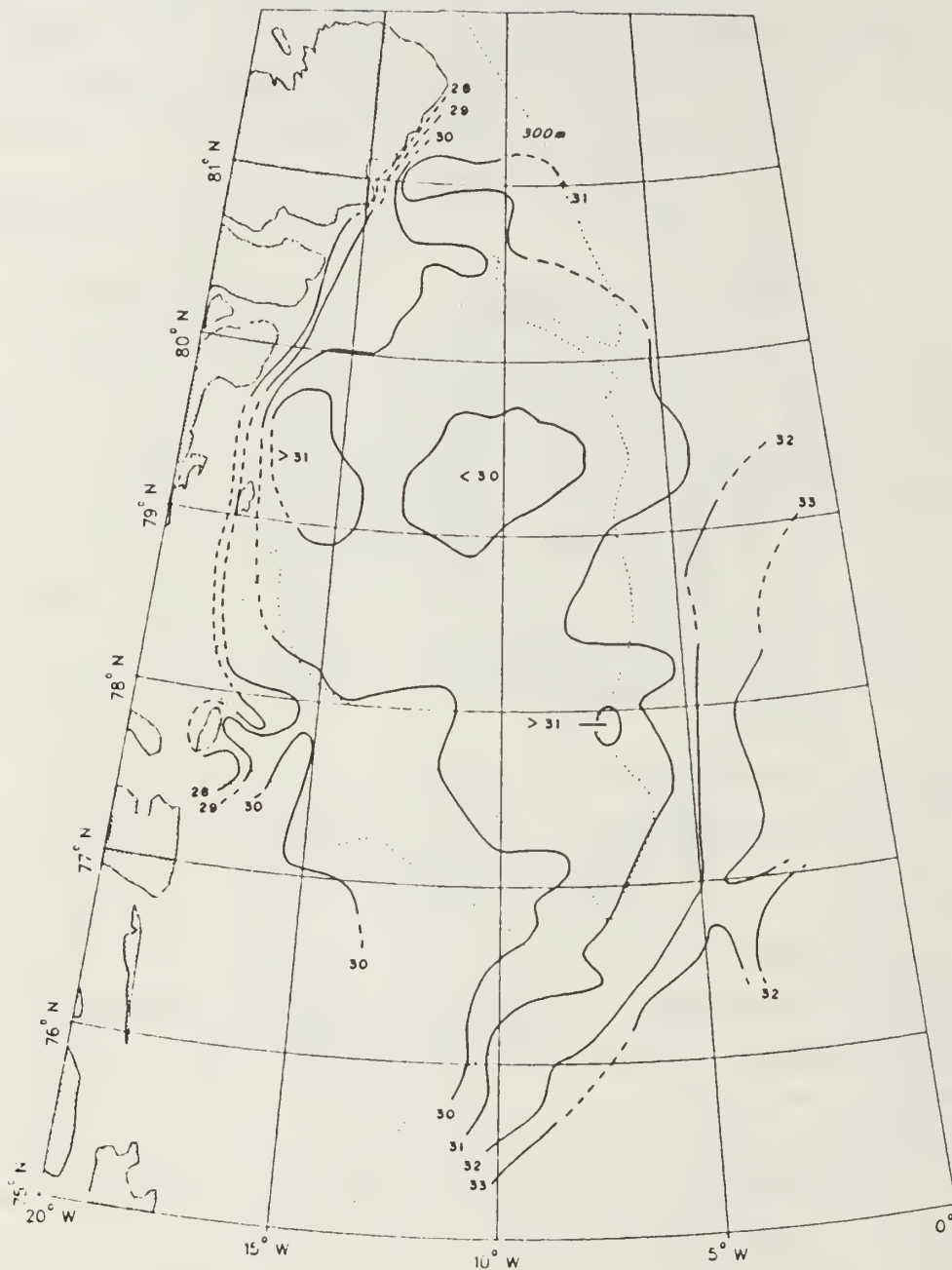


Figure 3.35 Bottom salinity. High salinity water at the bottom of the troughs has probably advected from the east.

the circulation of the EGC in the region of the EGPF and over the shelf will be estimated, using the dynamic topography, vertical baroclinic velocity cross-sections and the distribution of water properties as a guide.

## 2. Dynamic Topography

Surface dynamic heights were computed using the methods outlined in Chapter 2 with reference to the 150 dbar (Fig. 3.36), 200 dbar (Fig. 3.37), and the 500 dbar (Fig. 3.38) levels to assess the contribution that different levels of assumed no net motion would make to the dynamic height fields and to facilitate comparison with similar profiles produced by previous authors. A plot of the 150 dbar surface relative to 500 dbar was also constructed (Fig. 3.39).

The surface dynamic height topographies show a number of features in common. The obvious one is the high gradient region representing the EGPF. In all three surface plots, the maximum value of the gradient across the front remains relatively constant between  $81^{\circ}\text{N}$  to  $77^{\circ}30'\text{N}$ , suggesting baroclinic surface flows of 0.35 to 0.50 m/s. A westward turning of the isobars occurs at  $77^{\circ}15'\text{N}$ , north of the entrance to Belgica Trough, followed by a southward turn indicative of southwesterly surface flow over the trough itself. This is well developed in Figs. 3.36 and 3.37 but is less evident in Fig. 3.38. At this point, the frontal dynamic height gradient decreases to that which would support a 0.25 m/s baroclinic flow.

In the region of the front, changing the level of no net motion from 150 dbar or 200 dbar to 500 dbar made little difference to the spacing of the isobars (compare Figs. 3.36, 3.37 and 3.38) and thus, implicitly, in the baroclinic current flow. This suggests that little contribution to the pressure gradient is made by the AIW found below 150 m, at least in summer.

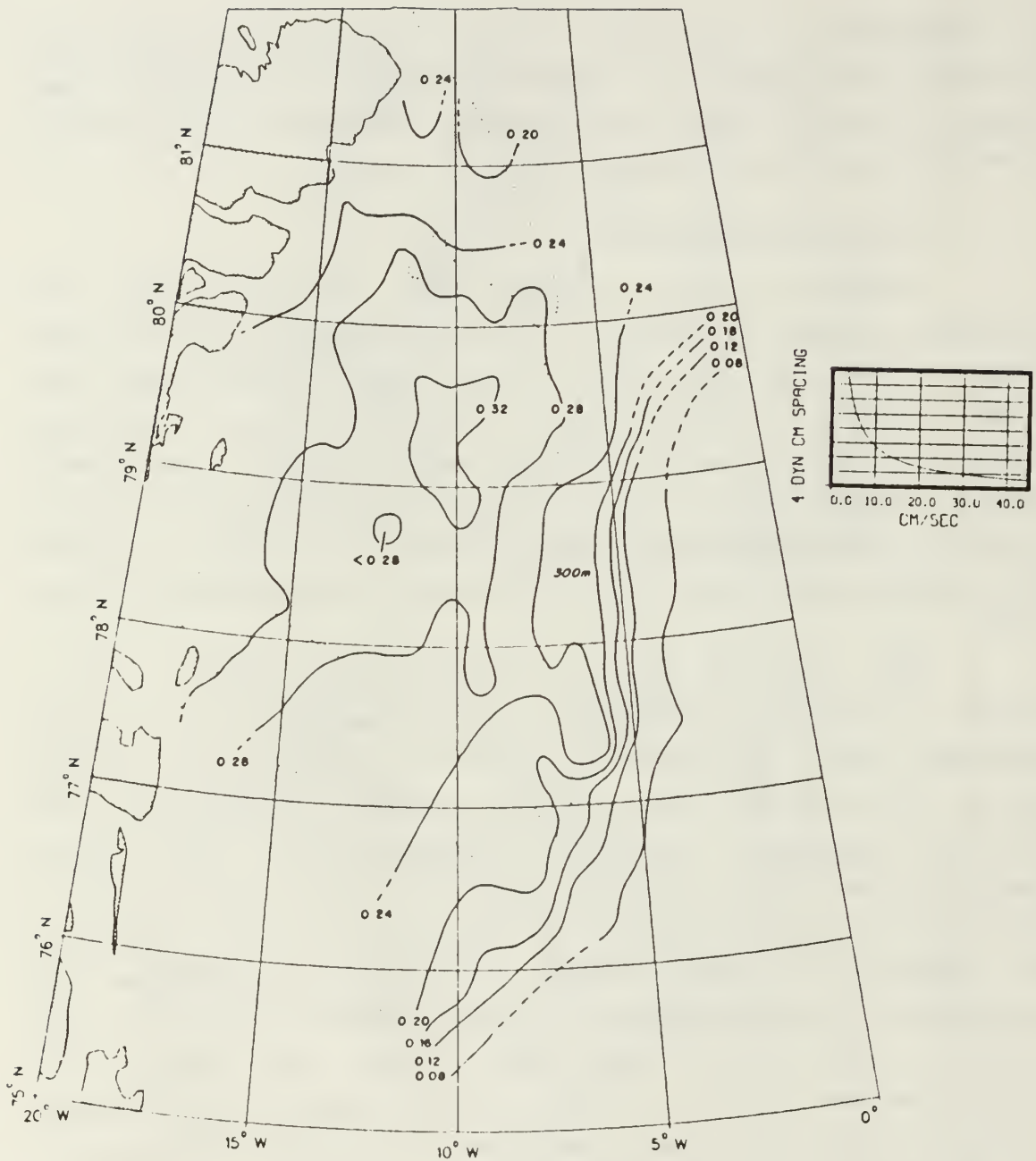


Figure 3.36 Surface dynamic topography referenced to 150 dbar in dynamic meters. A dynamic "hill" over the center of the shelf suggests anticyclonic circulation.



Figure 3.37 Surface dynamic topography referenced to 200 dbar in dynamic meters.



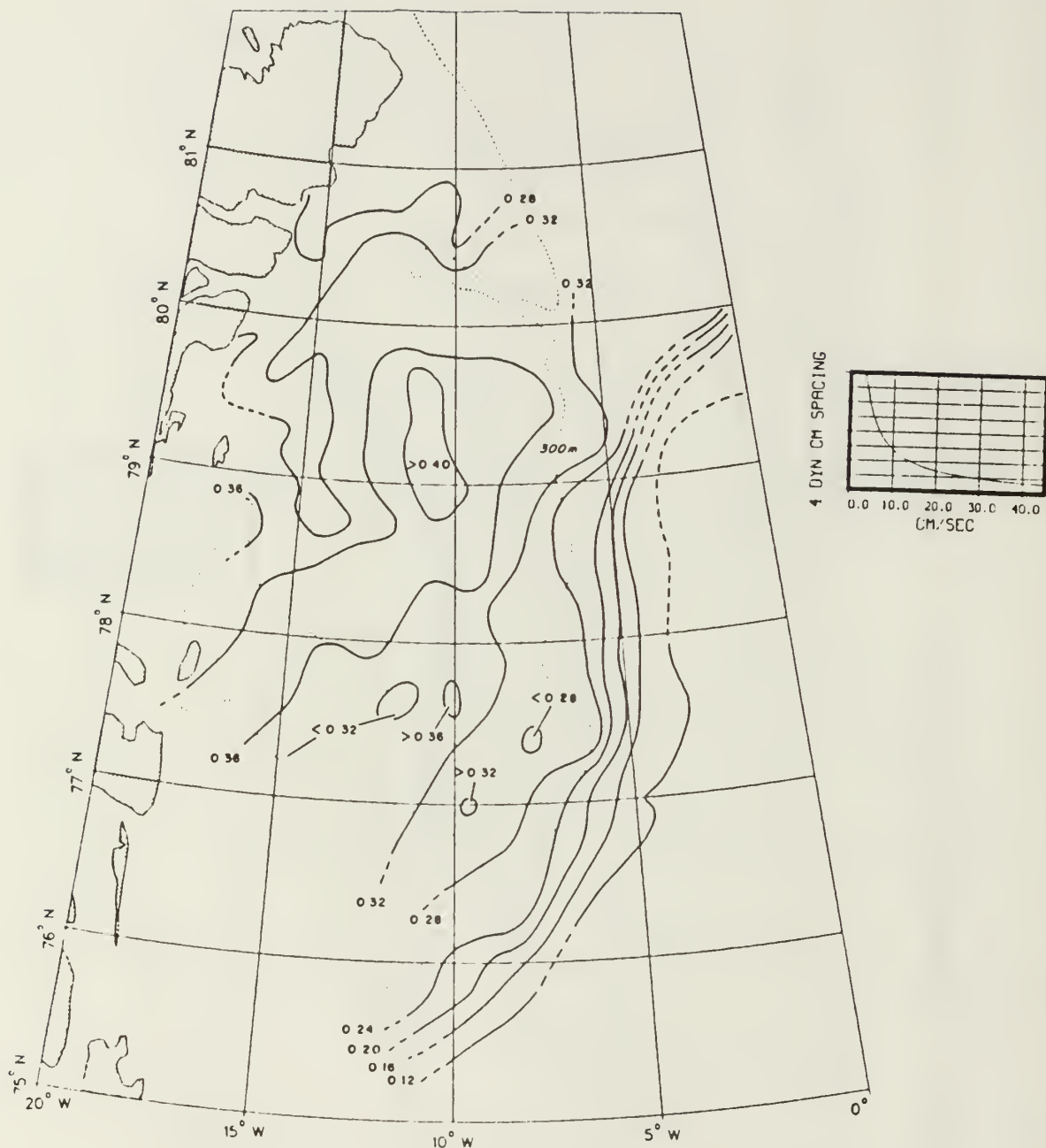


Figure 3.38 Surface dynamic topography referenced to 500 dbar in dynamic meters. The isobars over Westwind Trough suggests eastward flow there.

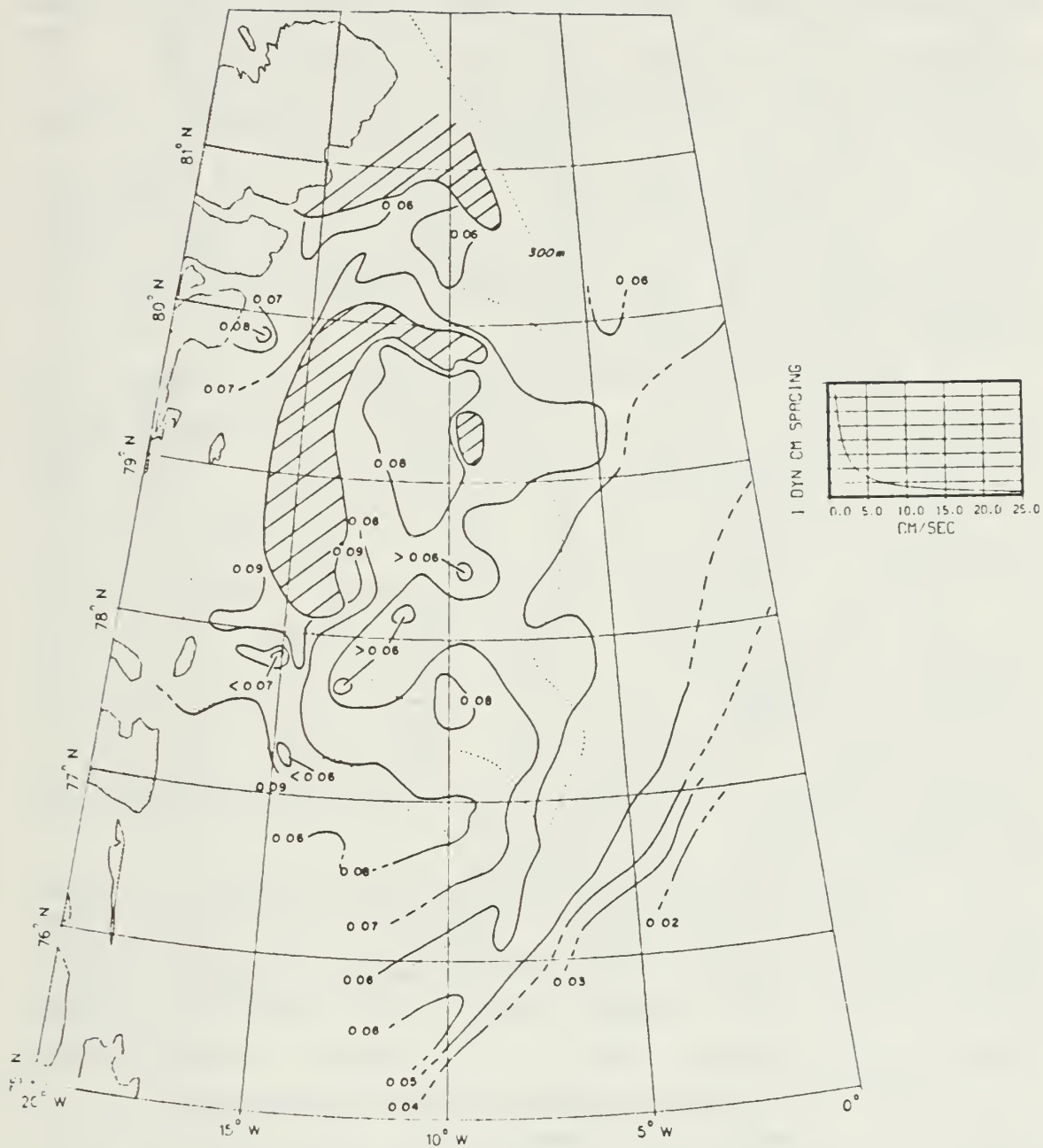


Figure 3.39 150 dbar dynamic topography referenced to 500 dbar. Hatched areas indicate bottom depths less than 150 m.

Another dominant feature is the dynamic "hill" over the central portion of Belgica Bank, which reflects the low salinities in the water column in that area (See Figs. 3.33 and 3.35). This feature suggests an anticyclonic geostrophic surface flow around and over the shallowest parts of the shelf. A secondary high region, over Ob' Bank evident in Figs. 3.36 and 3.37, implies a small region of anticyclonic flow centered there too, but the main sense of the current around  $80^{\circ}30'N$ , as implied by the dynamic topography, is eastward along Westwind Trough.

Generally, the dynamic topography at 150 dbar, as presented in Fig. 3.39 and contoured in 0.01 dynamic meter intervals, mirrors that of the surface (Fig. 3.38). The front is observed in the 150 dbar surface by a gradient which would support a baroclinic current of 0.05 to 0.07 m/s, a seven-fold reduction from the surface values. Over the shelf there is a generally southerly flow with perhaps a few meanders. However, one can have little faith in the large number of irregularities in the topography of this surface, especially over the shelf, because a contouring with a 0.01 dynamic meter spacing is approaching the "noise" level of the technique.

Dynamic topographies developed from previous cruises to the area show significant similarities to the features shown in Figs. 3.36 - 3.39. The baroclinic features developed from the the EDISTO summer 1964 and 1965 cruises (Aagaard and Coachman, 1968b, p. 279) show a strong gradient at the EGPF indicating baroclinic geostrophic currents of up to 0.23 m/s. Newton (in preparation), constructed a surface dynamic topography chart, relative to 200 dbar of the front and shelf regions based on the WESTWIND summer 1979 data. It shows a significant gradient corresponding to a geostrophic flow of about 0.3 m/s in the region of the EGPF and a dynamic "hill" over the center of Belgica Bank (although the

WESTWIND 1979 data were sparse there and some interpolations were indicated).

Paquette et al. (1985, p. 4876) developed dynamic height contours in the region of the front for the surface and the 150 dbar levels relative to 500 dbar from the NORTHWIND autumn 1981 data, thus including the effects of density gradients at greater depths than the two previous analyses. Additionally, they showed that with closer station spacing across the front, and a deeper reference level, geostrophic baroclinic current velocities up to 0.96 m/s (near 77°25'N) in the EGPF were evident. Their dynamic topographies show isobars turning westward between 76°30'N and 77°N at both the surface and 150 dbar levels suggesting a bathymetrically steered flow towards the entrance to Belgica Trough. This westward inflection of the isobars was also evident in the 1979 dynamic topography (Newton, in preparation) and is reflected in the westward turning of isopleths of water properties at the entrance to Belgica Trough also presented by Newton from the 1979 data. The westward turning at the entrance to Belgica Trough, however, is muted or non-existent in Figs. 3.36 - 3.39. Instead, the westward turning appears to take place north of the trough entrance. Thus considerable fluctuation in the current flow around the mouth of Belgica Trough can be expected (as previously suggested by the comparison made in Figs. 3.12 and 3.13).

### 3. Vertical Sections of Baroclinic Velocity

To further investigate the geostrophic current velocity and volume transport along the front and over the shelf, a sequence of vertical baroclinic current velocity sections was constructed. Seventeen sections cover the shelf break and, to varying degrees, the shelf; three were across Belgica Trough and two across Westwind Trough. The location of these sections is shown in Fig. 3.40.

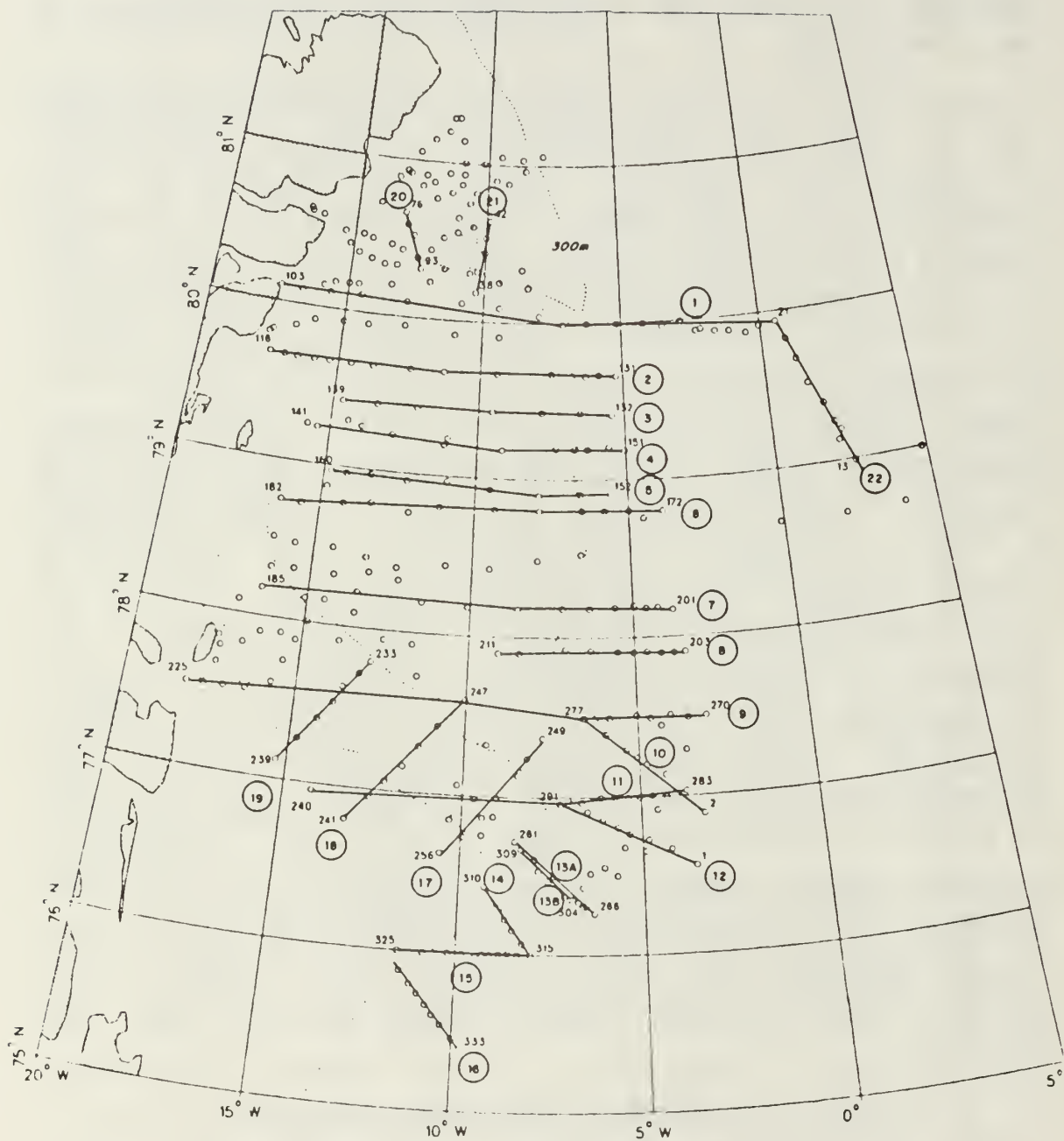


Figure 3.40 Location of vertical baroclinic current velocity sections.



As indicated in Chapter 2, a reference level of 500 dbar was selected for Sections 1 to 16 with horizontal extrapolation made for lesser bottom depths. Results of the geostrophic and transport calculations are shown in Table III.

Sections 1 - 16 are presented in Figs. 3.41 - 3.46. Most sections were made along a line of latitude and are arranged so that stations have the appropriate lateral reference to the  $10^{\circ}\text{W}$  and  $5^{\circ}\text{W}$  meridians. Some sections (those to the south where the EGC turns southwest) were made at a  $30^{\circ}$  -  $45^{\circ}$  angle to the parallels making the vertical stacking in the figures somewhat less accurate. Sections 1, 6, 7, 8, 9, and 11 covered significant portions of the front and shelf, Sections 2 - 5 do not include the front, while the remainder cover the frontal region only.

A sequential comparison of the sections reveals several aspects of the flow over the front and the shelf:

- As indicated in Table III, there is only a moderate variation in the maximum baroclinic current speed at the front which is consistent with the relatively uniform spacing of isobars of dynamic height noted in Figs. 3.36 - 3.38. Values varied from 0.30 to 0.47 m/s. The maximum values were at the surface except in the two northernmost frontal crossings (Sections 1 and 6) where peak speeds occurred at 15 to 20 m below the surface. However the salinity and density of the upper 5 m is affected by the adventitious presence or absence of melting ice which introduce anomalies on so short a time scale that they are not geostrophically balanced. Thus, baroclinic velocities in the upper 5 - 10 m of the profiles may be suspect.
- A core representing a high speed jet was present in all sections which crossed the EGPF. This core, as defined



TABLE III  
Frontal Geostrophic Current Sections

SECTION	MEAN LATITUDE	TOTAL VOLUME TRANSPORT (SVERDRUPS)		NET TRANSPORT CARRIED WEST OF SHELF BREAK (SVERDRUPS)	MAXIMUM GEOSTROPHIC CURRENT (m/s)	REMARKS
		Net.	Pos. Neg.			
1	79°55'N	0.82	1.54	0.72	1.02	0.37
2	79°40'N	0.44	1.03	0.58	N/A	*
3	79°25'N	0.32	0.61	0.29	N/A	*
4	79°12'N	0.05	0.46	0.41	N/A	*
5	78°55'N	0.49	0.99	0.50	N/A	*
6	78°48'N	0.37	1.46	0.49	0.70	0.39
7	78°11'N	1.49	1.60	0.12	0.58	0.38
8	77°54'N	1.19	1.47	0.21	0.58	0.32
9	77°30'N	1.42	1.86	0.44	1.12	0.46
10	77°15'N	1.55	1.55	0.0	1.55**	0.38
11	77°00'N	1.33	1.55	0.0	1.25	0.31
12	76°45'N	1.32	1.32	0.0	1.32**	0.30
13A	76°30'N	1.58	1.71	0.14	1.58**	0.38
13B	76°30'N	0.76	0.76	0.0	0.76**	0.38
14	76°10'N	0.69	0.72	0.03	0.69**	0.47
15	76°10'N	0.96	1.03	0.07	0.96**	0.36
16	75°45'N	0.96	1.03	0.07	0.96	0.36

N/A - No information east of shelf break.

\* - No relevant frontal velocities available.

\*\* - All transports include measurements east of shelf break only.

by a high velocity gradient, was typically less than 50 km in breadth and was confined generally to the upper 100 m in the region of the front. The core is occasionally split into two (or possibly more) portions (Section 11, Fig. 3.44, is an example), up to 30 km apart, indicating the filamental nature of the front.

- For those sections covering all or most of the front and shelf (Sections 1, 6, 7, 9, 11), the southward baroclinic volume transport (defined as positive transport in Table III) was about 1.6 Sv. A comparison of the contribution of the total southward transport over the shelf to the total transport (the difference between the total southward transport and the off-shelf transport) indicates that about 30 percent of the southerly transport in Section 1 is carried by water west of the 400 m isobath. In Sections 6, 7, 8, 9, and 11, this contribution rises to 40 - 60 percent. Such comparisons are tenuous, however, because of the uncertainties inherent in applying the Helland-Hansen technique over a wide shelf such as this. In deep water the contribution of layers deeper than 500 m to the baroclinicity has been ignored. While this might create only a small error in the computed surface velocities, the error in transports could be substantial. Additionally, errors are introduced because of the lack of ability to predict the barotropic component, especially in shallow water. Thus the figures given for surface velocities near the shelf break are probably a bit low and the sign of the errors in current velocities over portions of the shelf considerably westward of the EGPF is indeterminate.
- Sections 13A and 13B (Fig. 3.45) were constructed from the two lines of stations made three days apart and oriented axially through the mouth of Belgica Trough in

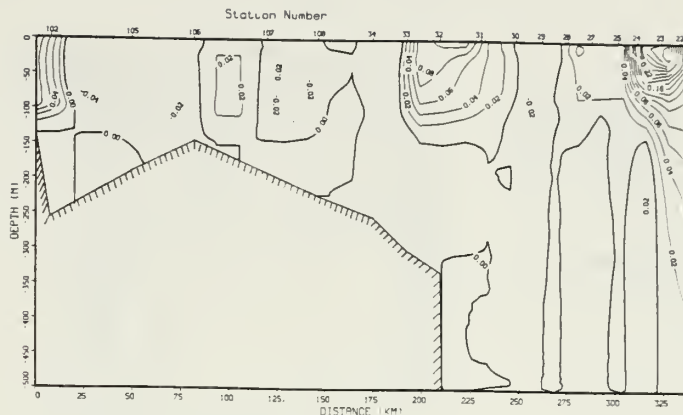
Transects 9 and 10. In Section 13A, the core of the jet has a considerably greater vertical development than in Section 13B.

- In several sections which extended far enough west to include it (Sections 1-6, 9), the northward flow of water in the westward parts of the shelf can be seen. Baroclinic current speeds here are up to 0.12 m/s with maxima occurring 25 - 100 m below the surface. The northerly transports, if accurate, are substantial - up to 0.5 Sv - suggesting that a significant portion of water in the northern part of the EGC recirculates northward over the shelf, at least in summer.

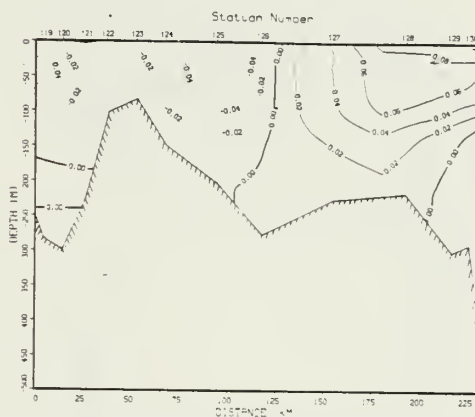
In 1984 maximum baroclinic current speeds along the front were reasonably constant with latitude, ranging from 0.30 to 0.47 m/s (Table III). No particular trend is obvious and variations are probably reflections of instabilities along the front. This fairly uniform behavior of the front from 80°N to 75°45'N is consistent with the suggestion of Paquette et al (1985, p. 4877) that the jet would probably be observed at a high velocity all along the EGPF if the CTD station density were high enough everywhere to resolve it. The maximum current speeds in 1984 are intermediate between the 0.80 to 0.96 m/s values computed from the autumn 1981 NORTHWIND cruise and the earlier EDISTO and WESTWIND values quoted previously.

The total southward volume transport calculated from the 1984 baroclinic measurements and integrated from the front to as close to the coast as possible, varied from 1.25 to 1.86 Sv. Based on the NORTHWIND 1981 data, Paquette et al., (1985, p. 4877) computed a transport of 1.2 Sv in the region of the front. They also estimated a total southward transport of 2 Sv from the ice edge to the coast by assuming that the current velocity decreased linearly to zero towards

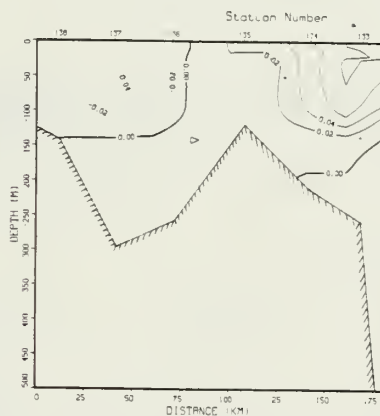
### SECTION 1



### SECTION 2



### SECTION 3

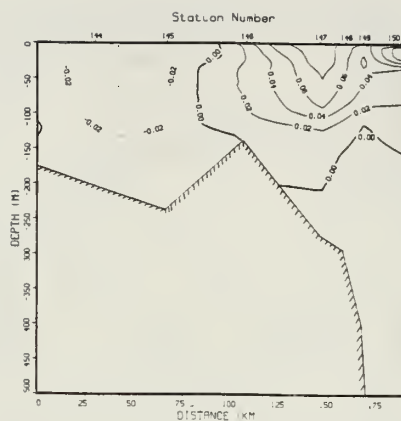


10°W

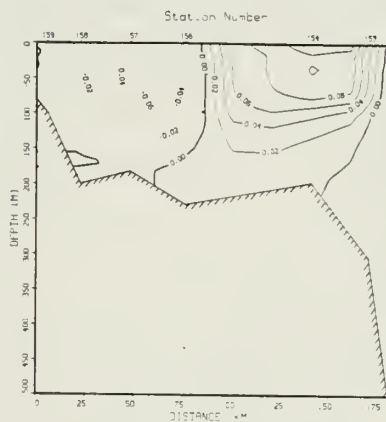
5°W

Figure 3.41 Sections 1 - 3. Solid isotachs indicate southerly movement, dashed isotachs indicate northerly movement. The high speed jet of the EGPF is at Station 23 in Section 1. Northward flowing water over the western portion of the shelf can be seen at Station 121 in Section 2. Sections 2 and 3 do not include the EGPF. Section locations are shown in Fig. 3.40

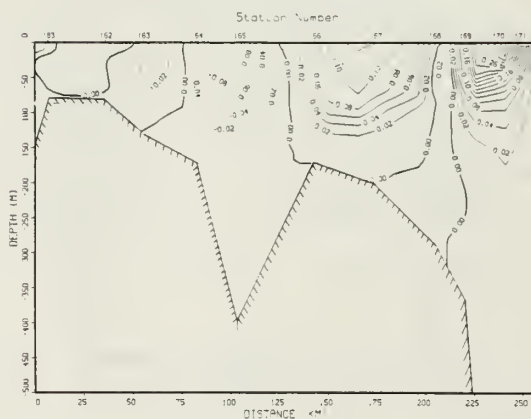
#### SECTION 4



#### SECTION 5



#### SECTION 6



10°W

5°W

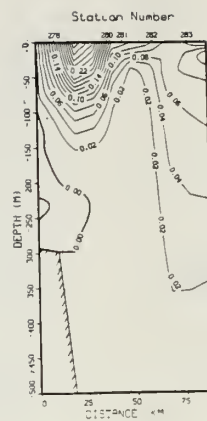
Figure 3.42 Sections 4 - 6. Sections 4 and 5 do not include the EGPF.

5°W

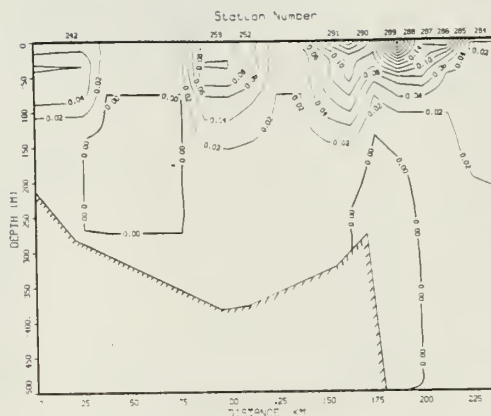
107



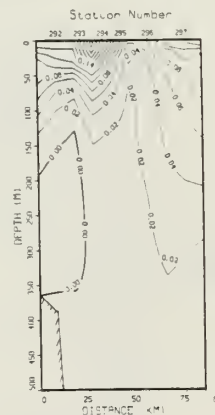
# SECTION 10



# SECTION 11



# SECTION 12



10°W

5°W

Figure 3.44 Sections 10 - 12. The high speed jet is broken into several filaments in Section 11.

SECTION 13A



SECTION 13B

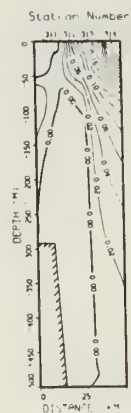


10°W

5°W

Figure 3.45 Sections 13A and 13B at the mouth of Belgica Trough. Note the change in vertical development of the jet over 3 days.

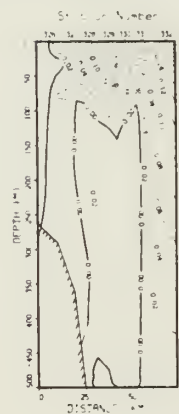
# SECTION 14



# SECTION 15



# SECTION 16



10'W

5'W

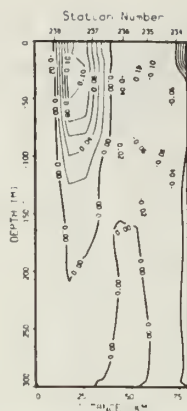
Figure 3.46 Sections 14 - 16. Meridional markings are accurate for Section 15 only.

the land. Given that there is probably a significant northward flow over the western half of the shelf, as implied by Figs. 3.36 - 3.38, this assumption appears to be invalid.

The motion of AIW up the bottom of Belgica Trough is not reflected in the dynamic topography or in vertical sections of baroclinic velocity. The latter, shown in Fig. 3.47 in which stations on the axis of the trough (Stations 335, 245, and 252/253) are superposed, appear to reflect local vortices such as that indicated by the "dynamic hill" in the center of the trough indicated in Fig. 3.37. As implied in this figure, the general sense of the baroclinic circulation in the eastern portion of the Belgica Trough area is southwesterly, although there may be some modifications to the flow producing some axial components in some parts of the trough. Presumably then, the shoreward advection of AIW as suggested by the modification of water properties in Belgica Trough is too slow to be reflected in the dynamic topography developed from the 1984 data or in winter ice drift and reflects water movement on a longer time scale.

Sections 20 and 21 (Fig. 3.48) are two transverse sections across Westwind Trough about 50 km apart and developed with reference to 300 dbar. They are characterized by a strong easterly baroclinic flow of water perpendicular to the sections: 0.37 m/s at the surface near Ob' Bank in Section 20 decreasing to 0.25 m/s at 40 m over the deepest portion of Westwind Trough in Section 21. Transports of about 0.5 Sv were calculated, suggesting that much of the northward moving water in the western part of the shelf is exhausted through Westwind Trough. This may contribute to the injection of shelf-conditioned PW into the EGPF and also contribute to the slightly lower salinities and temperatures of the AIW immediately west of the shelf break at the entrance to Westwind Trough compared to the AIW at the mouth of Belgica Trough.

# SECTION 19



# SECTION 18



# SECTION 17

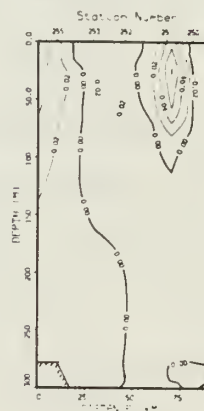
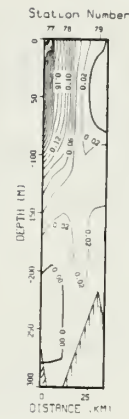


Figure 3.47 Sections 17 - 19 across Belgica Trough. The solid isotachs indicate eastward flow. These sections are arranged so that the stations on the axis of the trough are superposed. Velocities in this figure are referenced to 300 dbar.

# SECTION 20



# SECTION 21



Figure 3.48 Sections 20 - 21 across Westwind Trough. The solid isotachs indicate eastward flow. These sections are arranged so that the stations on the axis of the trough are superposed.



#### 4. Circulation

A map showing the circulation pattern inferred from the information obtained during the NORTHWIND 1984 cruise is presented in Fig. 3.49. As suggested by Newton (in preparation), the surface circulation implied by the dynamic height fields over the northern shelf is anticyclonic. A northward flow in Norske Trough resulting from a clockwise turning of the current around the southwest corner of Belgica Bank was postulated by Kiillerich (1945, p. 32) based on a few stations near Ile de France and the southern portion of Belgica Bank from the 1905 BELGICA expedition. He assumed that this turning of the current in this region was responsible for the ice-free water frequently observed near Ile de France (and also observed during NORTHWIND 1984) and for the transport of driftwood northward.

That there is a significant northward component to the surface current flow over the portion of the shelf nearest the coast between  $76^{\circ}\text{N}$  and  $80^{\circ}\text{N}$  was confirmed by observations of ice behaviour. The movement of several large, readily identifiable ice floes during the period 22 August to 14 September 1985, in the vicinity of the fast ice shelf from  $77^{\circ}30'\text{N}$  to  $79^{\circ}30'\text{N}$ , was observed from a sequence of NOAA 7 visual image photographs. During this period (in which winds were generally light and variable) the ice moved northward at about 2 km/day. This drift is consistent with the direction and magnitude of the flow provided by dynamic topographies.

Other observations of ice movement are consistent with the circulation pattern discussed in this section. Vinje (1978) tracked a number of buoys located on ice flows from the Nimbus 7 satellite in 1976. The tracks of these buoys are shown in the upper map in Fig. 3.50. The westernmost buoy appears to closely follow the course of Westwind

Trough; its average velocity from 31 August to 16 September is about 0.12 m/s. Vinje (1977) also observed the movement of ice from LANDSAT imagery in May and June 1976 (lower map Fig. 3.50). He suggested that this ice movement, during a period of relatively calm weather, probably reflects the local oceanographic circulation, consistent with the anticyclonic circulation pattern observed in this area by previous authors (Riis-Cristensen, 1938; Laktionov et al., 1960)

Kiillerich (1945, p. 27) also indicated a northward flow along the shore of water derived from the westward turning of a portion of the EGC up a trough south of Belgica Trough at 76°N. If this additional shorebound current exists, it might join the northward flow of water over Norkse Trough, reinforcing it.

Some interannual fluctuations in the circulation pattern are evident. As previously indicated, dynamic topography from the 1981 and 1979 NORTHWIND cruises and distribution of surface water characteristics from the 1979 data suggest a westward inflection of the EGC at the northern entrance to Belgica Dyb, while the 1984 data indicate that such a turning occurs farther north and farther westward. Certainly the presence of relatively warm AIW at the bottom of Belgica Trough and the intrusion of the cold saline fraction normally noted only at the front some distance down the trough (Fig. 3.18) indicated some sort of axial flow but its strength and consistency are not well established here.

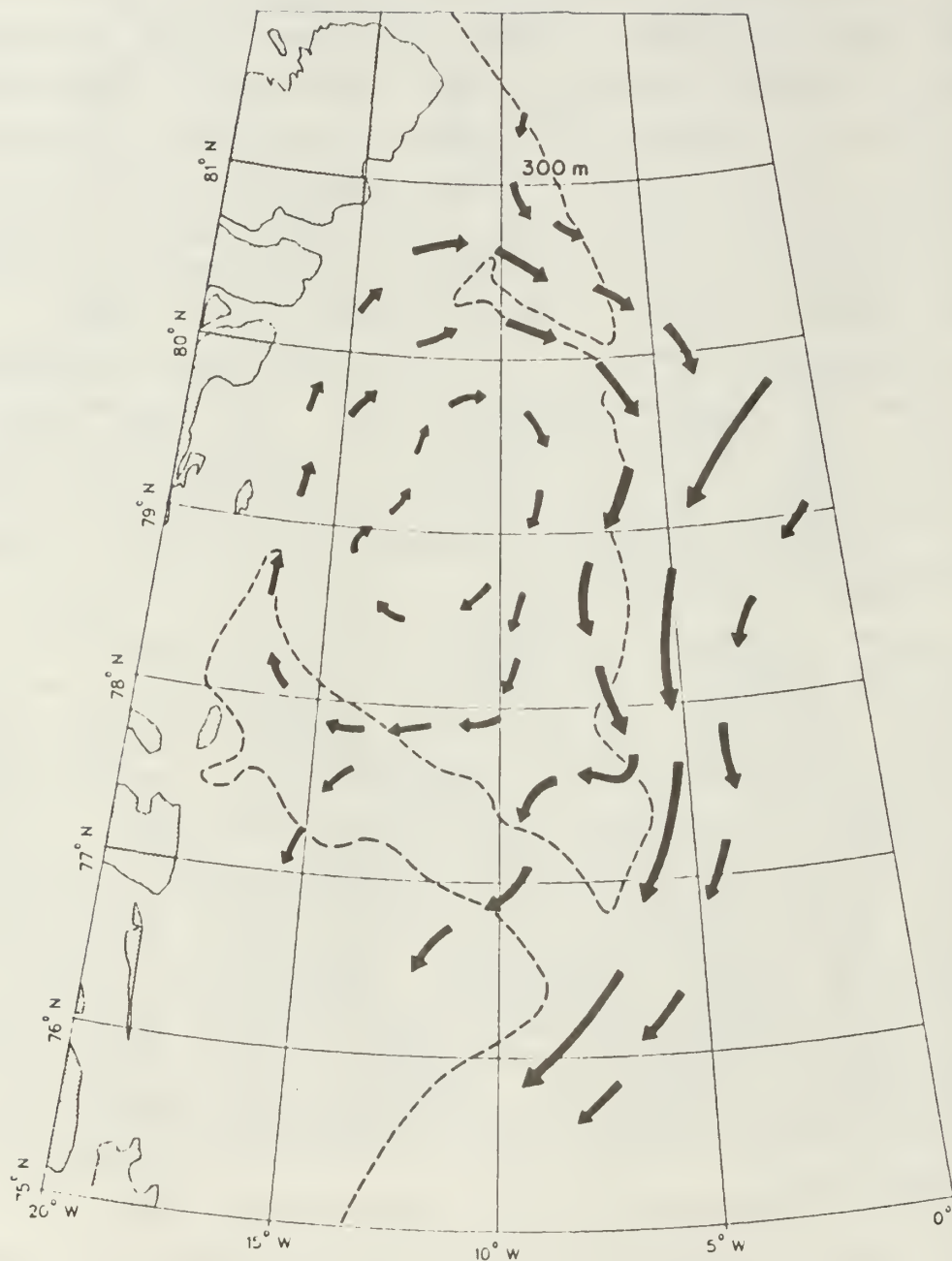


Figure 3.49 Estimated circulation pattern over the shelf and at the adjacent EGPF.

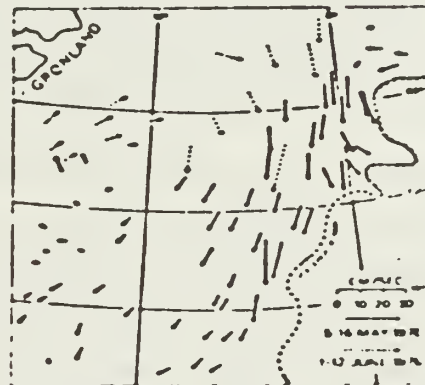


Figure 3.50 Two maps (after Vinje, 1977) indicating ice movement in 1976. The upper map indicates movement of buoys located on ice floes in August/September and tracked by the NIMBUS 7 satellite. The lower shows ice movement in May and June deduced from LANDAT imagery.

#### IV. CONCLUSIONS

The waters of the East Greenland Current both in the region of the front and over the adjacent continental shelf from  $75^{\circ}45'N$  to  $81^{\circ}20'N$  have been examined using a relatively dense network of CTD stations taken during the NORTHWIND 1984 cruise. Baroclinic geostrophic transport and current flow based on the distribution of water properties and dynamic topography were developed with the following major conclusions drawn:

- A number of characteristics of the EGPF observed by previous authors were also noted during the 1984 cruise. The front consisted of a marked east-west gradient in salinity and temperature giving rise to a baroclinic frontal jet with velocities of 0.30 to 0.47 m/s. Considerable finestructure development was noted in the southern portions of the front often consisting of parcels of AIW imbedded in the PW of the EGC surface layer. A warm core of the RAC was found pressed close against the eastern boundary of the front which often included filaments of slightly dilute AW.
- The EGPF approached the continental shelf break from a distance of 120 km at  $80^{\circ}N$  to 20 km at  $78^{\circ}48'N$ , after which it paralleled the 400 m isobath south to at least  $75^{\circ}45'N$ . The latitude at which the EGPF closes the shelf varies somewhat from year to year and may be a function of fluctuations in the WSC as well as interannual climatic variations.
- The warm core of RAC water found close to the east side of the EGPF cools significantly at latitudes below  $78^{\circ}N$ ,

suggesting that the majority of the input from the westward turning arm of the WSC is made north of that latitude.

- Southward volume transports were about 1.6 Sv. This figure is, no doubt, a minimum since there is presumably a significant contribution to the mass transport made by the large volume of more slowly moving water below the 500 dbar reference level used.
- Circulation on the shelf between 76°N and 80°N is dominated by a large anticyclonic gyre centered over the shallowest portions of the shelf. Transports within this gyre can be significant, with up to 0.5 Sv (or more) of water moving northward on the western portion of the shelf.
- The surface and bottom water characteristics and dynamic height topographies developed suggest that water advects westward at the bottom of the entrances to Belgica and Westwind Troughs. Flow at the surface of Belgica Trough is generally southward, perhaps with local modifications, while in Westwind Trough the surface flow is eastward and southeastward.



APPENDIX A  
MOLLOY DEEP

A large (60 km diameter) cyclonic ice and water eddy has frequently been noted on the eastern edge of the East Greenland Current at about  $79^{\circ}40'N$ ,  $001^{\circ}E$  and described by various authors (Vinje, 1977; Wadhams, 1979; Wadhams and Squire, 1983). This eddy, which consists of relatively warm near-surface water at its center, is marked by a characteristic ice feature characterized by Wadhams and Squire (1983, p. 2770) as a "backward breaking wave shape". The feature is shown in Fig. A.1 (after Smith et al., 1984) which depicts the ice edge observed in August 1980 (Wadhams and Squire, 1983) and May 1976 (Vinje, 1977) superimposed on a map of local bathymetry (Perry et al., 1980).

The mechanism for the formation of this eddy has been the subject of some speculation. Wadhams and Squire (1983, p. 2776) argued that the East Greenland Current is baroclinically unstable and presented a two layer model for the generation of an eddy by such a mechanism. They established that wavelengths of 50 km would have the highest growth rates (which is similar to the observed diameter of the eddy) but that such disturbances should travel slowly downstream. Such propagation has not yet been observed and the repeated observations of the eddy in the same position led Wadhams and Squire to speculate on the possibility of a local triggering mechanism - possibly the Molloy Deep, a 5770 m depression located nearby at  $79^{\circ}10'N$ ,  $002^{\circ}50'E$ .

Smith et al. (1984), in arguing that the principle of conservation of vorticity could explain the generation of an eddy in this region, developed a two layer model in a 2500 m rectangular ocean basin centered on a 3500 m Gaussian shaped

depression and driven by a 0.1 m/s jet from the north-east. The model generated a cyclonic eddy with a barotropic and subsequently a baroclinic component. They suggest that their results indicate that an eddy generated under the conditions of their model should remain trapped in the vicinity of the depression.

Over a 24 hour period on 24/25 August 1984, NORTHWIND occupied a sequence of CTD stations from 79°N - 80°N adjacent to the Molloy Deep and through an ice edge feature similar to that described above. The position of the stations is shown in Fig. A.1. A narrow band (5 - 10 km) of ice oriented generally east-west and comprised of densely spaced small fragments of ice was observed in the vicinity of Station 14. Ice concentrations at Stations 16 - 18 were less than one tenth and an ice edge was encountered between Stations 18 and 19 at which latter station a concentration of six tenths was observed.

A temperature and salinity transect summarizing the results of the CTD measurements made through this feature is shown in Fig. A.2. The location of the band of ice at Station 14 is reflected in the sharply cooler near-surface water which, as indicated by Bourke (1984), has a horizontal gradient of temperature of 4°C in 5 km. The ice edge north of Station 18 is marked by a surface layer of water less than 0°C.

The center of the eddy is characterized by a layer of >4°C water 100 m thick and 65 km in diameter near the surface. Below 200 m, isohalines and isotherms at the center are depressed at least 100 m deeper than their positions at the apparent edges of the eddy. As Bourke (1984) points out, such depression of the isotherms continues to at least 900 m, suggesting that the eddy exists to at least that depth.

A vertical cross-section of the geostrophic baroclinic velocity of this section was constructed (Fig. A.3) with reference to 1000 dbar. The cross-section, in which positive values indicate westward motion, shows cyclonic flow with regions of maximum speeds located some 30 km from the center. The swirl transport calculated from these baroclinic velocities was 1 Sv. The current velocity values in Fig. A.3 and the transport value quoted above may be low for two reasons. The barotropic component, which may be significant if the eddy is bathymetrically driven, is not included. Additionally, the transect probably does not run through the exact center of the eddy. Adjustments for the gradient current in this eddy suggest that the geostrophic velocities indicated in Fig. A.3 should be reduced by a maximum of 3% for a 30 km radius eddy.

The large vertical scale of this eddy is consistent with a topographic genesis, and as indicated by the model of Smith et al. (1984), some displacement of the center of an eddy from the center of a triggering depression as is suggested in Figs. A.1 and A.2 is not inconsistent with a topographically trapped eddy. However, further information on the long term absolute velocity field in this area will probably be required to resolve the issue of the generative mechanism for this eddy.

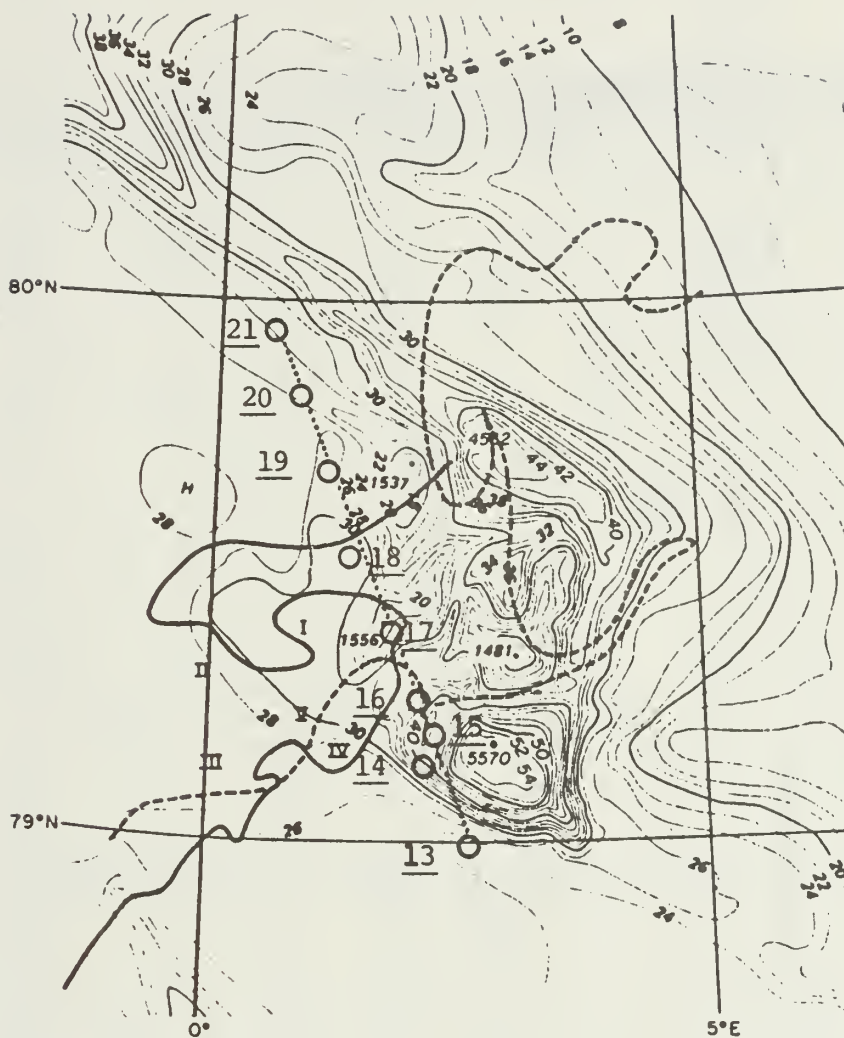


Figure A.1 The bathymetry and ice edge features in the vicinity of Molloy Deep (after Smith et al., 1984). The position of the NORTHWIND 1984 CTD Stations (underlined figures) is also shown.

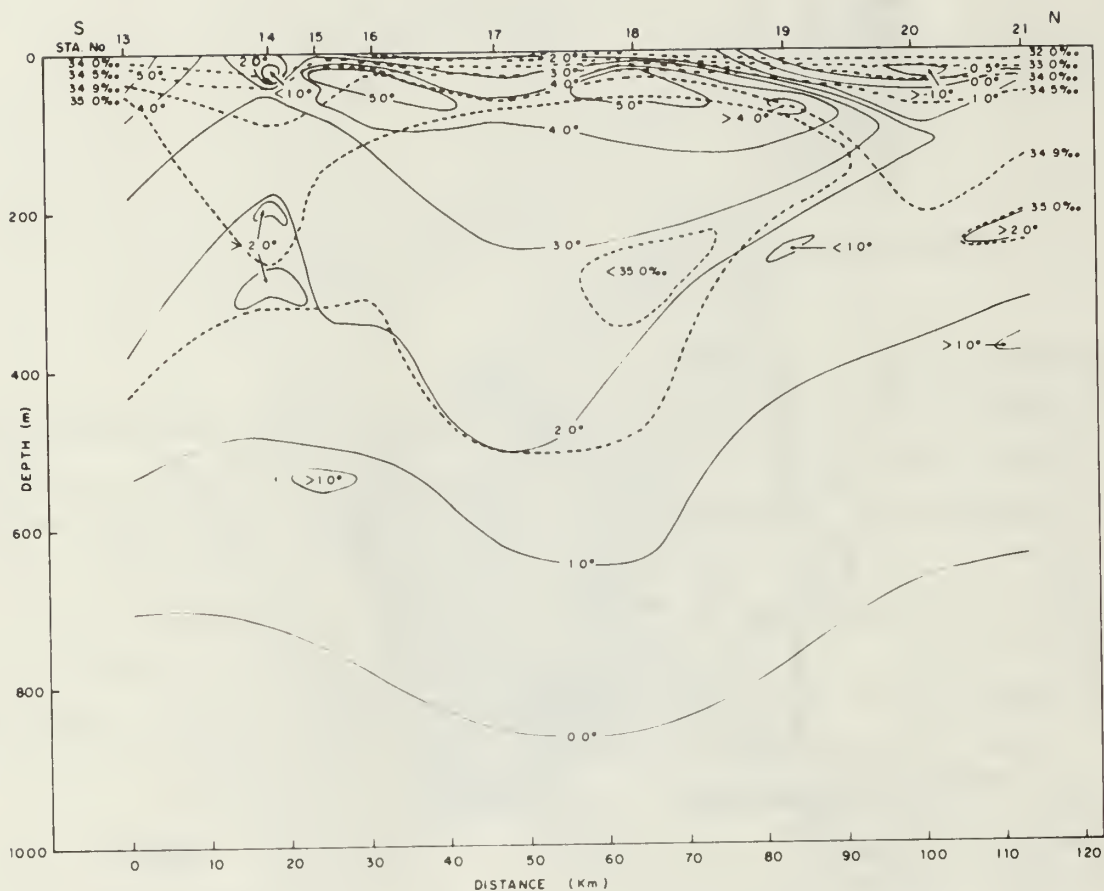


Figure A.2 A temperature and salinity transect across the Molloy Deep eddy feature. A band of brash ice was located in the vicinity of Station 14 and the ice margin was again encountered between Stations 18 and 19.



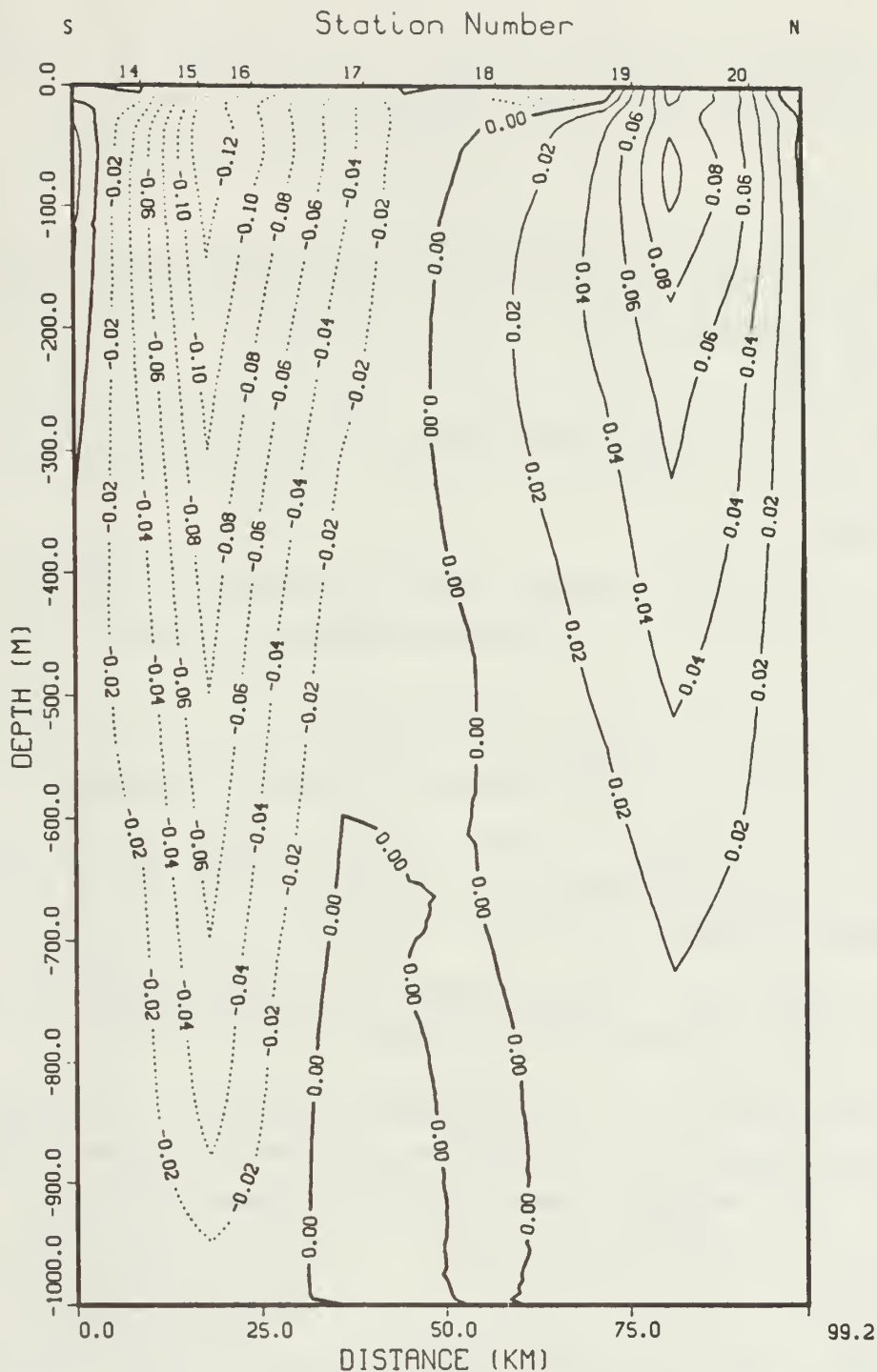


Figure A.3 The baroclinic velocity field relative to 1000 dbar near Molloy Deep. Westward flow is indicated by positive isotachs.



## LIST OF REFERENCES

- Aagaard, K., and L.K. Coachman, The East Greenland Current north of the Denmark Strait, I, Arctic, 21(3), 181-200, 1968a
- Aagaard, K., and L.K. Coachman, The East Greenland Current north of the Denmark Strait, II, Arctic 21(4), 267-290, 1968b.
- Aagaard, K., L.K. Coachman, and E. Carmack, On the halocline of the Arctic Ocean, Deep-Sea Research, 28A(6), 529-545, 1981.
- Bourke, R.H., Preliminary results of the oceanographic cruise of the USCGC Northwind to the Greenland Sea: August - September, 1984, Tech. Rep. NPS 69-84-019, Dept. of Oceanography, Naval Postgraduate School, Monterey, Calif., 1984.
- Fomin, L.M., The Dynamic Method in Oceanography, Elsevier Publishing Company, N.Y., 1964.
- Helland-Hansen, B., The Sognefjord Section - oceanographic observations in the northernmost part of the North Sea and the southern part of the Norwegian Sea, James Johnstone Memorial Volume, Lancashire Sea-Fish. Lab., Liverpool, 1934.
- Kiilerich, A.B., On the hydrography of the Greenland Sea, Meddelser om Gronland, 144(2), 63 pp., 1945.
- Laktionov, V.A et al., Okeanograficheskii ocherk severnoi chast Grenlandskogo morya, Sovietskije Ribokh. Issled. y Moryakh Evropeiskogo Severa, Moskva: Vniro-Pinro, 1960.

- Mosby, H., Water, salt, and heat balance of the North Polar Sea and of the Norwegian Sea, Geofysiske Publikasjoner, 24, 289-313, 1962.
- Newton, J.L., Hydrographic structure of the northeast Greenland shelf; Fall 1979, in preparation.
- Newton, J.L., and L.E. Piper, Oceanographic data from the northwest Greenland Sea: Arctic East 1979 survey of the USCGC Westwind, Rep. SAI-202-81-003-1j, Sci. Appl, Inc., San Diego, Calif., 1981.
- Paquette, R.G., R.H. Bourke, J.L. Newton, and W.F. Perdue, The East Greenland Polar Front in Autumn, J. Geophys. Res., 90(C3), 4866-4882, 1985.
- Perdue, W.F., Oceanographic investigation of the East Greenland Polar Front, Master's Thesis, Naval Postgraduate school, Monterey, California, 1982.
- Perry, R.K., H.S. Flemming, N.Z. Cherkis, R.H. Feden, and P.R. Vogt, Bathymetry of the Norwegian-Greenland and western Barents Seas, U.S. Naval Research Laboratory - Acoustics Division, Environmental Sciences Group, William and Heintz Map Corporation, Washington, D.C. 1980.
- Reid, J.L., and A.W. Mantyla, The effect of the geostrophic flow upon coastal sea elevations in the northern North Pacific Ocean, J. Geophys. Res., 81(18), 3100-3110, 1976.
- Riis-Carstensen, E., Fremsettelse av et dynamisk-topographisk kort over Ostgronlandsstrommen Mellom 74° og 79° N.Br. paa grundlag af hidtidige gjorte undersogelser i disse egne, Geografisk Tidsskrift 41(1), 1938.
- Smith, D.C., J.H. Morison, J.A. Johannessen, and N. Untersteiner, Topographic generation of an eddy at the

edge of the East Greenland Current, J. Geophys. Res., 89 (C5), 8205-8208, 1984.

Swift, J.H., and K. Aagaard, Seasonal transitions and water mass formation in the Iceland and Greenland Seas, Deep Sea Res., 28A (10), 1107-1129, 1981.

Tripp, R.B. and K. Kusunoki, Physical, chemical and current data from Arlis II Eastern Arctic Ocean, Greenland Sea and Denmark Strait area February 1964 - May 1965, Tech. Rep. 185 Vols. 1 and 2, Ref. M07-29 Dept. of Oceanogr., Univ. Wash., Seattle, 1967.

Vinje, T.E. Landsat Rep. E77-10206, National Technical Information Service, Springfield, 1977.

Vinje, T.E., On the use of data buoys in sea ice studies, paper presented at WMO Workshop on Remote Sensing of Sea Ice, World Meteorological Organization, Washington, D.C., Oct 16-20, 1978.

Wadhams, P., A.E. Gill, and P.F. Linden, Transect by submarine of the East Greenland Polar Front, Deep Sea Res., 26 (12A), 1311-1328, 1979.

Wadhams, p., Sea ice thickness distribution in Fram Strait, Nature, 303 (3930), 108-111, 1983.

Wadhams, P., and V.A. Squire, An ice-water vortex at the edge of the East Greenland Current, J. Geophys. Res., 88 (C5), 2770-2780, 1983.

# INITIAL DISTRIBUTION LIST

	No. Copies
1. Director	
Applied Physics Laboratory	
Attn: Mr. Robert E. Francois	1
Mr. E.A. Pence	1
Mr. G.R. Garrison	1
Library	1
University of Washington	
1013 Northeast 40th Street	
Seattle, Washington 98105	
2. Director	5
Arctic Submarine Laboratory	
Code 54, Building 371	
Naval Ocean Systems Center	
San Diego, California 92152	
3. Superintendent	
Naval Postgraduate School	
Attn: Library, Code 0142	2
Dr. R.H. Bourke, Code 68Bf	5
Dr. R.G. Paquette, Code 68Pa	5
Monterey, California 93943	
4. Mr. Beaumont M. Buck	1
Polar Research Laboratory, Inc.	
6309 Carpinteria Ave.	
Carpinteria, California 93103	
5. Chief of Naval Operations	
Department of the Navy	
Attn: NOP-02	1
NOP-22	1
NOP-964D2	1
NOP-095	1
NOP-098	1
Washington, District of Columbia 20350	
6. Commander	1
Submarine Squadron THREE	
Fleet Station Post Office	
San Diego, California 92132	
7. Commander	1
Submarine Group FIVE	
Fleet Station Post Office	
San Diego, California 92132	

8. Dr. John L. Newton 2  
10211 Rookwood Drive  
San Diego, California 92131
9. Director 1  
Marine Physical Laboratory  
Scripps Institution of Oceanography  
San Diego, California 92132
10. Commanding Officer 1  
Naval Intelligence Support Center  
4301 Suitland Road  
Washington, District of Columbia 20390
11. Commander 1  
Space and Naval Warfare Systems Command  
Department of the Navy  
Washington, District of Columbia 20360
12. Director 1  
Woods Hole Oceanographic Institution  
Woods Hole, Massachusetts 02543
13. Commanding Officer 1  
Naval Coastal Systems Laboratory  
Panama City, Florida 32401
14. Commanding Officer 1  
Naval Submarine School  
Naval Submarine Base, New London  
Groton, Connecticut 06349-5700
15. Assistant Secretary of the Navy 1  
(Research and Development)  
Department of the Navy  
Washington, District of Columbia 20350
16. Director of Defense Research and Engineering 1  
Office of Assistant Director (Ocean Control)  
The Pentagon  
Washington, District of Columbia 20301
17. Commander, Naval Sea Systems Command 1  
Department of the Navy  
Washington, District of Columbia 20362
18. Chief of Naval Research  
Department of the Navy  
Attn: Code 102-OS 1  
Code 220 1  
Code 425 Arctic 1  
800 N. Quincy Street  
Arlington, Virginia 22217

19. Fisheries-Oceanography Library 1  
Oceanography Teaching Bldg., WG-30  
University of Washington  
Seattle, WA 98195
20. Commanding Officer 1  
Naval Underwater Systems Center  
Newport, Rhode Island 02840
21. Commander 1  
Naval Air Systems Command  
Headquarters  
Department of the Navy  
Washington, District of Columbia 20361
22. Commander  
Naval Oceanographic Office  
Attn: Library Code 3330 1  
Washington, District of Columbia 20373
23. Director 1  
Advanced Research Project Agency  
1400 Wilson Boulevard  
Arlington, Virginia 22209
24. Commander SECOND Fleet 1  
Fleet Post Office  
New York, New York 09501
25. Commander THIRD Fleet 1  
Fleet Post Office  
San Francisco, California 96601
26. Commander  
Naval Surface Weapons Center  
White Oak  
Attn: Mr. M.M. Kleinerman 1  
Library 1  
Silver Springs, Maryland 20910
27. Officer-in-Charge 1  
New London Laboratory  
Naval Underwater Systems Center  
New London, Connecticut 06320
28. Commander  
Submarine Development Squadron Twelve 1  
Naval Submarine Base  
New London  
Groton, Connecticut 06349



29. Commander  
Naval Weapons Center  
Attn: Library 1  
China Lake, California 93555
30. Commander  
Naval Electronics Laboratory Center  
Attn: Library 1  
271 Catalina Boulevard  
San Diego, California 92152
31. Director 1  
Naval Research Laboratory  
Attn: Technical Information Division  
Washington, District of Columbia 20375
32. Director 1  
Ordnance Research Laboratory  
Pennsylvania State University  
State College, Pennsylvania 16801
33. Commander Submarine Force 1  
U.S. Atlantic Fleet  
Norfolk, Virginia 23511
34. Commander Submarine Force  
U.S. Pacific Fleet 1  
Attn: N-21  
FPO San Francisco, CA 96860
35. Commander 1  
Naval Air Development Center  
Warminster, Pennsylvania 18974
36. Commander 1  
Naval Ship Research and Development Center  
Bethesda, Maryland 20084
37. Commandant 1  
U.S. Coast Guard Headquarters  
400 Seventh Street, S.W.  
Washington, DC 20590
38. Commander 1  
Pacific Area, U.S. Coast Guard  
630 Sansome Street  
San Francisco, California 94126
39. Commander 1  
Atlantic Area, U.S. Coast Guard  
159E, Navy Yard Annex  
Washington, District of Columbia 20590

- |     |  |             |
|-----|--|-------------|
| 40. | Commanding Officer<br>U.S. Coast Guard Oceanographic Unit<br>Building 159E, Navy Yard Annex<br>Washington, District of Columbia 20590                                  | 1           |
| 41. | Scientific Liaison Office<br>Office of Naval Research<br>Scripps Institute of Oceanography<br>La Jolla, California 92037   | 1           |
| 42. | SIO Library<br>Scripps Institute of Oceanography<br>P.O. Box 2367<br>La Jolla, California 92037  | 1           |
| 43. | School of Oceanography, WB-10<br>University of Washington<br>Attn: Dr. L.K. Coachman<br>Dr. K. Aagaard<br>Dr. S. Martin<br>Seattle, Washington 98195                   | 1<br>1<br>1 |
| 44. | Library, School of Oceanography<br>Oregon State University<br>Corvallis, Oregon 97331  | 1           |
| 45. | CRREL<br>U.S. Army Corps of Engineers<br>Attn: Library<br>Hanover, New Hampshire 03755-1290  | 1           |
| 46. | Commanding Officer<br>Fleet Numerical Oceanography Center<br>Monterey, California 93940  | 1           |
| 47. | Commanding Officer<br>Naval Environmental Prediction Research Facility<br>Monterey, California 93940   | 1           |
| 48. | Defense Technical Information Center<br>Cameron Station<br>Alexandria, Virginia 22304-6145   | 2           |
| 49. | Commander<br>Naval Oceanography Command<br>NSTL Station<br>Bay St. Louis, Mississippi 39529  | 1           |
| 50. | Commanding Officer<br>Naval Ocean Research and Development Activity<br>Attn: Technical Director<br>Dr. J.P. Welsh,<br>NSTL Station<br>Bay St. Louis, Mississippi 39529 | 1<br>1      |

51. Commanding Officer 1  
Naval Polar Oceanography Center, Suitland  
Washington, District of Columbia 20373
52. Director 1  
Naval Oceanography Division  
Naval Observatory  
34th and Massachusetts Ave. NW  
Washington, District of Columbia 20390
53. Commanding Officer 1  
Naval Oceanographic Command  
NSTL Station  
Bay St. Louis, Mississippi 39522
54. Scott Polar Research Institute  
University of Cambridge  
Attn: Library 1  
Sea Ice Group 1  
Cambridge, England  
CB2 1ER
55. Chairman 1  
Department of Oceanography  
U.S. Naval Academy  
Annapolis, Maryland 21402
56. Dr. James Morison 1  
Polar Science Center  
4059 Roosevelt Way, NE  
Seattle, Washington 98105
57. Dr. Kenneth Hunkins 1  
Lamont-Doherty Geological Observatory  
Palisades, New York 10964
58. Dr. David Paskowsky, Chief 1  
Oceanography Branch  
U.S. Department of the Coast Guard  
Research and Development Center  
Avery Point, Connecticut 06340
59. Science Applications, Inc. 1  
Attn: Dr. Robin Muench  
13400B Northrup Way  
Suite 36  
Bellevue, Washington 98005
60. Institute of Polar Studies 1  
Attn: Library  
103 Mendenhall  
125 South Oval Mall  
Columbus, Ohio 43210

61. Institute of Marine Science  
University of Alaska  
Attn: Library  
Fairbanks, Alaska 99701 1
  
62. Department of Oceanography  
University of British Columbia  
Attn: Library  
Vancouver, B.C. Canada  
V6T 1W5 1
  
63. Geophysical Institute  
University of Alaska  
Attn: Dr. H.J. Niebauer  
Fairbanks, Alaska 99701 1
  
64. Bedford Institute of Oceanography  
Attn: Library  
P.O. Box 1006  
Dartmouth, Nova Scotia  
Canada  
B2Y 4A2 1
  
65. Carol Pease  
Pacific Marine Environmental Lab/NOAA  
7600 Sand Point Way N.E.  
Seattle, Washington 98115 1
  
66. Department of Oceanography  
Dalhousie University  
Halifax, Nova Scotia  
Canada  
B3H 4J1 1
  
67. Mr. Richard Armstrong  
MIZEX Data Manager  
National Snow and Ice Data Center  
Cooperative Institute for Research  
in Environmental Sciences  
Boulder, Colorado 80309 2
  
68. Royal Roads Military College  
Faculty of Science and Engineering  
FMO Victoria, B.C.  
CANADA  
VOS IBO 1
  
69. National Defence Headquarters  
Ottawa, Ontario  
CANADA  
K1V 0K2  
Attn: DGRET 3

70. LCDR M.D. Tunncliffe  
Canadian Forces Fleet School Halifax  
Halifax, N.S.  
CANADA  
B3K 2X0

3











216375

Thesis  
T9343  
c.1

Tunnicliffe

An investigation of  
the waters of the  
East Greenland cur-  
rent.

5 OCT 92

80451

5 OCT 92

80451

216375

Thesis  
T9343  
c.1

Tunnicliffe

An investigation of  
the waters of the  
East Greenland cur-  
rent.





An investigation of the waters of the Ea



3 2768 000 65637 5

DUDLEY KNOX LIBRARY